CONJUGATED SCHIFF-BASE MACROCYCLES AND THEIR METAL COMPLEXES

by

Joseph Hui

B.Sc. (Hon.), The University of British Columbia, 2001

A THESIS SUBMITTED IN PARTIAL FULFILLMENT OF
THE REQUIREMENTS FOR THE DEGREE OF
MASTER OF SCIENCE

in

THE FACULTY OF GRADUATE STUDIES

(DEPARTMENT OF CHEMISTRY)

We accept this thesis as conforming
to the required standard

THE UNIVERSITY OF BRITISH COLUMBIA

APRIL 2004

Library Authorization

In presenting this thesis in partial fulfillment of the requirements for an advanced degree at the University of British Columbia, I agree that the Library shall make it freely available for reference and study. I further agree that permission for extensive copying of this thesis for scholarly purposes may be granted by the head of my department or by his or her representatives. It is understood that copying or publication of this thesis for financial gain shall not be allowed without my written permission.

JOSEPH HUI

Name of Author *(please print)*

05/04/2004

Date (dd/mm/yyyy)

Title of Thesis: CONJUGATED SCHIFF-BASE MACROCYCLES AND THEIR ~~MA~~ METAL COMPLEXES

Degree: M.Sc Year: 2004

Department of CHEMISTRY

The University of British Columbia
Vancouver, BC Canada

Abstract

The [3+3] Schiff-base macrocycles (**37-40**) were obtained by reacting 3,6-diformyl-1,2-dihydroxybenzene (**31**) and 4,5-diamino-1,2-dialkoxybenzene (**33-36**). The resulting macrocycles were characterized by ^{1}H and ^{13}C NMR spectroscopy, IR spectroscopy, UV-Vis spectroscopy, ESI mass spectrometry, DSC and POM. The macrocycles with long alkoxy substituents have the potential to exhibit liquid crystallinity; however, no mesomorphic characteristics were observed. Macrocycle **37** was metallated with most of the first-row transition metals. The metal-containing [3+3] Schiff-base macrocycles (**47-53**) were characterized by ^{1}H NMR spectroscopy, IR spectroscopy, UV-Vis spectroscopy, and ESI and MALDI-TOF mass spectrometry. ESR spectroscopy has been performed on the vanadyl-containing macrocycle **47**. The ESR spectrum shows that there appears to be a significant interaction between the unpaired electrons of the vanadium atoms, leading to a single broad ESR signal. Several attempts have been made to obtain the [6+6] Schiff-base macrocycle, but only a fragment of it (compound **65**) could be synthesized successfully.

Table of Contents **Page**

List of Symbols and Abbreviations

Å	angstroms (1 Å = $1x10^{-10}$ m)
a.m.u.	atomic mass units
^{o}C	degrees Celsius
^{o}C/min	degree per minute
ca	circa (about)
^{13}C NMR	carbon-13 nuclear magnetic resonance
cm	centimetres
d	days
d	deuterium
δ	chemical shift (NMR)
DSC	differential scanning calorimetry
ε	molar extinction coefficient
e.g.	for example
eq.	equivalents
ESI-MS	electrospray ionization mass spectrometry
ESR	electron spin resonance
Et_3N	triethylamine
EtOH	ethanol
Fig.	figure
g	grams
G	gauss

h	hours
^{1}H NMR	proton nuclear magnetic resonance
HMBC	heteronuclear multiple bond correlation
HMQC	heteronuclear multiple quantum correlation
HOAc	acetic acid
HR-ESI-MS	high resolution electrospray ionization mass spectrometry
I	nuclear spin
IR	infrared
L	litres
λ	wavelength
LMCT	ligand-to-metal charge transfer
m	multiplet (NMR) / medium (IR)
M	molecular weight / transition metals
μM	micromolar
$M(acac)_2$	transition metal(II) acetylacetonate
MALDI-TOF-MS	Matrix-assisted laser desorption/ionisation time-of-flight mass spectrometry
MBBA	4-methoxybenzylidene-4'-n-butylaniline
Me	methyl group
MeCN	acetonitrile
MeOH	methanol
MHz	megahertz
min	minutes
mL	millilitres

MLCT	metal-to-ligand charge transfer
mmol	millimoles
Mp	melting point
mW	milliwatts
m/*z*	mass-to-charge ratio
ñ	director
ν	frequency
$Ni(OAc)_2 \cdot 4H_2O$	nickel(II) acetate tetrahydrate
NLO	nonlinear optical
nm	nanometres
NMR	nuclear magnetic resonance
%	percent
θ	angle with respect to the director
POM	polarizing optical microscope
ppm	parts per million (NMR)
R, R', R"	alkyl group / functional group
s	singlet (NMR) / strong (IR)
S	total spin angular momentum
S	order parameter of the liquid crystal
salen	2,2'-*N*,*N*'-bis(salicylidene)ethylenediamine
salphen	2,2'-*N*,*N*'-bis(salicylidene)phenylenediamine
sh	shoulder (IR)
t	triplet (NMR)

Temp.	temperature
TOF	time-of-flight
THF	tetrahydrofuran
UV-Vis	ultraviolet-visible
vs	very strong
w	weak (IR)
$Zn(OAc)_2 \cdot 2H_2O$	zinc(II) acetate dihydrate

List of Tables **Page**

List of Figures **Page**

List of Schemes **Page**

Acknowledgement

I would like to thank Dr. Mark J. MacLachlan for giving me the opportunity to study and do research in his lab. He has given me plenty of valuable advice and support. I have learned a great deal from him and that helped me in strengthening my skills as an independent chemist. I would also like to thank the rest of the MacLachlan group for their encouragement and supports for the past two years. I have had a lot of good times with them, both inside and outside the lab. Thanks to the people in the Chemistry Department who have helped me in my research, especially Dr. Yun Ling and the staff of the UBC Microanalytical Services Laboratory for help in obtaining the mass spectra. Lastly, I would like to thank my family and friends who have supported me both emotionally and physically during my graduate studies.

Chapter 1: Introduction

1.1 Liquid Crystals

Before the end of the nineteenth century, it was believed that there are only three states of matter: solid, liquid, and gas. However, this belief was shattered in 1888 when Friedrich Reinitzer, an Austrian botanist and chemist, discovered the first liquid crystal, cholesteryl benzoate (**1**) (Fig. 1-1). The name "liquid crystal" was used by Otto Lehmann to describe this new state of matter which possesses physical properties that are between those of solid and liquid phases. Liquid crystalline phases are also known as mesophases or mesomorphic phases (from the Greek *mesos*, meaning middle or intermediate).

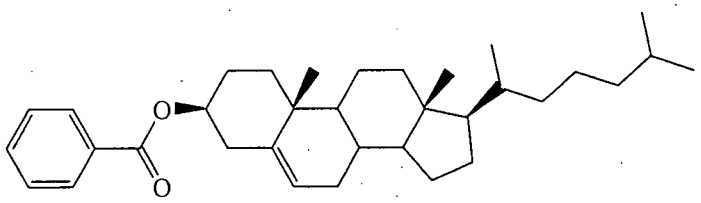

1

Figure 1-1: Chemical structure of cholesteryl benzoate

In crystalline solids, each molecule is located at a specific position and is oriented with respect to other molecules. Therefore, the solid phase has both positional and orientational order. In the liquid phase, all molecules are moving randomly, having neither positional nor orientational order. As a substance changes from the solid phase to the liquid crystalline phase, its positional ordering may be lost, but it retains a certain

degree of orientational order.[1] Although the molecules are free to move as a fluid, they are on average oriented in one direction, which is denoted by the director (ñ) (Fig. 1-2). Each molecule is oriented at a certain angle (θ) with respect to the director. The higher the orientational order, the closer the average of the angles is to zero. The magnitude of the orientational order can be quantified by the order parameter of the liquid crystal (S),[1,2] the average of the function $(3\cos^2\theta - 1)/2$. The typical values of the order parameter are between 0.3 and 0.9 for liquid crystals, decreasing as the temperature increases.

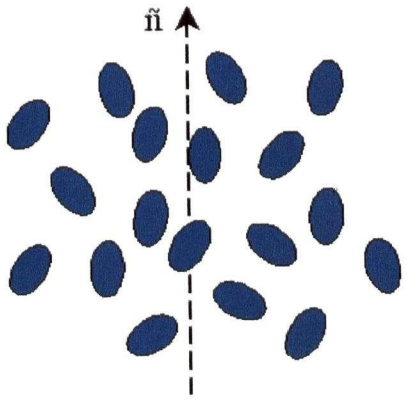

Figure 1-2: Director of liquid crystal

According to the rule of Daniel Vorländer, molecules that exhibit liquid crystalline properties must have a shape that is as linear as possible, although there are several exceptional cases.[2] Liquid crystals can be classified into two types - lyotropic and thermotropic. They differ in that the former one is concentration dependent, while the latter one is temperature dependent. Lyotropic liquid crystals exist only in mixtures consisting of amphiphilic species and certain solvents, an example being the mixture of soap and water.[2] Thermotropic liquid crystals exist within certain temperature ranges,

depending on the molecular structures. Thermotropic mesophases can be divided into three categories according to the shape of the mesogen: calamitic, discotic and sanidic liquid crystals are formed by molecules with rod-like, disc-like, and board-like shapes, respectively. Examples of these are given in Fig. 1-3.

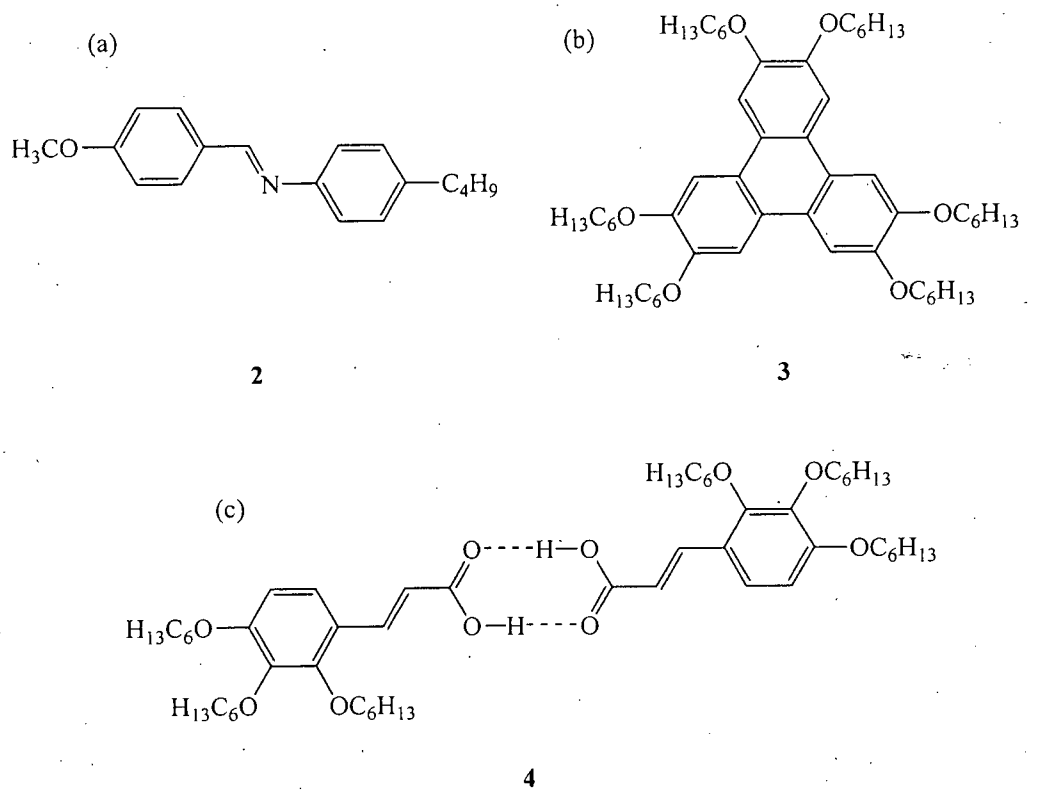

2 **3**

4

Figure 1-3: Examples of (a) calamitic (4-methoxybenzlidene-4-n'-butylaniline, **2**), (b) discotic (hexahexyloxytriphenylene, **3**), and (c) sanidic liquid crystals (2,3,4-trishexyloxycinnamic acid, **4**)

The calamitic liquid crystals can be classified into three types: nematic, chiral nematic and smectic. Nematic (from the Greek *νημα*, meaning thread) liquid crystals are rod-like molecules that only possess orientational order. This type of mesogen has a director that is parallel to the molecular axis of the molecules (Fig. 1-4). When the

nematic mesogens are placed under the polarizing optical microscope (POM) equipped with a heating stage, they exhibit a texture as shown in Fig. 1-5. Chiral nematic liquid crystals, also known as cholesteric liquid crystals, are similar to the nematic liquid crystals except that the director is in a twisted structure (Fig. 1-6). The director takes a certain distance to complete one full turn and that distance is called the pitch of the liquid crystal. At one-half of the pitch, the twisted structure of the director repeats itself. The

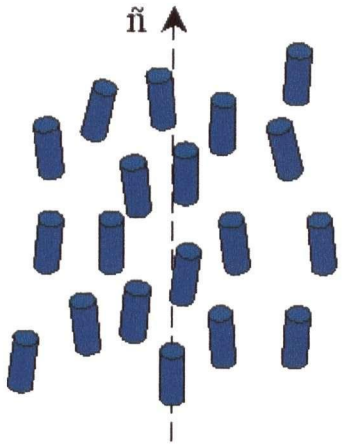

Figure 1-4: Schematic representation of a nematic liquid crystal

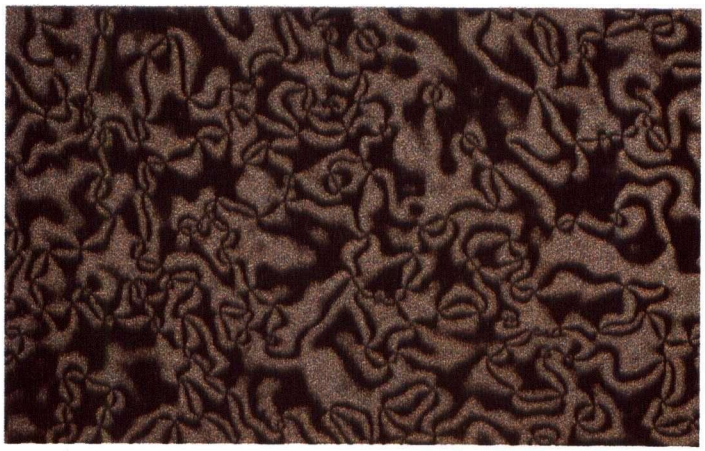

Figure 1-5: Texture of a nematic liquid crystal[1]

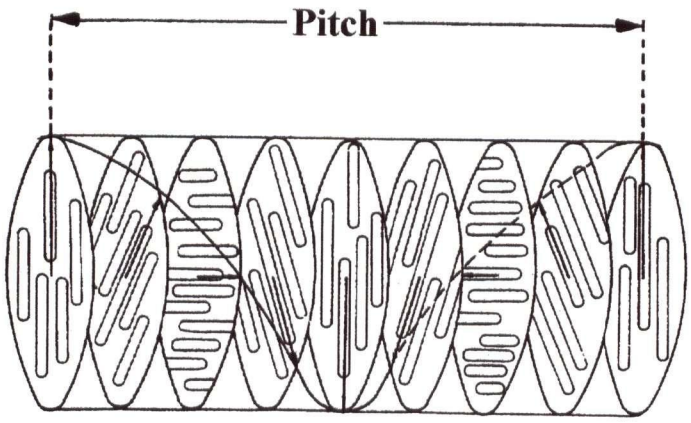

Figure 1-6: Schematic representation of a chiral nematic liquid crystal[2]

chiral nematic liquid crystal has its own texture under the POM as shown in Fig. 1-7. Mesogens can possess either the nematic phase or the chiral nematic phase, but never both.

Figure 1-7: Texture of a chiral nematic liquid crystal[1]

Smectic (from the Greek $\sigma\mu\eta\gamma\mu\alpha$ = soap) liquid crystals possess both positional and orientational order (Fig. 1-8). Moreover, the molecules tend to arrange themselves in layers. There are different kinds of smectic mesophase, such as smectic A, smectic B, and smectic C, depending on the arrangement of the layers. Each smectic phase exhibits a different texture under the POM. An example of the smectic mesophase is shown in Fig. 1-9.

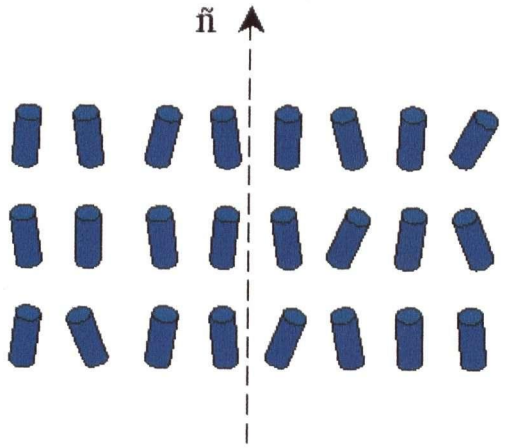

Figure 1-8: Schematic representation of a smectic A liquid crystal

Figure 1-9: Texture of a smectic A liquid crystal[3]

The sanidic liquid crystals are a new type of mesogen that was discovered in 1986. These mesogens were found to occur in board-like molecules and they arrange themselves into stacks parallel to one another (Fig. 1-10).[4] However, the structural packing of the sanidic liquid crystal is still not fully resolved due to the lack of unambiguous experimental proof.

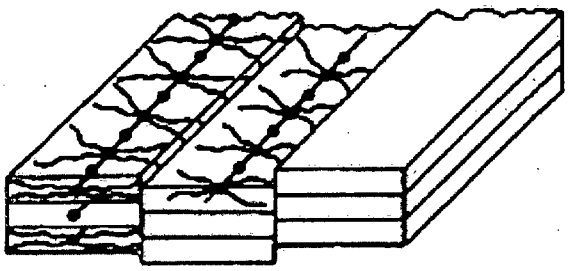

Figure 1-10: Schematic representation of a sanidic liquid crystal[4]

Since their discovery, numerous studies on liquid crystals have been performed by chemists and physicists throughout the world. In the mid-1950s, researchers focused on the potential applications of liquid crystals. During that period, the electro- and magneto-optic characteristics of calamitic liquid crystals were discovered. As a result, the development of electronic display devices using liquid crystals emerged and has since grown rapidly. Today, many electronic devices, such as digital watches, computer monitors, and calculators, use liquid crystal technologies in their display component. Moreover, liquid crystals have been used as temperature sensors since some of them are very sensitive to small changes in temperature.

1.2 Discotic Liquid Crystals

Discotic liquid crystals were discovered in 1977 by Chandrasekhar while investigating different derivatives of hexaalkanoyloxybenzene (**5**) (Fig. 1-11).[5] By the end of the twentieth century, over 1500 discotic liquid crystals had been synthesized.[6,7] In general, the cores of discotic liquid crystals are flat and rigid, allowing them to easily stack. There are usually six or eight long, flexible chain substituents attached to the core.[6-8] The flexibility of the long chains lowers the transition temperature from the solid phase to the liquid crystalline phase[2] and maintains a certain distance between the molecules as they flow.[1]

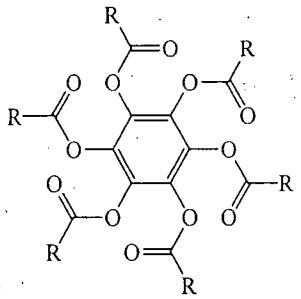

$R = {}^{n}C_mH_{2m+1}$; m = 4 to 9

5

Figure 1-11: Chemical structure of the first discotic liquid crystal

Discotic liquid crystals can be classified into three categories: nematic discotic, columnar and lamellar. In nematic discotic liquid crystals (Fig. 1-12), disc-like molecules move randomly in space with no positional order. However, they orient along

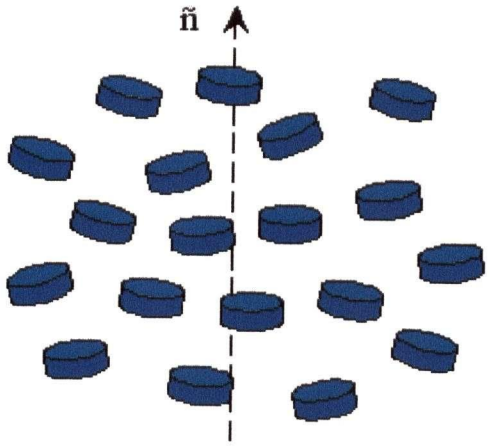

Figure 1-12: Schematic representation of a nematic discotic liquid crystal

the director, in the direction perpendicular to the plane of the core. Under the POM, nematic discotic mesogens display a texture as shown in Fig. 1-13.

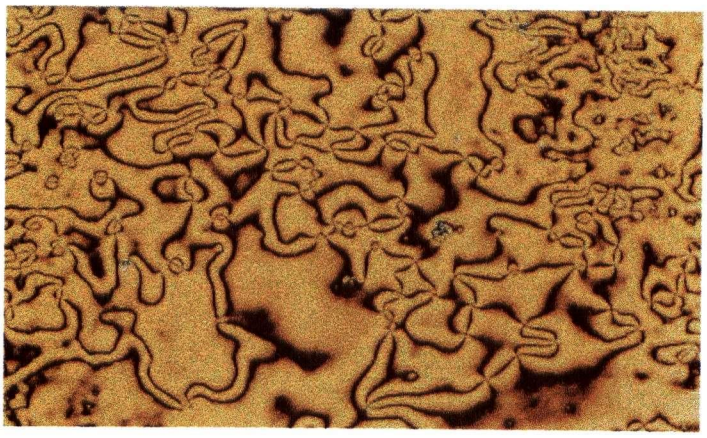

Figure 1-13: Texture of a nematic discotic liquid crystal[10]

The columnar liquid crystalline phase is the most common mesophase for discotic liquid crystals.[2,9] In this phase, the molecules stack on top of each other forming upright

or tilted columns (Fig. 1-14). Moreover, they can organize into hexagonal or rectangular two-dimensional lattices. Within each column, the distance between molecules is neither uniform nor fixed. Therefore, columnar liquid crystals possess positional order in only two-dimensions. Columnar liquid crystals exhibit a fan-like texture under the POM (Fig. 1-15). There are examples of columnar mesophases possessing a conical or pyramidal

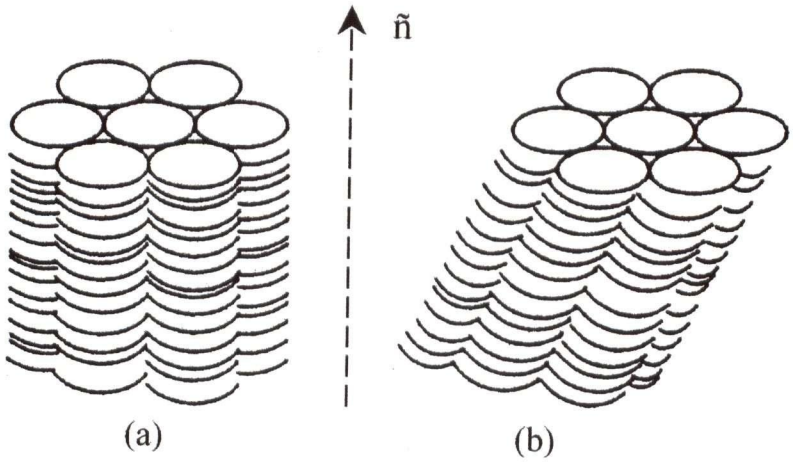

Figure 1-14: Schematic representation of a columnar liquid crystal: a) upright columns and b) tilted columns[6]

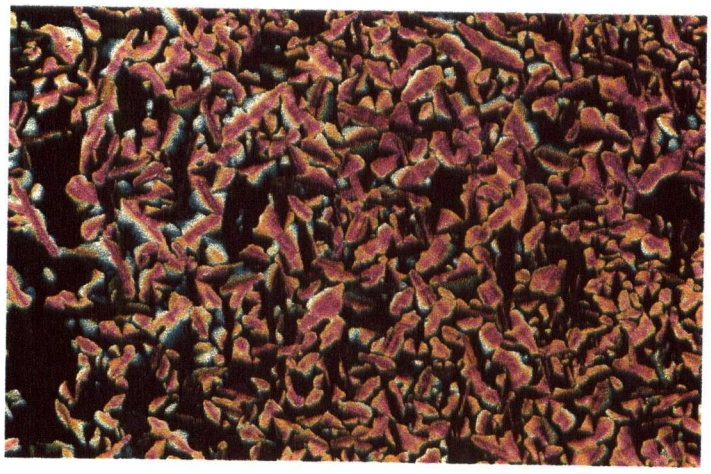

Figure 1-15: Texture of a columnar liquid crystal[11]

core, and others with no core (Fig. 1-16). Most columnar liquid crystals contain heteroatoms, and it is speculated that the presence of heteroatoms induces the formation of this particular type of mesophase.[12]

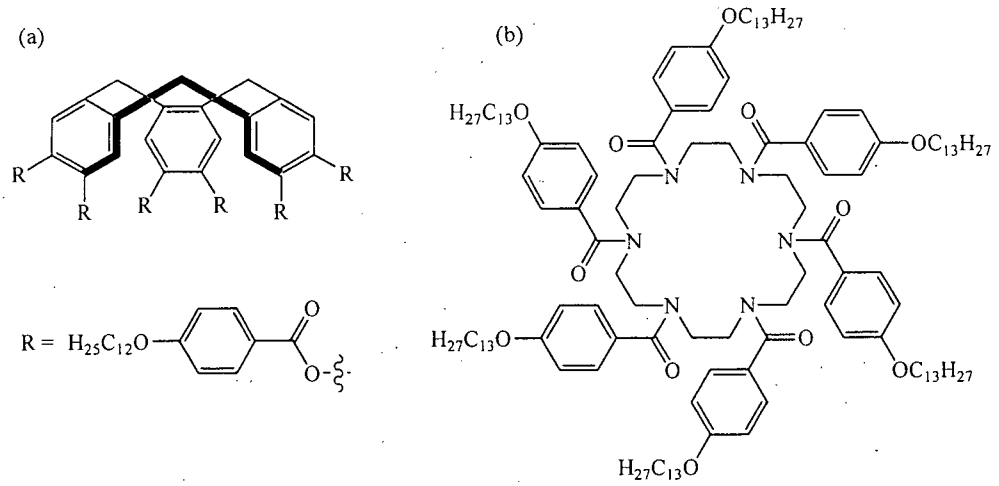

6 **7**

Figure 1-16: (a) Examples of columnar mesogens with conical or pyramidal cores (**6**) and (b) Columnar mesogens without a core (**7**)

The lamellar liquid crystalline phase is very similar to the columnar mesophase, except that each molecule is tilted at an angle with respect to the column axis (Fig. 1-17).

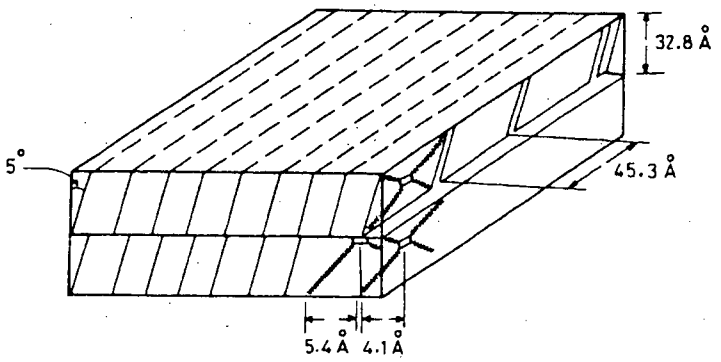

Figure 1-17: Schematic representation of a lamellar liquid crystal[6]

An example of a lamellar liquid crystal is the first metal-containing discotic liquid crystal (**8**), first synthesized by Giroud-Godquin and Billard (Fig. 1-18).[7] Although it is certain that these molecules are tilted within the column, the disposition of the molecules in each layer is still not completely known.[6,7]

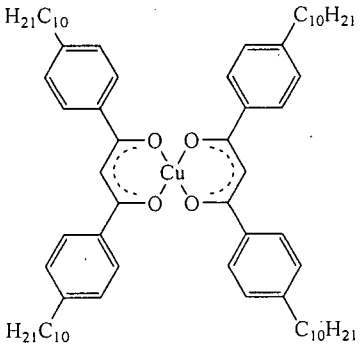

8

Figure 1-18: Chemical structure of the first metal-containing discotic liquid crystal (bis(*p*-n-decylbenzoyl)methanato copper (II), **8**)

Discotic liquid crystals can be formed in polymers of two types: (i) Polymers with the disc-shaped repeat units on the main chain of the polymer backbone (Fig. 1-19a); and (ii) polymers with disc-shaped side groups (Fig. 1-19b). The disc-shaped components of the discotic polymer liquid crystals will stack into columns, which results in the formation of columnar liquid crystalline phases.

Since the discovery of the first metal-containing discotic liquid crystal in 1981, numerous metal-containing discotic liquid crystals have been synthesized and they exhibit either columnar or lamellar liquid crystalline phases. Metal-containing discotic liquid crystals are of interest because of their unusual electrical and magnetic

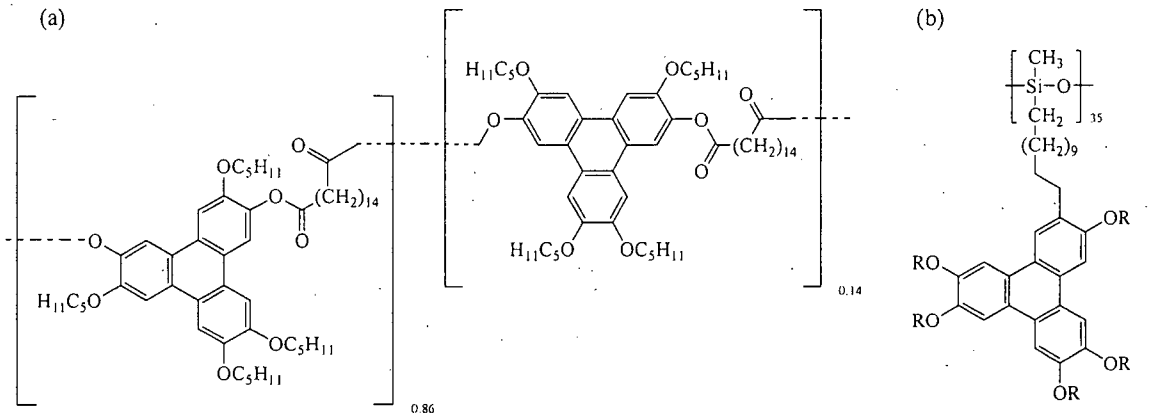

9 10

Figure 1-19: Discotic polymer liquid crystals with disc-shaped units (a) on the main chain and (b) on the side groups

properties.[7,13] These mesogens usually have different liquid crystalline properties than their organic counterparts due to the rich electron density of the metal atoms, and it is anticipated that metal-containing liquid crystals will have superior optical, electrical and magnetic properties than their organic analogues.[13,14]

The cores of most columnar liquid crystals are considered to be electron-rich. Within a column, the aromatic cores are separated by *ca* 3.5 Å.[11,15] Therefore, the π-orbital of one core can overlap with that of the neighboring one, providing good conductivity along the column. However, the energy gap for the propagation of electrons perpendicular to the columns is large, making the liquid crystals good insulators.[16,17] When the columnar mesogens are doped with electron acceptors, such as 2,4,7-trinitro-9-fluorenone and its derivatives,[9] they became p-type semiconductors. The electrons can then travel along the cores of the columns, which are protected by the insulating side chain, making them one-dimensional conducting wires.[6,9,16] The conductivity data for metal-containing columnar liquid crystals shows that they are semiconductors.[7] In

addition, columnar mesophases display photoconductivity and can be used as a 1-dimensional charge transfer material.

1.3 Tubular Liquid Crystals

Generally, discotic mesogens are flat, rigid, disc-shaped molecules with long, flexible chain substituents. In addition, numerous macrocyclic molecules exhibit columnar liquid crystallinity (e.g., **11-14**, Fig. 1-20).[8,18] Metal-containing macrocycles have also been shown to exhibit columnar mesomorphism (e.g., Barber's metallacrown, **15**) (Fig. 1-21).[19]

Macrocycles form columnar mesophases by stacking on top of one another and arrange themselves into tubular mesophases containing hollow columns.[20-25] If the backbone of the macrocycle is not rigid, such as in azacrowns, the central cavity of the column may be partially collapsed.[20,24] The empty channel within each column of the resulting structure provides sites for potential applications, such as trapping metal ions and other molecules within the empty channels. It is desirable that the ions or molecules trapped within the tubes do not inhibit the liquid crystalline order, but can travel through the hollow tubes.[26] This type of columnar mesogen is expected to find applications in the development of ion-conducting channels,[27] and to be useful as hosts for chemical reactions and for selective trapping of molecules.

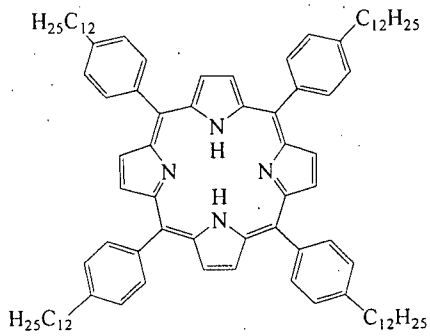

11

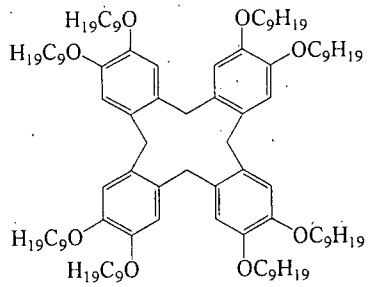

12

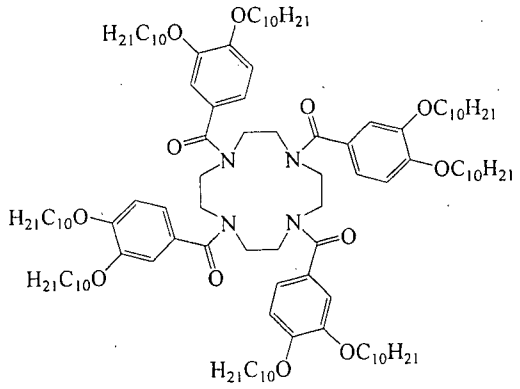

13

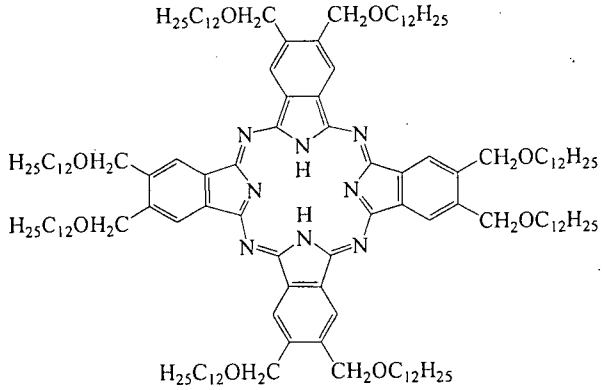

14

Figure 1-20: Examples of macrocyclic columnar mesogens

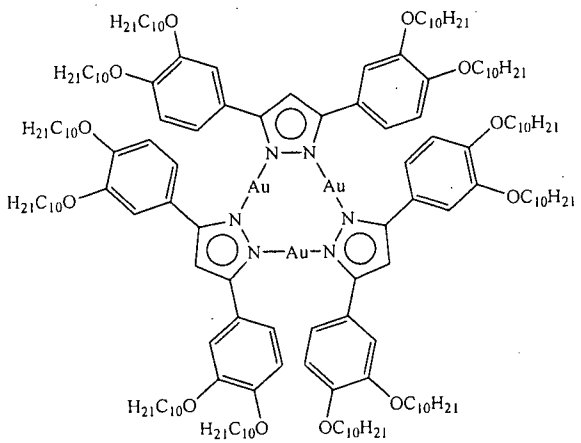

15

Figure 1-21: Example of metal-containing macrocyclic columnar mesogen

1.4 Schiff-Base Liquid Crystals

Schiff-base chemistry offers a convenient route to assemble new mesogens. Schiff-base compounds have found applications in numerous fields, such as dye and liquid crystal technology. Among liquid crystals, the first stable room temperature mesogen, 4-methoxybenzylidene-4'-n-butylaniline (MBBA, **16**), is a Schiff-base compound (Fig. 1-22).[1,2] Liquid crystalline Schiff-base molecules with HO···CH=NR groups have also been applied in coordination chemistry to form metal-containing Schiff-base complexes (Fig. 1-23).

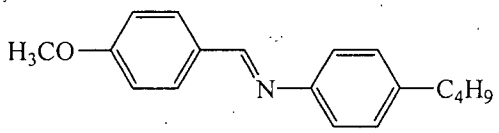

16

Figure 1-22: Chemical structure of 4-methoxybenzylidene-4'-n-butylaniline

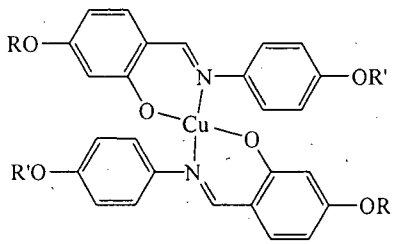

17

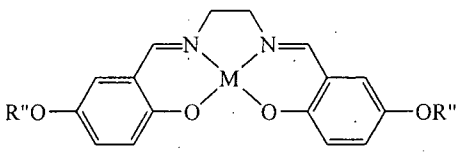

18

Figure 1-23: Examples of transition-metal-containing Schiff-base liquid crystals

The transition-metal-containing Schiff-base mesogens have different shapes and properties than those of their organic counterparts.[28] In particular, when paramagnetic

metal atoms such as oxovanadium(IV) and copper(II) coordinate to the Schiff-base liquid crystals, their orientation can be switched by a weak external magnetic field.[29] Furthermore, these transition-metal containing liquid crystals have the tendency to display intermolecular dative interactions, leading to the formation of liquid crystalline linear polymer chains.[28] Most of the Schiff-base metallomesogens that have been synthesized exhibit a nematic or smectic mesophase.[13] However, columnar liquid crystalline phases have been obtained for some Schiff-base metal-containing mesogens.[29,30]

Salen (2,2'-*N*,*N*'-bis(salicylidene)ethylenediamine) compounds are a class of Schiff-base molecules that are widely used as ligands to coordinate transition metal atoms within their N_2O_2 pockets. Besides being useful as catalysts, these complexes can form the rigid centre of new metallomesogens. It was found that in order for mesomorphism to occur for the organic salen compounds, alkoxy substituents must be on the salicylidene benzene ring and *para* to the imine bond. For the metal-containing Schiff-base complexes, the chain substituents are also on the salicylidene moieties, but are *para* to the hydroxyl groups.[31] The length and the position of the substituents play an important role in controlling the melting temperature and symmetry of the mesogens. On the other hand, if the substituents of the metallomesogens are unsymmetrical, the melting temperature can be lowered because the polarizability and molecular symmetry have been changed.[32] By altering the chain length and the functional group of the substituents, the rigidity of the Schiff-base ligand, and the metal atom chelated to the pocket, the stability and the type of the mesophase can be modified.

1.5 Schiff-Base Macrocycles

A macrocycle is a molecular ring, which can be rigid or flexible (Fig. 1-24). Numerous types of macrocycles have been synthesized and studied for many years. In order to promote solubility of the macrocycles, substituents like alkyl or alkoxy side chains are usually attached to the periphery. Macrocycles can be synthesized through a step-wise pathway, by templating methodology, or by self-assembly.[33-38] By changing one or more of the moieties of the macrocycle, such as adding the fluorophore 1,3,4-oxadiazole within the ring,[39] the properties of the macrocycles can be modified. These substances are of interest because they can be applied in the fields of biology and materials science.[40] For instance, porphyrins are present in biological systems as hemoglobin and myoglobin. Moreover, some macrocycles (e.g., crown ethers) can trap molecules and metal ions within their cavities. Other macrocycles can aggregate into nanotubes through π-stacking interaction[23] or by coordinating transition metal atoms to the macrocycles and link them together through bridging ligands.[41]

One type of macrocycle that has attracted enormous scientific interest is the Schiff-base macrocycle. It is formed by the condensation of a formyl group and an amine to give an imine. Schiff-base macrocyclic chemistry has been applied to the study of expanded porphyrins, generating larger π-conjugated core systems. Sessler and co-workers synthesized the first Schiff-base type expanded porphyrins in 1998 (Fig 1-25).[42] Expanded porphyrins are of interest because their pore size is larger and thus can coordinate rare-earth metals and can act as anion binding agents.[30] Schiff-base chemistry can be applied in the modification of the core of those expanded porphyrins previously synthesized.

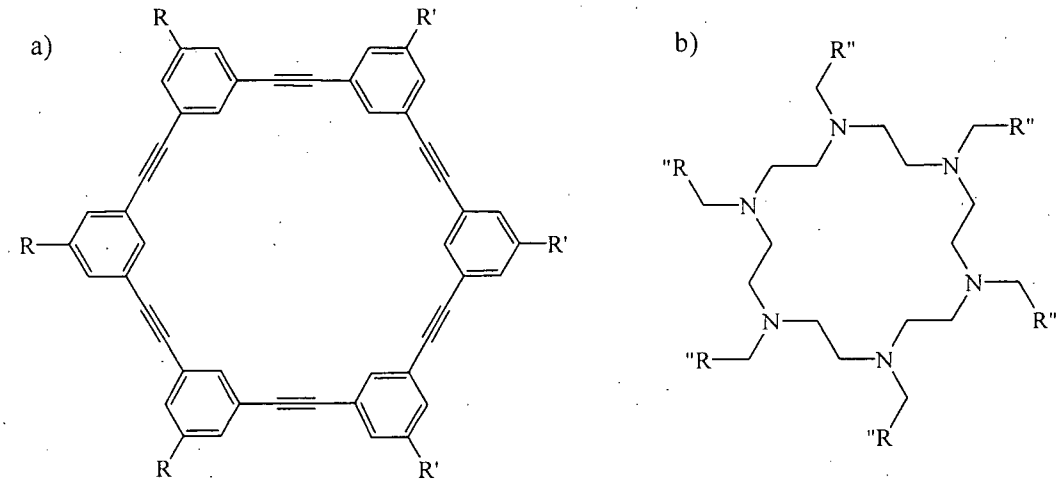

19 20

Figure 1-24: Examples of macrocycles with a) rigid core and b) flexible core

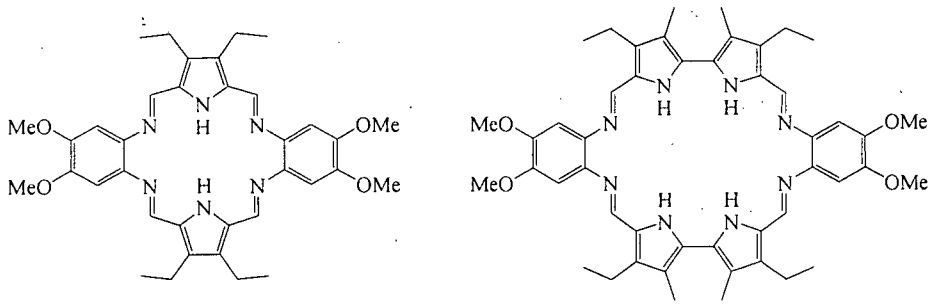

21 22

Figure 1-25: Chemical structures of expanded porphyrins

Among all types of Schiff-base macrocycles, Robson-type macrocycles and its derivatives (Fig. 1-26a) are very popular and have been studied for over 30 years. They are [2+2] Schiff-base macrocycles formed from condensation of two diamines with two dialdehydes and are capable of coordinating two transition metal atoms within their cavity. Robson-type macrocycles are of interest because the two metal atoms within the

cavity are in close proximity to each other, which can induce metal-metal interactions and magnetic exchange, and binuclear metal reactivity.[33,43] Two expanded versions of Robson-type macrocycle have been reported by McKee and co-workers (Fig. 1-26b).[44-46] One of the macrocycles has four identical binding sites that can coordinate transition metal atoms. The resultant metal complex can be dinuclear or tetranuclear, and can be two pairs of different metal atoms for the tetranuclear case. The other expanded Robson-type macrocycle has three different binding sites, which can bind up to four metal atoms. Since the expanded Robson-type macrocycle can coordinate more transition metal atoms in close proximity, they are expected to exhibit different metal-metal interactions and magnetochemistry, and to find applications in other areas such as catalysis.

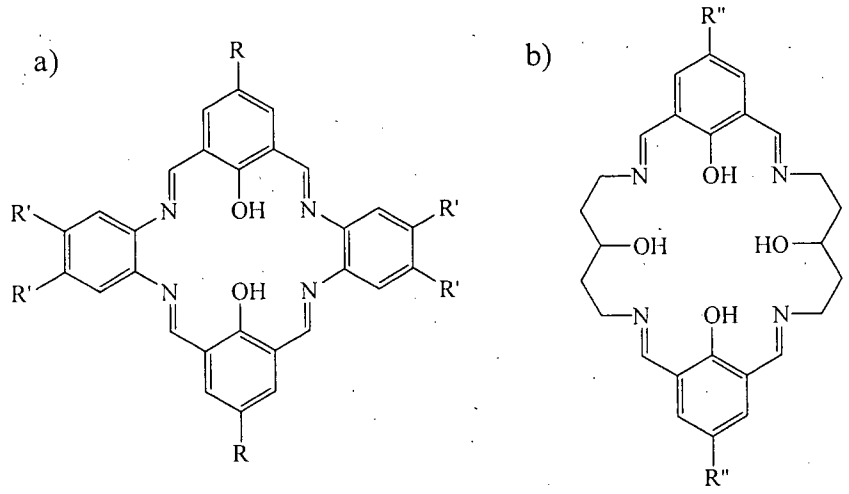

23 **24**

Figure 1-26: a) Robson-type (**23**) and b) McKee-type (**24**) macrocycles

Akine and co-workers synthesized a [3+3] Schiff-base macrocycle without any substituents attached (Fig. 1-27),[47] but the resultant macrocycle was not soluble in most

solvents. The macrocycle has three N_2O_2 binding sites that are analogous to three salphens, which are good ligands to bind to transition metal atoms.

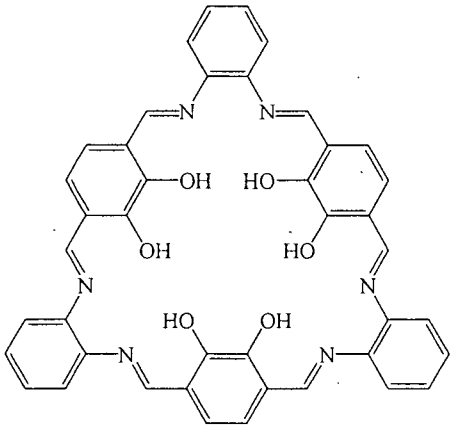

25

Figure 1-27: [3+3] Schiff-base macrocycle

1.6 Thesis Objective

The goal of this project was to develop the first porous metallomesogens, molecules that could be used to form chemical sensors. This thesis will highlight the synthesis and characterization of [3+3] Schiff-base macrocycles with different alkoxy chain substituents attached to their periphery (**26**) (Fig. 1-28a). The [3+3] Schiff-base macrocycles with long alkoxy chains have the potential to exhibit discotic liquid crystallinity since they have the same symmetry as hexaalkoxytriphenylene derivatives, which are discotic mesogens.[48] Since the core of the macrocycle has an empty cavity, it is possible that the resulting discotic mesophase would be a tubular mesophase[20] if the

macrocycles stack on top of one another. Metal complexes of the macrocycle with decyloxy substituents (**27**) will also be discussed (Fig. 1-28b). The metal-containing macrocycles also have the potential to exhibit liquid crystallinity.[13] In addition, attempts to synthesize the [6+6] Schiff-base macrocycle (**28**) (Fig. 1-28c) will be discussed in Chapter 4.

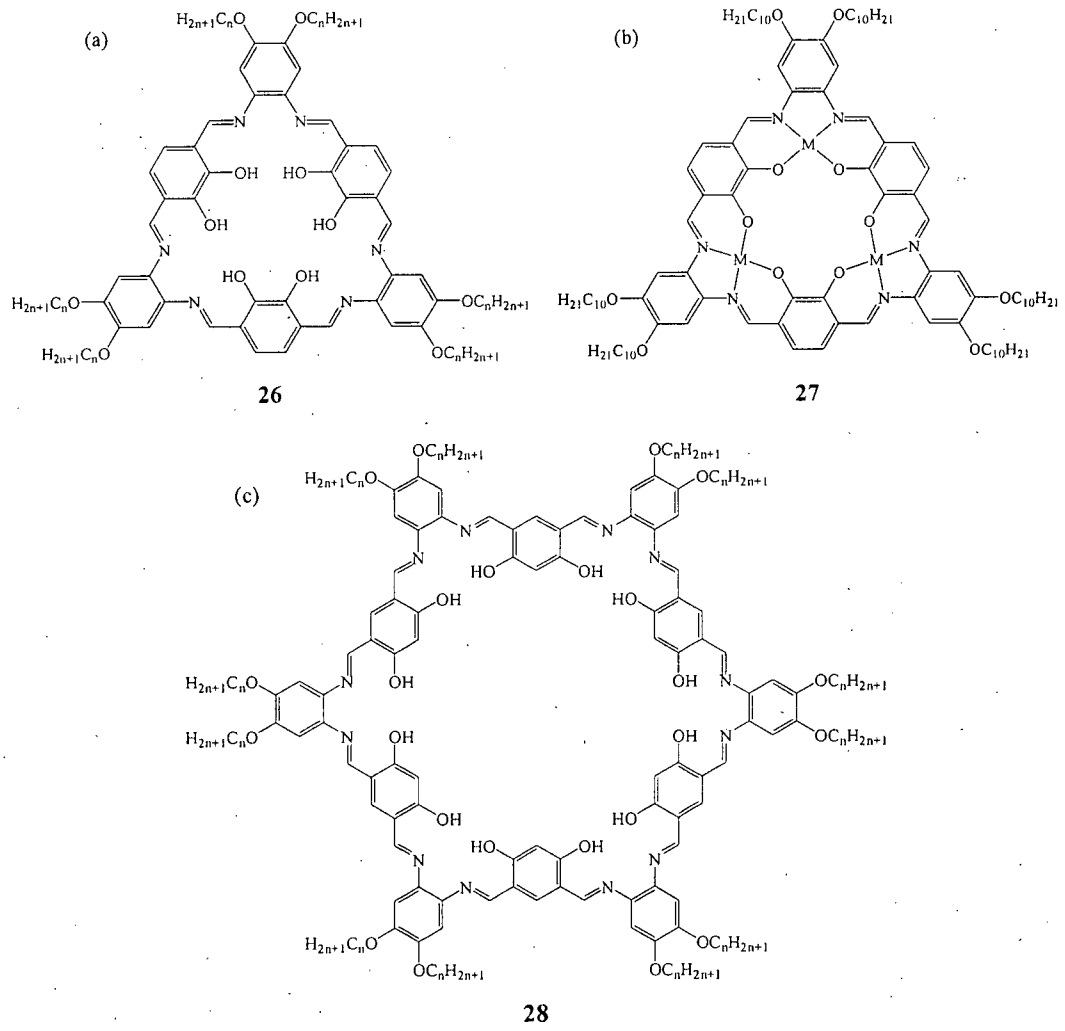

26 **27**

28

Figure 1-28: Chemical structures of the target (a) [3+3] Schiff-base macrocycle (**26**), (b) [3+3] metal-containing Schiff-base macrocycle (**27**), and (c) [6+6] Schiff-base macrocycle (**28**)

1.7 References

(1) Collings, P. J. In *Liquid Crystals: Nature's Delicate Phase of Matter*; Princeton University Press: New Jersey, 2002; pp 1-27.

(2) Stegemeyer, H. In *Liquid Crystals*; Steinkopff: Darmstadt; Springer: New York, 1994; pp 1-50.

(3) Nguyen, H. L.; Horton, P. N.; Hursthouse, M. B.; Legon, A. C.; Bruce, D. W. *J. Am. Chem. Soc.* **2004**, *126*, 16.

(4) Barón, M. *Pure Appl. Chem.* **2001**, *76*, 845.

(5) Chandrasekhar, S.; Sadashiva, B. K.; Suresh, K. A. *Pramana* **1977**, *9*, 471.

(6) Chandrasekhar, S. In *Handbook of Liquid Crystals*; Demus, D., Goodby, J. W., Gray, G. W., Spiess, H. W., Vill, V., Eds.; Wiley VCH: New York, 1998; Vol. 2B, pp 749-780.

(7) Chandrasekhar, S. *Liq. Cryst.* **1993,** *14*, 3.

(8) Cammidge, A. N.; Bushby, R. J. In *Handbook of Liquid Crystals*; Demus, D., Goodby, J. W., Gray, G. W., Spiess, H. W., Vill, V., Eds.; Wiley VCH: New York, 1998; Vol. 2B, pp 693-748.

(9) Kouwer, P. H. J.; Jager, W. F.; Mijs, W. J.; Picken, S. J. *Macromolecules* **2002**, *35*, 4322.

(10) Kumar, S.; Varshney, S.K. *Org. Lett.* **2002**, *4*, 157.

(11) Levitsky, I. A.; Kishikawa, K.; Eichhorn, S. H.; Swager, T. M. *J. Am. Chem. Soc.* **2000**, *122*, 2474.

(12) Christoph, P. H.; Kayser, W.; Müllen, K.; Spiess, H. W. *Adv. Mater.* **1996**, *8*, 510.

(13) Giroud-Godquin, A. M. In *Handbook of Liquid Crystals*; Demus, D., Goodby, J. W., Gray, G. W., Spiess, H. W., Vill, V., Eds.; Wiley VCH: New York, 1998; Vol. 2B, pp 901-932.

(14) Chung, K. L; Wu, H. C.; Sung, J. H.; Yang, C. D. *Liq. Cryst.* **2001**, *28*, 411.

(15) Donovan, K. J.; Kreouzis, T.; Boden, N.; Clements, J. *J. Chem. Phys.* **1998**, *109*, 10400.

(16) Boden, N.; Movaghar, B. In *Handbook of Liquid Crystals*; Demus, D., Goodby, J. W., Gray, G. W., Spiess, H. W., Vill, V., Eds.; Wiley VCH: New York, 1998; Vol. 2B, pp 781-798.

(17) Balagurusamy, V. S. K.; Prasad, S. K.; Chandrasekhar, S.; Kumar, S.; Manickam, M.; Yelamaggad, C. V. *Pramana* **1999**, *53*, 3.

(18) Hegmann, T.; Neumann, B.; Kain, J.; Diele, S.; Tschierske, C. *J. Mater. Chem.* **2000**, *10*, 2244.

(19) Date, R. W.; Iglesias, E. F.; Rowe, K. E.; Elliott, J. M.; Bruce, D. W. *J. Chem. Soc., Dalton Trans.* **2003**, 1914.

(20) Lehn, J.-M.; Malthête, J.; Levelut, A.-M. *J. Chem. Soc., Chem. Commun.* **1985**, 1794.

(21) Malthête, J.; Levelut, A.-M.; Lehn, J.-M. *J. Chem. Soc., Chem. Commun.* **1992**, 1434.

(22) Zhao, M.; Ford, W. T.; Idziak, S. H. J.; Maliszewskyj, N. C.; Heiney, P. A. *Liq. Cryst.* **1994**, *16*, 583.

(23) Zhang, J.; Moore, J. S. *J. Am. Chem. Soc.* **1992**, *114*, 9701.

(24) Zhang, J.; Moore, J. S. *J. Am. Chem. Soc.* **1994**, *116*, 2655.

(25) Zhao, D.; Moore, J. S. *J. Chem. Soc., Chem. Commun.* **2003**, 807.

(26) Mindyuk, O. Y.; Stetzer, R.; Heiney, P. A.; Nelson, J. C.; Moore, J. S. *Adv. Mater.* **1998**, *10*, 1363.

(27) Demus, D. In *Handbook of Liquid Crystals*; Demus, D., Goodby, J. W., Gray, G. W., Spiess, H. W., Vill, V., Eds.; Wiley VCH: New York, 1998; Vol. 2B, pp 133-187.

(28) Serrette, A.; Carroll, P. J.; Swager, T. M. *J. Am. Chem. Soc.* **1992**, *114*, 1887.

(29) Binnemans, K.; Lodewyckx, K.; Donnio, B.; Guillon, D. *Chem. Eur. J.* **2002**, *8*, 1101.

(30) Sessler, J. L.; Callaway, W.; Dudek, S. P.; Date, R. W.; Lynch, V.; Bruce, D. W. *Chem. Commun.* **2003**, 2422.

(31) Berdagué, P.; Courtieu, J.; Maitlis, P. M. *J. Chem. Soc., Chem. Commun.* **1994**, 1313.

(32) Paschke, R.; Balkow, D.; Sinn, E. *Inorg. Chem.* **2002**, *41*, 1949.

(33) Atkins, A. J.; Black, D.; Blaske, A. J.; Marin-Becerra, A.; Parson, S.; Rui-Ramirez, L.; Schröder, M. *Chem. Commun.* **1996**, 457.

(34) Tian, Y.; Tong, J.; Frenzen, G.; Sun, J.-Y. *J. Org. Chem.* **1999**, *64*, 1442.

(35) Cox, B. G.; Schneider, H. In *Coordination and Transport Properties of Macrocyclic Compounds in Solution*; Elsevier: New York, 1992; pp 335-400.

(36) Curtis, N. F. *J. Chem.Soc.* **1960**, 4409.

(37) Curtis, N. F. *Coord. Chem. Rev.* **1968**, *3*, 3.

(38) Blight, M. M.; Curtis, N. F. *J. Chem. Soc.* **1962**, *1204*, 3016.

(39) Wang, S.; Li, Z.; Hua, W. *Synth. Commun.* **2002**, *32*, 3339.

(40) James, S.; Kumar, D. S.; Alexander, V. *J. Chem. Soc., Dalton Trans.* **1999**, 1773.

(41) Wojaczyński, J.; Latos-Grażyński, L. *Coord. Chem. Rev.* **2000**, *204*, 113.

(42) Meyer, S.; Andrioletti, B.; Sessler, J. L.; Lynch, V. *J. Org. Chem.* **1998**, *63*, 6752.

(43) Pilkington, N. H.; Robson, R. *Aust. J. Chem.* **1970**, *23*, 2225.

(44) Tandon, S. S.; Thompson, L. K.; Bridson, J. N.; McKee, V.; Downard, A. J. *Inorg. Chem.* **1992**, *31*, 4635.

(45) Kruger, P. E.; McKee, V. *Chem. Commun.* **1997**, 1341.

(46) McCrea, J.; McKee, V.; Metcalfe, T.; Tandon, S. S.; Wikaira, J. *Inorg. Chim. Acta* **2000**, *297*, 220.

(47) Akine, S.; Taniguchi, T.; Nabeshima, T. *Tetrahedron Lett.* **2001**, *42*, 8861.

(48) Destrade, C.; Mondon, M. C.; Malthete, J. *Journal de Physique* **1979**, *40*, C3.

Chapter 2: [3+3] Schiff-Base Macrocycles

2.1 Background

Schiff-base condensation between a formyl group and an amino group to form an imine moiety has been widely used for many years. As this reaction is straightforward and reversible, supramolecular chemists have employed this chemistry to construct macrocycles, such as expanded porphyrins,[1-3] Robson-type macrocycles,[4,5] and McKee-type macrocycles.[6-8] Some of the macrocyclic Schiff-base compounds can form metal complexes because they have one or more binding sites within their core. The macrocycles have various different shapes, depending on the structure of the dialdehyde and diamine starting materials used in the cyclocondensation. Triangular macrocycles can be obtained by [3+3] cyclocondensation of suitable dialdehyde and diamine building units (Fig. 2-1).[9-11] Akine and co-workers reported the synthesis of a [3+3] triangular Schiff-base macrocycle[12] that has the identical core ring as the target macrocycle (Fig. 2-2). The resultant compound was insoluble in nearly all solvents because of the lack of peripheral chain substituents. Side chain substituents, such as alkyl, alkoxy and alkanoyl chains, are expected to enhance their solubility in common solvents. If the chain substituents are long enough, it is possible that the [3+3] macrocycles will exhibit discotic liquid crystallinity since the core ring is rigid and flat, and the symmetry is the same as triphenylene derivatives, which have previously been reported to possess discotic mesomorphism. The macrocyclic [3+3] Schiff-base compound may exhibit a columnar

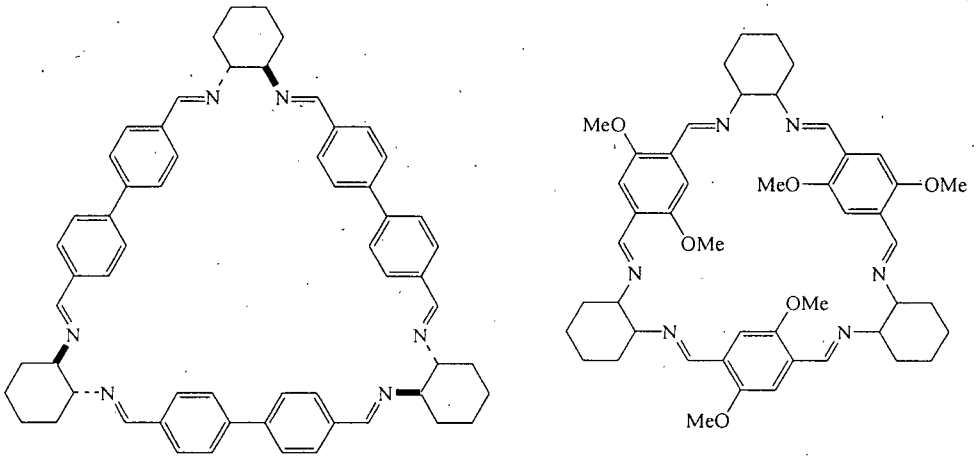

29 **30**

Figure 2-1: Examples of triangular [3+3] Schiff-base macrocycles

mesophase. Since there is an empty cavity within the macrocycle, a hollow channel will be obtained. Columnar liquid crystal phases with a channel, tubular mesophases,[13-18] can potentially be applied in guest-host chemistry, and ion and charge transfer.

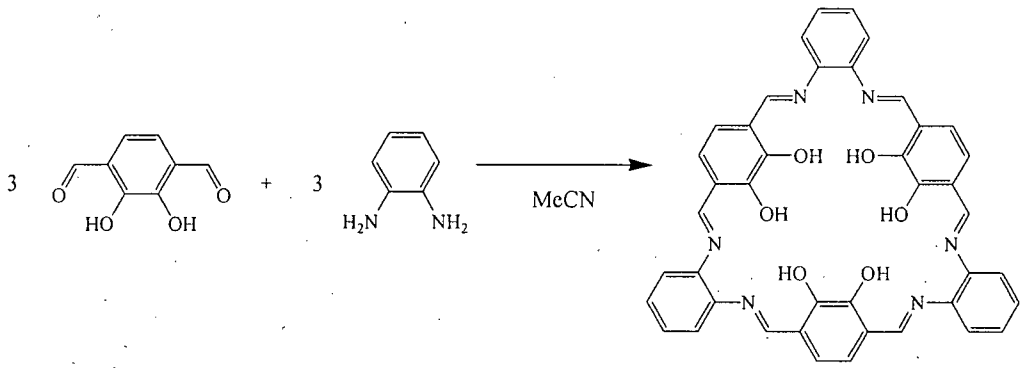

31 **32** **25**

Figure 2-2: [3+3] Schiff-base macrocycle

2.2 Experimental

Materials: Deuterated solvents were obtained from Cambridge Isotope Laboratories, Inc.. Diethylether and dichloromethane were dried by passage over alumina columns. Dimethylformamide, ethanol, toluene, chloroform, and acetonitrile were purged with nitrogen gas before use. 3,6-Diformyl-1,2-dihydroxybenzene (**31**) and 4,5-diamino-1,2-dialkoxybenzene (**33-36**) were prepared by literature methods.[12,19]

Equipment: All reactions were carried out under nitrogen unless otherwise noted. The 300MHz ^{1}H and 75.5 MHz ^{13}C NMR spectra were recorded on a Bruker AV-300 spectrometer. The IR spectra were obtained from dispersions in potassium bromide using a Bomens MB-series spectrometer. The UV-Vis spectra were obtained in dichloromethane on a Varian Cary 5000 UV-Vis/near-IR spectrometer using a 1 cm cuvette. The electrospray (ESI) mass spectra were obtained at the UBC Microanalytical Services Laboratory on a Micromass LCT time-of-flight (TOF) mass spectrometer equipped with an electrospray ion source. The sample was analyzed in methanol:dichloromethane at 1 μM. The differential scanning calorimetry (DSC) thermograms were obtained on a Perkin Elmer Diamond DSC. An Olympus BX41 polarizing optical microscopy (POM) equipped with a heating stage was used to look for the liquid crystalline texture. Melting points were obtained on a Fisher-John's melting point apparatus and are corrected.

Synthesis of Compound 37. 3,6-Diformyl-1,2-dihydroxybenzene (**31**) (0.100 g, 0.602 mmol) and 4,5-diamino-1,2-didecyloxybenzene (**33**) (0.229 g, 0.545 mmol) were added

to a 100 mL Schlenk flask under nitrogen. Toluene (20 mL) and acetonitrile (20 mL) were sequentially added via syringe into the flask, giving a deep red solution. The solution was stirred under reflux at 90 °C for 24 h. After cooling the solution to room temperature, a deep red precipitate formed. The red solid isolated by filtration was crystallized from chloroform and acetonitrile to yield compound **37** (0.196 g, 59%).

Data for Compound 37. ^{1}H NMR (300 MHz, chloroform-d_1) δ 13.31 (s, 6H, O*H*), 8.50 (s, 6H, C*H*=N), 7.04 (s, 6H, aromatic C*H*), 6.64 (s, 6H, aromatic C*H*), 3.94 (broad, 12H, OCH_2), 1.81 (broad, 12H, CH_2), 1.46 (broad, 12H, CH_2), 1.27 (broad, 74H, CH_2), 0.87 (broad, 18H, CH_3) ppm; ^{13}C NMR (75.5 MHz, chloroform-d_1) δ 162.6 (*C*H=N), 152.0, 150.4, 136.3, 122.7, 122.1, 105.5 (aromatic *C*H), 71.0 (O*C*H$_2$), 33.4, 31.3, 31.1, 31.0, 30.8, 27.5, 24.1 (*C*H$_2$), 15.5 (*C*H$_3$) ppm; UV-Vis (dichloromethane): λ_{max} (ε) = 307 nm (4.59×10^4 cm^{-1}M^{-1}), 344 nm (5.50×10^4 cm^{-1}M^{-1}), 403 nm (8.61×10^4 cm^{-1}M^{-1}); ESI-MS: m/*z* = 1653.2 ((M+H)$^+$, 100%); HR-ESI-MS (M+H)$^+$: 1652.1390 (calculated), 1652.1393 (found); IR (KBr): υ = 3513 (w), 2953 (sh), 2924 (vs), 2853 (s), 1609 (s), 1517 (m), 1496 (m), 1468 (m), 1424 (w), 1378 (m), 1302 (m), 1260 (s), 1218 (m), 1193 (s), 1116 (m), 1007 (m), 922 (w), 842 (m), 794 (w), 720 (s) cm^{-1}; Mp = 182-185 °C.

Synthesis of Compound 38. Compound **38** was prepared by a procedure analogous to that for compound **37**. Yield: 0.124 g (34%).

Data for Compound 38. ^{1}H NMR (300 MHz, chloroform-d_1) δ 13.42 (s, 6H, O*H*), 8.50 (s, 6H, C*H*=N), 7.07 (s, 6H, aromatic C*H*), 6.64 (s, 6H, aromatic C*H*), 3.96 (broad, 12H, OCH_2), 1.84 (broad, 12H, CH_2), 1.49 (broad, 12H, CH_2), 1.29 (broad, 98H, CH_2), 0.90

(broad, 18H, CH_3) ppm; ^{13}C NMR (75.5 MHz, chloroform-d_1) δ 160.6 (*C*H=N), 150.6, 149.0, 134.9, 121.1, 120.7, 103.7 (aromatic *C*H), 69.5 (O*C*H_2), 31.9, 29.7, 29.5, 29.4, 26.1, 22.7 (*C*H_2), 14.1 (*C*H_3) ppm; UV-Vis (dichloromethane): λ_{max} (ε) = 306 nm (5.50×10^4 $cm^{-1}M^{-1}$), 343 nm (6.56×10^4 $cm^{-1}M^{-1}$), 403 nm (1.06×10^5 $cm^{-1}M^{-1}$); ESI-MS: m/*z* = 1821.5 ($(M+H)^+$, 100%); HR-ESI-MS $(M+H)^+$: 1820.3268 (calculated), 1820.3303 (found); IR (KBr): υ = 3458 (w), 2923 (vs), 2853 (s), 1610 (s), 1515 (m), 1494 (m), 1468 (m), 1426 (w), 1415 (w), 1379 (m), 1301 (m), 1262 (s), 1218 (w), 1193 (m), 1117 (m), 1008 (m) , 965 (w), 932 (w), 842 (m), 710 (s) cm^{-1}; Mp = 160-162 °C.

Synthesis of Compound 39. Compound **39** was prepared by a procedure analogous to that for compound **37**. Yield: 0.144 g (36%).

Data for Compound 39. ^{1}H NMR (300 MHz, chloroform-d_1) δ 13.29 (s, 6H, O*H*), 8.50 (s, 6H, C*H*=N), 7.00 (s, 6H, aromatic C*H*), 6.67 (s, 6H, aromatic C*H*), 3.97 (broad, 12H, OCH_2), 1.82 (broad, 12H, CH_2), 1.47 (broad, 12H, CH_2), 1.25 (broad, 122H, CH_2), 0.86 (broad, 18H, CH_3) ppm; ^{13}C NMR (75.5 MHz, chloroform-d_1) δ 160.8 (*C*H=N), 150.6, 149.0, 134.8, 121.2, 120.6, 103.7 (aromatic *C*H), 69.5 (O*C*H_2), 31.9, 29.8, 29.6, 29.4, 26.1, 22.7 (*C*H_2), 14.1 (*C*H_3) ppm; UV-Vis (dichloromethane): λ_{max} (ε) = 303 nm (4.51×10^4 $cm^{-1}M^{-1}$), 349 nm (6.16×10^4 $cm^{-1}M^{-1}$), 398 nm (9.64×10^4 $cm^{-1}M^{-1}$); ESI-MS: m/*z* = 1989.2 ($(M+H)^+$, 100%); HR-ESI-MS $(M+H)^+$: 1989.5180 (calculated), 1989.5137 (found); IR (KBr): υ = 3513 (w), 2953 (sh), 2922 (s), 2870 (sh), 2852 (s), 1609 (vs), 1517 (m), 1497 (m), 1468 (m), 1420 (w), 1414 (w), 1378 (m), 1303 (m), 1259 (s), 1218 (m), 1192 (m), 1117 (s), 1007 (m), 924 (w), 843 (s), 822 (m), 800 (m), 720 (s) cm^{-1}; Mp = 150-153 °C.

Synthesis of Compound 40. 3,6-Diformyl-1,2-dihydroxybenzene (**31**) (0.100 g, 0.602 mol) and 4,5-diamino-1,2-dihexadecyloxybenzene (**36**) (0.355 g, 0.602 mol) were added to a 100 mL Schlenk flask under nitrogen. Chloroform (45 mL) and acetonitrile (15 mL) were sequentially added via syringe into the flask, giving a deep red solution. The solution was stirred under reflux at 90 °C for 24 h. After cooling the solution to room temperature, the solvent was removed by rotary evaporation and a red solid was obtained. The red solid was recrystallized from chloroform and ethanol to yield compound **40** (0.076 g, 18%).

Data for Compound 40. ^{1}H NMR (300 MHz, chloroform-d_1) δ 13.34 (s, 6H, O*H*), 8.49 (s, 6H, C*H*=N), 7.00 (s, 6H, aromatic C*H*), 6.68 (s, 6H, aromatic C*H*), 3.99 (broad, 12H, OCH_2), 1.83 (broad, 12H, CH_2), 1.48 (broad, 12H, CH_2), 1.25 (broad, 144H, CH_2), 0.86 (t, 18H, CH_3) ppm; ^{13}C NMR (75.5 MHz, chloroform-d_1) δ 160.4 (*C*H=N), 150.1, 149.3, 135.0, 121.0, 120.6, 103.9 (aromatic *C*H), 69.8 (O*C*H$_2$), 31.9, 29.7, 29.6, 29.4, 26.1, 22.7 (*C*H$_2$), 14.1 (*C*H$_3$) ppm; UV-Vis (dichloromethane): λ_{max} (ε) = 306 nm (5.98x10^4 cm^{-1}M^{-1}), 344 nm (7.29x10^4 cm^{-1}M^{-1}), 403 nm (1.11x10^5 cm^{-1}M^{-1}); ESI-MS: m/*z* = 2158.0 ((M+H)$^+$, 100%); HR-ESI-MS (M+H)$^+$: 2157.7058 (calculated), 2157.6982 (found); IR (KBr): υ = 3504 (w), 2922 (vs), 2851 (s), 1609 (s), 1574 (w), 1516 (m), 1496 (m), 1468 (m), 1425 (w), 1378 (m), 1303 (m), 1260 (s), 1218 (m), 1193 (s), 1117 (m), 1005 (m), 965 (w), 933 (w), 843 (m), 791 (w), 720 (m) cm^{-1}; Mp = 126-128 °C.

Synthesis of Compound 41. 3,6-Diformyl-1,2-dihydroxybenzene (**31**) (0.050 g, 0.301 mol) and 4,5-diamino-1,2-didodecyloxybenzene (**34**) (0.322 g, 0.677 mol) were added to

a 100 mL Schlenk flask under nitrogen. Toluene (15 mL) and acetonitrile (25 mL) were sequentially added via syringe into the flask, giving a mixture of red solution and red precipitate. The mixture was stirred overnight at room temperature. The red precipitate was filtered and washed with acetonitrile to yield compound **37** (0.222 g, 98.6 %).

Data for Compound 41. ^{1}H NMR (300 MHz, chloroform-d_1) δ 13.47 (s, 2H, O*H*), 8.54 (s, 2H, C*H*=N), 6.97 (s, 2H, aromatic C*H*), 6.80 (s, 2H, aromatic C*H*), 6.34 (s, 2H, aromatic C*H*), 3.94 (m, 8H, OCH_2), 3.86 (broad, 4H, NH_2), 1.79 (m, 8H, CH_2), 1.43 (m, 8H, CH_2), 1.25 (broad, 64H, CH_2), 0.86 (m, 12H, CH_3) ppm; ^{13}C NMR (75.5 MHz, chloroform-d_1) δ 157.1 (*C*H=N), 151.3, 149.3, 142.4, 136.9, 126.0, 121.0, 120.9, 106.0, 102.1 (aromatic *C*H), 71.2, 69.1 (O*C*H_2), 31.9, 29.7, 29.5, 29.4, 26.1, 22.7 (*C*H_2), 14.1 (*C*H_3) ppm; UV-Vis (dichloromethane): λ_{max} (ε) = 306 nm (8.99x10^3 cm^{-1}M^{-1}), 336 nm (6.39x10^3 cm^{-1}M^{-1}), 473 nm (1.44x10^4 cm^{-1}M^{-1}); ESI-MS: m/*z* = 1083.9 ((M+H)$^+$, 510%); HR-ESI-MS (M+H)$^+$: 1083.8817 (calculated), 1083.8823 (found); IR (KBr): υ = 3378 (m), 3296 (w), 3169 (m), 2956 (s), 2919 (vs), 2849 (vs), 1611 (s), 1525 (s), 1502 (s), 1467 (s), 1432 (s), 1390 (m), 1378 (m), 1350 (w), 1325 (w), 1306 (m), 1260 (s), 1234 (s), 1206 (s), 1141 (s), 1118 (s), 1070 (m), 1043 (w), 1021 (w), 1001 (m), 955 (w), 921 (w), 889 (w), 837 (s), 808 (m), 772 (m), 720 (m) cm^{-1}; Mp = 118-119 ^{O}C.

2.3 Discussion

3,6-Diformyl-1,2-dihydroxybenzene (**31**) reacts with 4,5-diamino-1,2-dialkyloxy-

benzene (**33-36**) under nitrogen to form the [3+3] Schiff-base macrocycles (**37-40**) (Scheme 2-1). The reaction needs to be carried out under nitrogen because the diamine starting material is air sensitive. It is surprising that the reaction proceeds in moderate to good yield to give the macrocycle without yielding any polymer or oligomer. Although the equilibrium could be driven to the product side by the removal of water that is generated during the cyclocondensation by using the Dean-Stark apparatus or by adding drying agents, we have found this to be unnecessary. We believe that the macrocycle is a thermodynamically stable product and the reversibility of the imine condensation allows the intermediates to arrange themselves in order to form the desired product.

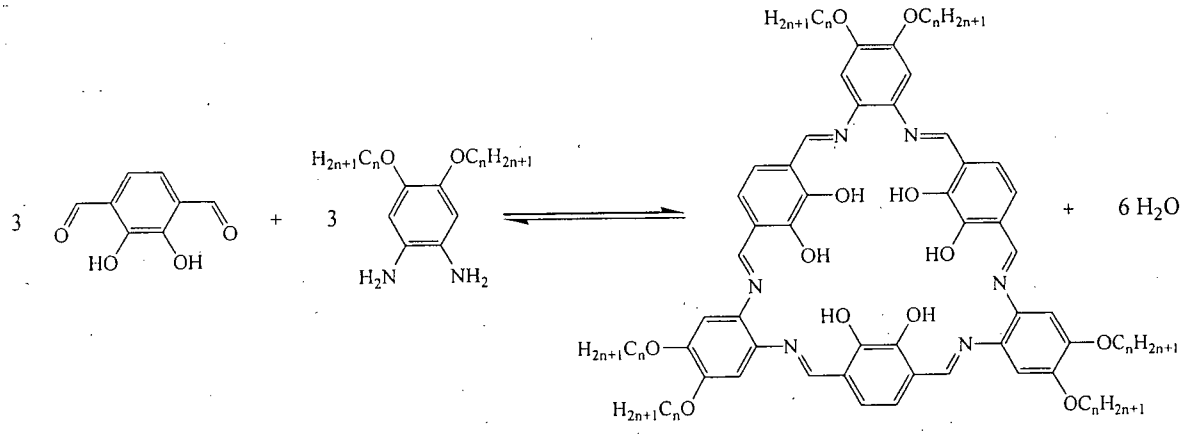

31 **33** n = 10, **34** n = 12, **35** n = 14, **36** n = 16 **37** n = 10, **38** n = 12, **39** n = 14, **40** n = 16

Scheme 2-1: Synthesis of [3+3] Schiff-base macrocycles

When the ratio of starting materials (**29** and **32**) was modified, compound **41** could be isolated. To prove that compound **41** is an intermediate in the macrocyclic reaction and to demonstrate the reversibility of the macrocyclic reaction, compound **41**

was reacted with an equimolar quantity of compound **31** (Scheme 2-2). Macrocycle **38** was obtained as the major product. In order for the macrocycle to form from compound **41**, the imine bonds must be broken at some point during the reaction. Presumably the reaction occurred with hydrolysis and the reconstruction of imine bonds until the thermodynamically stable macrocyclic product was obtained.

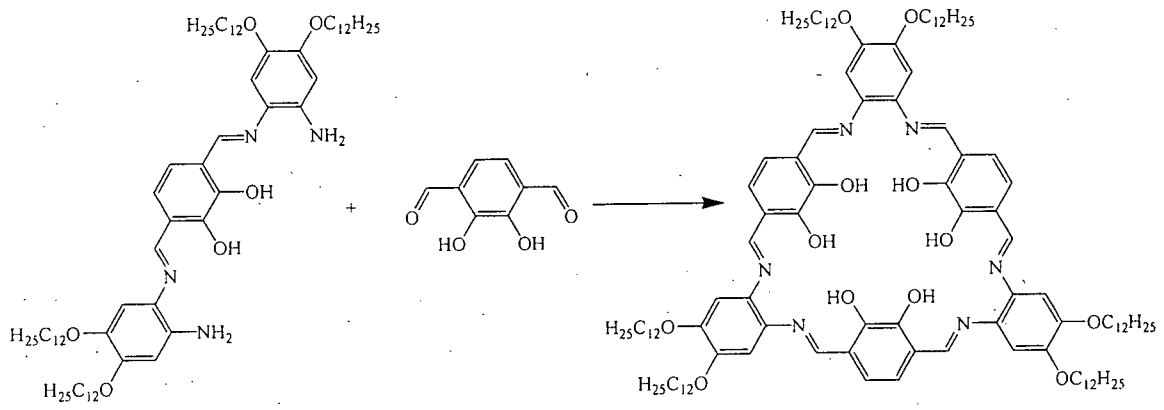

41 **31** **38**

Scheme 2-2: Synthesis of hexakisdodecyloxy [3+3] Schiff-base macrocycle (**38**) from compound **41** and 3,6-diformyl-1,2-dihydroxybenzene (**31**)

The macrocycles were characterized by ^{1}H and ^{13}C NMR spectroscopies. The ^{1}H NMR spectra of the Schiff-base macrocycles (Fig. 2-3) show only one environment for each of the hydroxyl and imine protons and two aromatic proton environments, consistent with overall 3-fold symmetry. The ^{13}C NMR spectra (Fig. 2-4) also confirm the structure. Heteronuclear Multiple Quantum Correlation (HMQC) and Heteronuclear Multiple Bond Correlation (HMBC) experiments (Fig. 2-5) of hexakishexyloxy [3+3] Schiff-base macrocycle allowed the aromatic protons in the NMR spectra to be assigned.

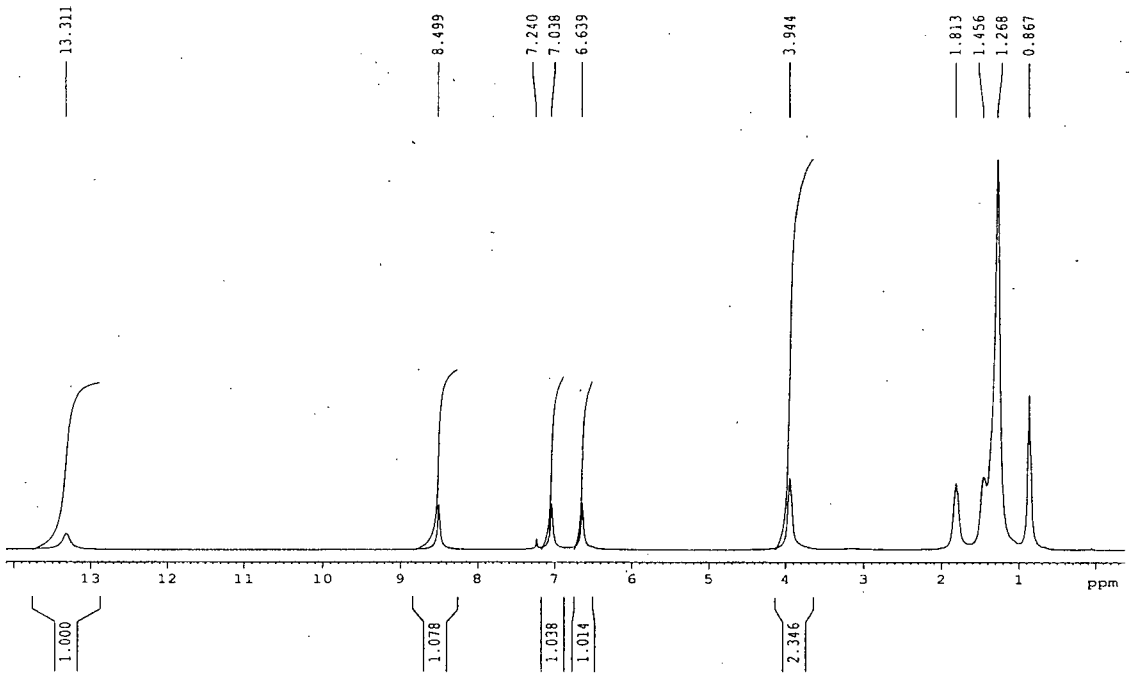

Figure 2-3: ^{1}H NMR spectrum of hexakisdecyloxy [3+3] Schiff-base macrocycle (**37**)

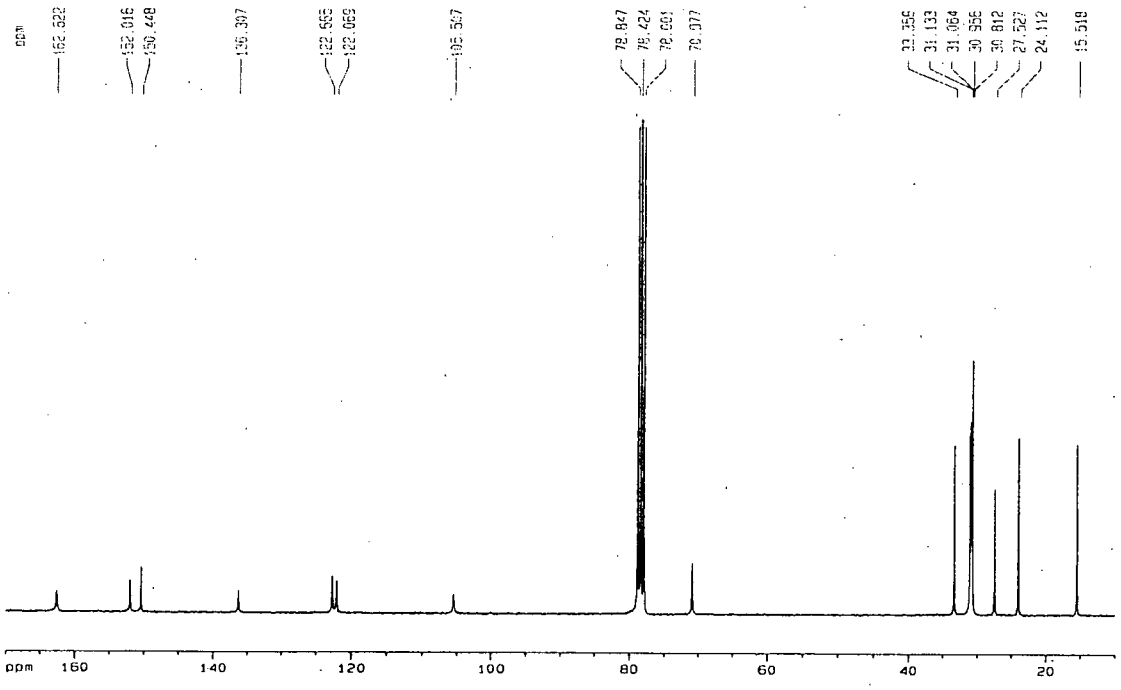

Figure 2-4: ^{13}C NMR spectrum of hexakisdecyloxy [3+3] Schiff-base macrocycle (**37**)

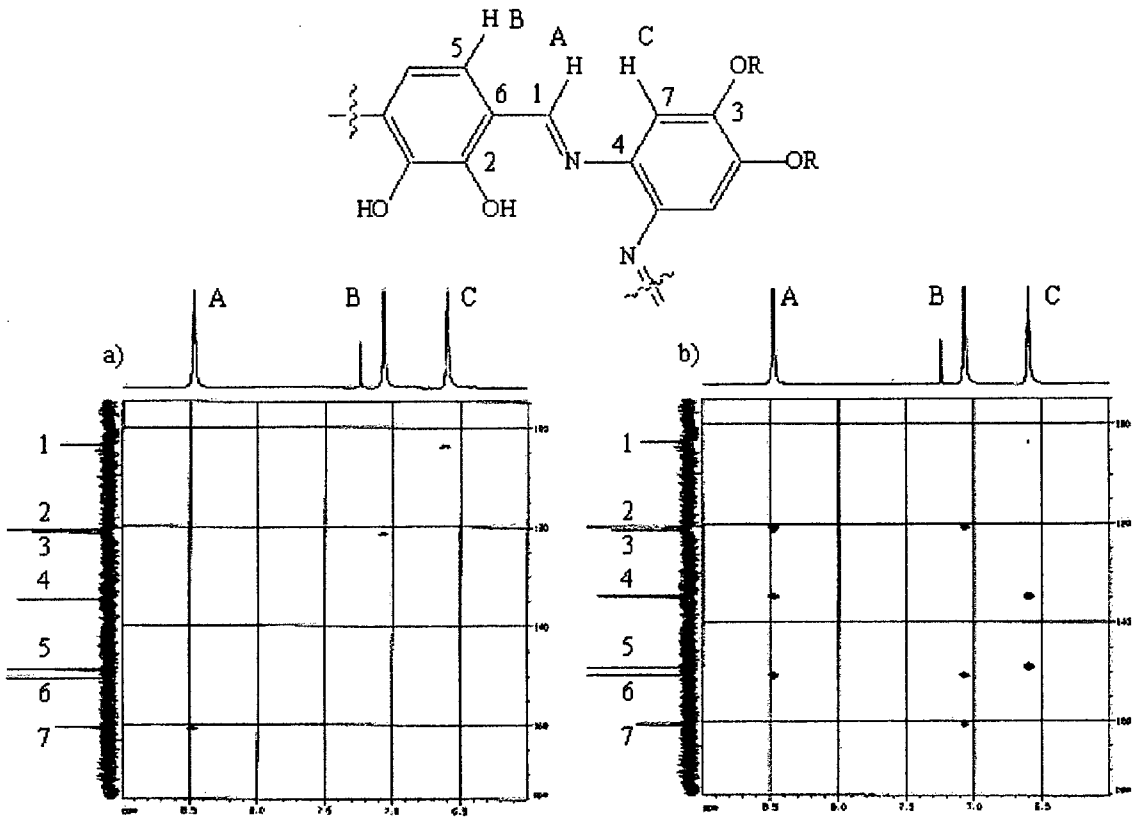

Figure 2-5: a) Heteronuclear Multiple Quantum Coherence (HMQC) and b) Heteronuclear Multiple Bond Correlation (HMBC) experiments on hexakishexyloxy [3+3] Schiff-base macrocycle

The IR spectra of the macrocycles were obtained (Fig. 2-6). Two strong IR bands at 2920 and 2850 cm^{-1} are the C-H stretching frequencies of the alkoxy substituents on the periphery. A single intense absorption band at 1609 cm^{-1} corresponds to the stretching frequency of the imine C=N bond. The absence of any C=O stretches at 1660-1715 cm^{-1} or N-H stretches at 3300-3500 cm^{-1} confirmed that starting materials or intermediate amines or aldehydes were not present in the product.

The UV-Vis spectra of macrocycles **37-40** (Fig. 2-7) all showed three peaks centred near 300, 340 and 400 nm (Table 2-1). The UV-Vis spectrum of compound **41** is

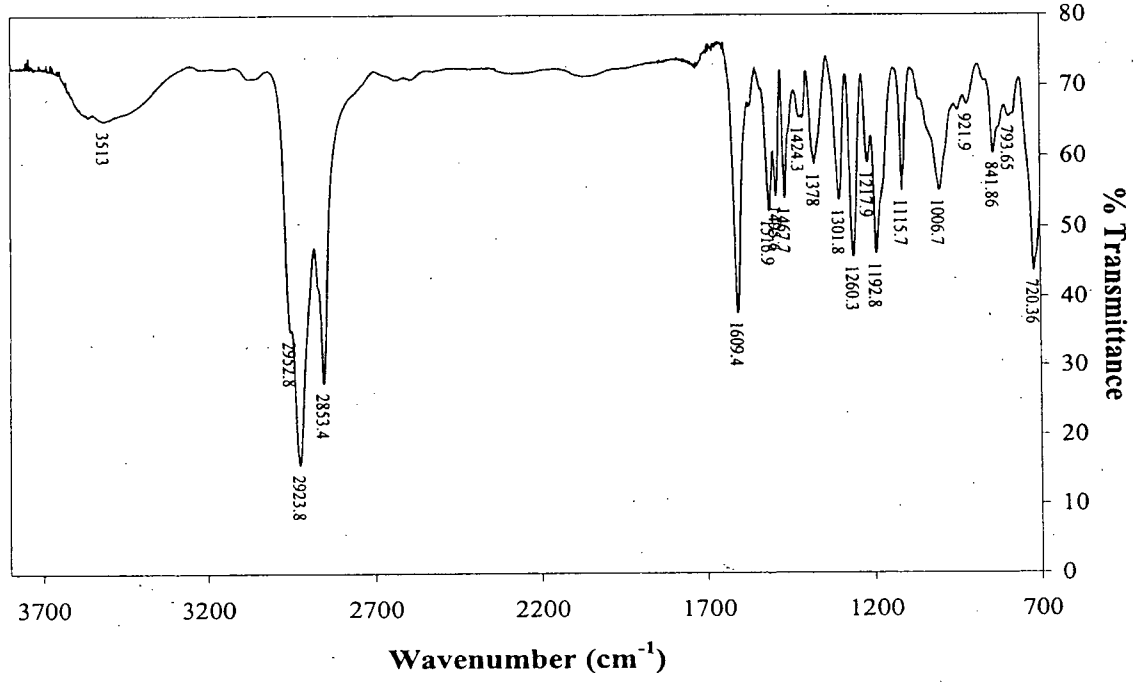

Figure 2-6: IR spectrum of hexakisdecyloxy [3+3] Schiff-base macrocycle (**37**)

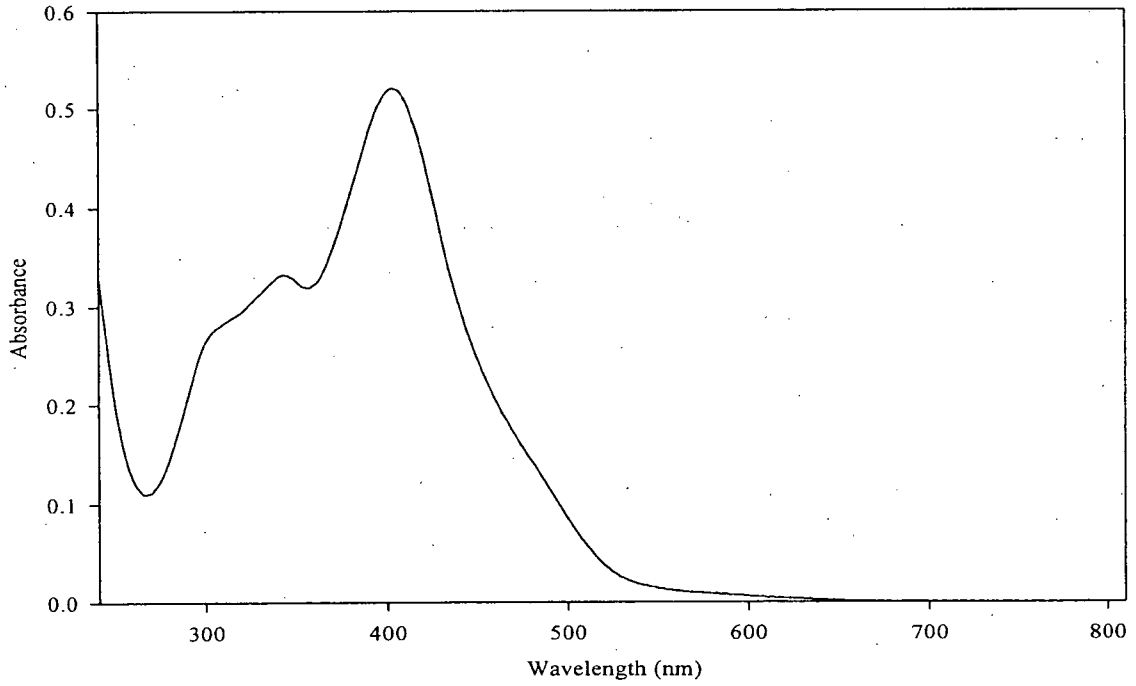

Figure 2-7: UV-Vis spectrum of hexakisdecyloxy [3+3] Schiff-base macrocycle (**37**)

Table 2-1: The values of λ_{max} and molar extinction coefficient (ε) of macrocycles **37-40**

Chain Length	Wavelength (nm)	ε ($cm^{-1}M^{-1}$)	Wavelength (nm)	ε ($cm^{-1}M^{-1}$)	Wavelength (nm)	ε ($cm^{-1}M^{-1}$)
10	307	$4.59x10^4$	344	$5.50x10^4$	403	$8.61x10^4$
12	306	$5.50x10^4$	343	$6.59x10^4$	403	$1.06x10^5$
14	303	$4.51x10^4$	349	$6.16x10^4$	398	$9.64x10^4$
16	306	$5.98x10^4$	344	$7.29x10^4$	403	$1.11x10^4$

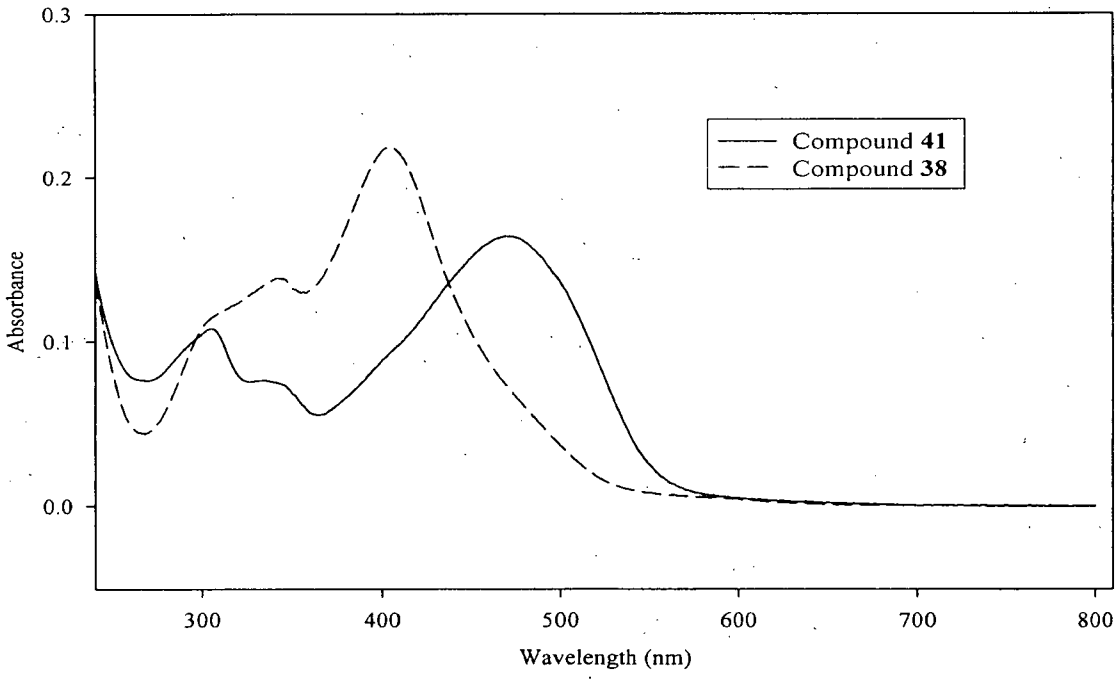

Figure 2-8: UV-Vis spectra of compound **41** and macrocycle **38**

similar to that of the other macrocycles (Fig. 2-8). It is interesting that the shorter molecule, compound **41**, absorbs at a longer wavelength than macrocycle **38**. PM3 calculations show that compound **41** is twisted at both ends of the molecule (Fig. 2-9), whereas the macrocycle is not planar and is twisted at the diformylcatechol moieties (Fig.

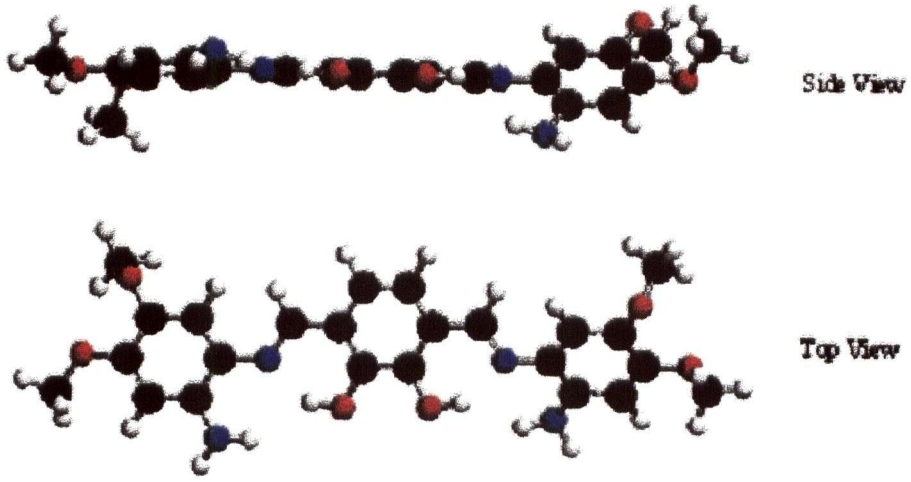

Figure 2-9: PM3 calculation of compound **41** (methoxy substituents are used for clarity)

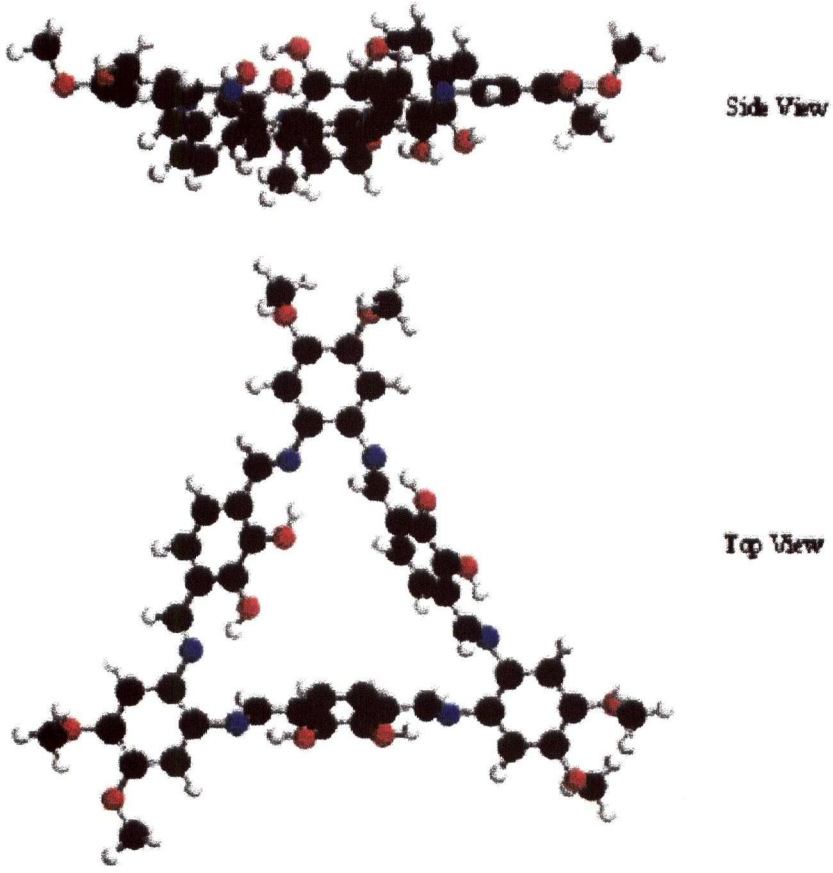

Figure 2-10: PM3 calculation of [3+3] Schiff-base macrocycle (methoxy substituents are used for clarity)

2-10). The twist in the macrocycle causes the imine bonds to be out-of-plane from the core ring and that weakens the conjugation. However, the imine bonds in compound **41** are still co-planar. Therefore, compound **41** has a longer conjugation length than the macrocycle, leading to a lower π-π^* separation.

All target [3+3] Schiff-base macrocycles were characterized by electrospray mass spectrometry (ESI-MS). The correct molecular weight (M+1) was observed for each target macrocycle (Fig. 2-11). In some occasion, a molecular weight of 23 a.m.u. heavier than the target macrocycle was also observed, corresponding to the coordination of a sodium ion to the macrocycle. The affinity of sodium ions for the [3+3] Schiff-base macrocycle has been previously reported.[20]

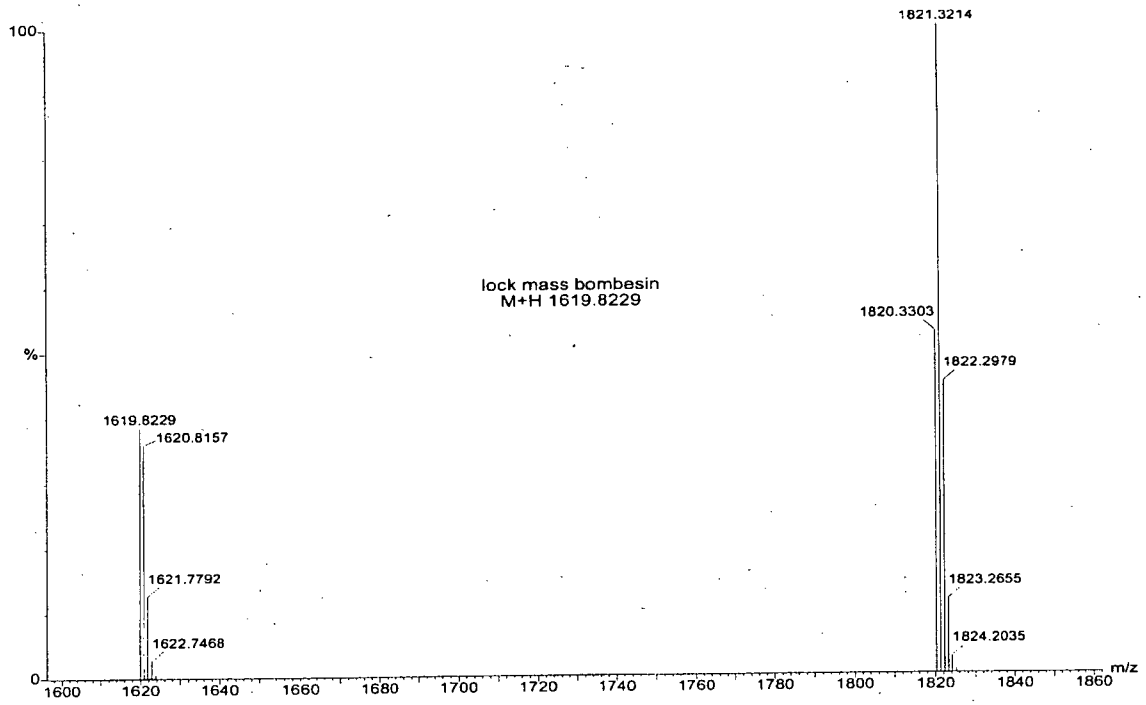

Figure 2-11: ESI mass spectrum of hexakisdodecyloxy [3+3] Schiff-base macrocycle (**38**)

To explore the possible liquid crystallinity of [3+3] Schiff-base macrocycles, macrocycles **37-40** were investigated by differential scanning calorimetry (DSC) and polarizing optical microscopy (POM). Macrocycle **38** showed an endothermic peak at 162 °C (rate = 30 °C/min) and exothermic decomposition at *ca* 233 °C (Fig. 2-12). A ^{1}H NMR spectrum of the sample after heating to 245 °C (Fig. 2-13) showed the hydroxyl and imine peaks were absent and the aromatic proton peaks were diminished in the spectrum. However, the alkyl proton peaks still remained on the spectrum.

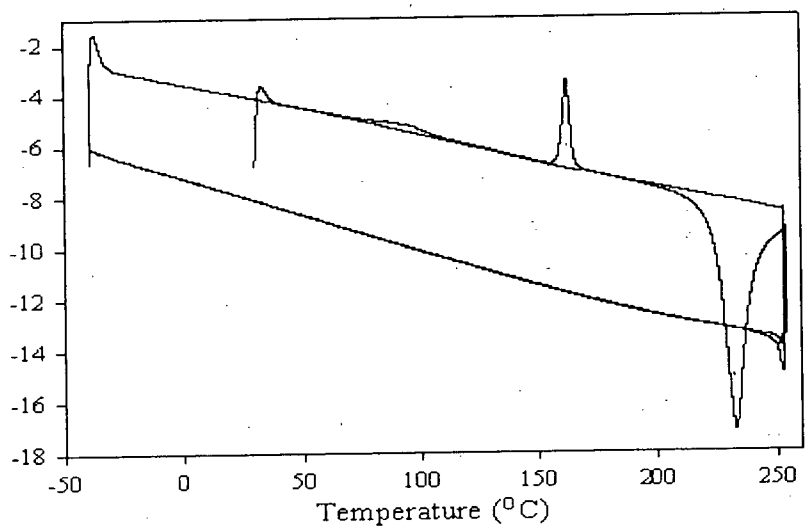

Figure 2-12: DSC thermogram of macrocycle **38** from -40 °C to 245 °C

A second sample of macrocycle **38** was examined at the same heating rate, but the heating was stopped when the temperature reached 195 °C. During the cooling period to -40 °C (rate = 20 °C/min), no thermal transition was observed. The sample was then reheated at a rate of 30 °C/min back to 195 °C. When the sample reached 89 °C, an exothermic transition was observed. The exothermic peak at 89 °C may be due to the

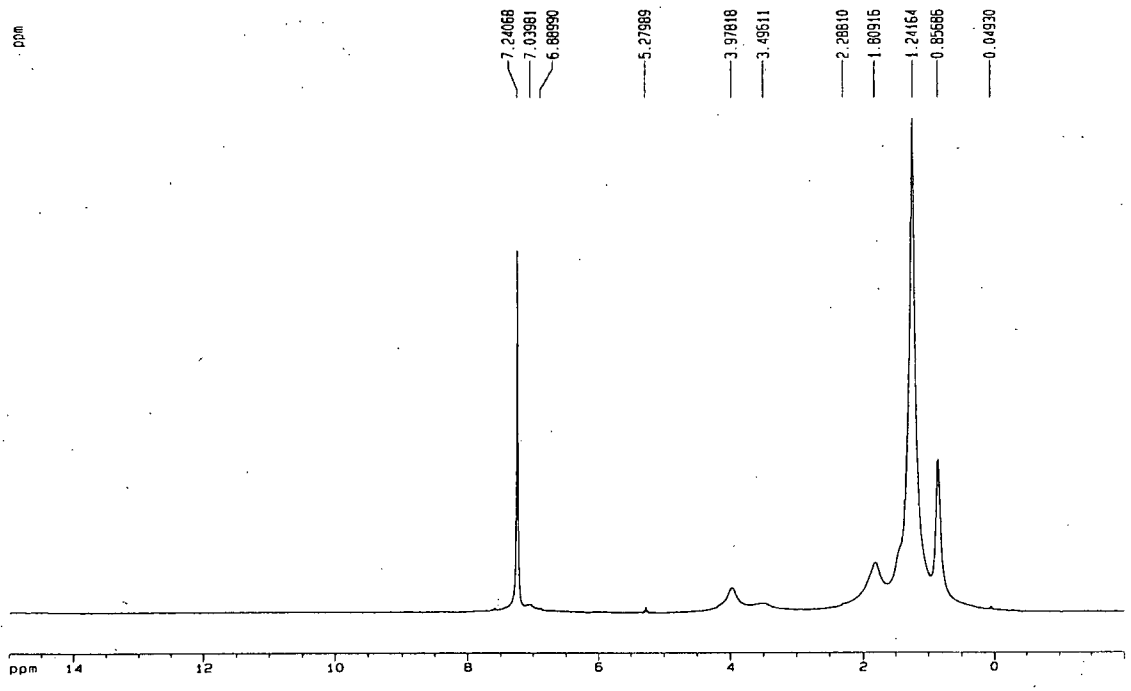

Figure 2-13: ^{1}H NMR spectrum of the decomposed hexakisdodecyloxy [3+3] Schiff-base macrocycle

change of the sample from a less ordered phase back to the solid state. The thermal behavior of the macrocycle was not reversible; the macrocycle nay be undergoing partial hydrolysis or decomposition.

When another sample of hexakisdodecyloxy [3+3] Schiff-base macrocycle (**38**) was heated at a rate of 5 °C/min, two endothermic peaks separated by 3 °C were observed near 160 °C (Fig. 2-14). It is possible that a liquid crystalline phase exists between the two transitions, or that the compound exists in two different phases (dimorphs) with slightly different melting points. Those possibilities could be resolved by using high temperature powder X-ray diffraction. Hexakishexadecyloxy [3+3] Schiff-base macrocycle (**40**) was also investigated by DSC. Its DSC plot is similar to that of the hexakisdodecyloxy macrocycle, except the endothermic peak shifted to 118 °C.

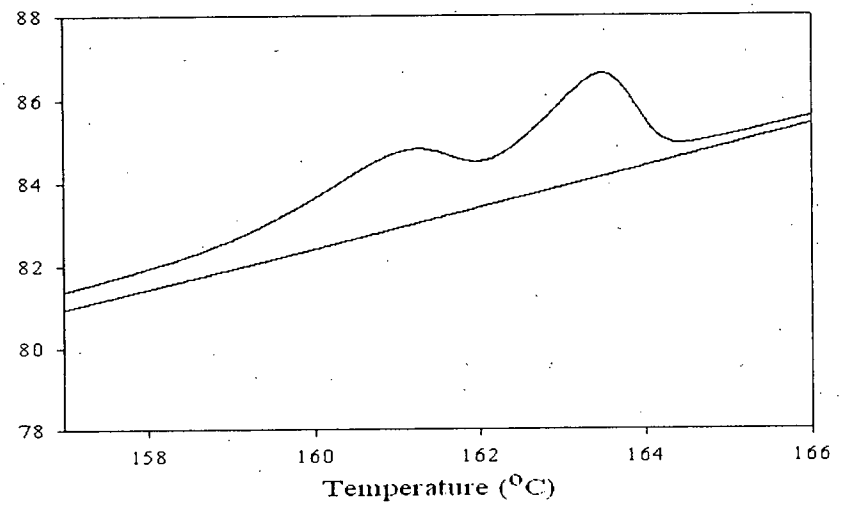

Figure 2-14: DSC thermogram of macrocycle **38** heated at 5 °C/min

Macrocycle **38** was investigated by variable temperature POM. No liquid crystalline texture was observed under crossed polarizers above the melting point. When the sample was heated to 220 °C, the color changed from red to black. A new sample heated to 10 °C above its melting point showed no liquid crystallinity upon cooling at 5 °C/min. Another sample was heated to 160 °C at 5 °C/min, then it was cooled to 100 °C and held at that temperature for 30 minutes. It was then heated back up to 160 °C at 5 °C/min. The reason for doing this was to allow the macrocyclic molecules to have enough time to align, which helps in exhibiting liquid crystallinity when heated back up to the melting point. However, the melted sample still looked like an isotropic liquid, without any sign of being liquid crystalline. The hexakishexadecyloxy [3+3] Schiff-base macrocycle (**38**) also did not show mesomorphism.

It is surprising that macrocycles **37-40** with long alkoxy chains are not liquid crystalline. There are several possible reasons for this aspect. First, the diameter of the macrocycles is quite large and the alkoxy chains may be too short to adequately fill the

space between the molecules. Second, the nature of the functional group of the substituents may be not suitable for these macrocycles. Third, the position of the substituents on the macrocycles may be not appropriate, since the organic salen mesogens have the alkoxy substituents on the salicylidene benzene ring and *para* to the imine bond.[21]

Several structural modifications can be made to the [3+3] Schiff-base macrocycles in order to promote liquid crystallinity. First, the linear alkoxy substituents can be replaced by chiral branched alkoxy chains, such as 2-ethylhexyloxy groups. The chiral branched alkoxy substituents inhibit crystalline packing of the molecules and make them more likely to exhibit a liquid crystalline phase. Moreover, the branched chains can lower the melting point and stabilize the mesophase.[22] Second, the alkoxy substituents can be replaced by other functional groups, such as ester (RCOO-), amide (RCONH-), and alkylsulfone (RSO_2-).[23] Those functional groups are proven to be good substituents for mesogens. By modifying the side chains of the [3+3] Schiff-base macrocycle, it is anticipated that macrocyclic liquid crystals may be obtained. Third, substituents with multiple chains that can occupy more space may be used.

In summary, the target [3+3] Schiff-base macrocycles and a smaller fragment of the macrocycle, compound **41**, were obtained. They were characterized by ^{1}H and ^{13}C NMR spectroscopy, IR spectroscopy, UV-Vis spectroscopy, ESI mass spectrometry, DSC and POM. No liquid crystallinity was observed for macrocycles **38** and **40**. In the future, modifications on the side chains will be performed to enhance the possibility of observing liquid crystallinity in these compounds.

2.4 References

(1) Meyer, S.; Andrioletti, B.; Sessler, J. L.; Lynch, V. *J. Org. Chem.* **1998**, *63*, 6752.

(2) Sessler, J. L.; Davis, J. M. *Acc. Chem. Res.* **2001**, *34*, 989.

(3) Sessler, J. L.; Callaway, W.; Dudek, S. P.; Date, R. W.; Lynch, V.; Bruce, D. W. *Chem. Commun.* **2003**, 2422.

(4) Atkins, A. J.; Black, D.; Blaske, A. J.; Marin-Becerra, A.; Parson, S.; Rui-Ramirez, L.; Schröder, M. *Chem. Commun.* **1996**, 457.

(5) Pilkington, N. H.; Robson, R. *Aust. J. Chem.* **1970**, *23*, 2225.

(6) Tandon, S. S.; Thompson, L. K.; Bridson, J. N.; McKee, V.; Downard, A. J. *Inorg. Chem.* **1992**, *31*, 4635.

(7) Kruger, P. E.; McKee, V. *Chem. Commun.* **1997**, 1341.

(8) McCrea, J.; McKee, V.; Metcalfe, T.; Tandon, S. S.; Wikaira, J. *Inorg. Chim. Acta* **2000**, *297*, 220.

(9) Gawroński, J.; Kolbon, H.; Kwit, M.; Katrusiak, A. *J. Org. Chem.* **2000**, *65*, 5768.

(10) Kuhnert, N.; Straßnig, C.; Lopez-Periago, A. M. *Tetrahedron: Asymmetry* **2002**, *13*, 123.

(11) Gawroński, J.; Kwit, M. *Tetrahedron: Asymmetry* **2003**, *14*, 1303.

(12) Akine, S.; Taniguchi, T.; Nabeshima, T. *Tetrahedron Lett.* **2001**, *42*, 8861.

(13) Lehn, J.-M.; Malthête, J.; Levelut, A.-M. *J. Chem. Soc., Chem. Commun.* **1985**, 1794.

(14) Malthête, J.; Levelut, A.-M.; Lehn, J.-M. *J. Chem. Soc., Chem. Commun.* **1992**, 1434.

(15) Zhao, M.; Ford, W. T.; Idziak, S. H. J.; Maliszewskyj, N. C.; Heiney, P. A. *Liq. Cryst.* **1994**, *16*, 583.

(16) Zhang, J.; Moore, J. S. *J. Am. Chem. Soc.* **1992**, *114*, 9701.

(17) Zhang, J.; Moore, J. S. *J. Am. Chem. Soc.* **1994**, *116*, 2655.

(18) Zhao, D.; Moore, J. S. *J. Chem. Soc., Chem. Commun.* **2003**, 807.

(19) Yilmaz, I.; Bekâroğlu, Ö. *J. Chem. Res* **1998**, (*S*) 374; (*M*) 1585.

(20) Gallant, A. J.; MacLachlan, M. J. *Angew. Chem. Int. Ed.* **2003**, *42*, 5307.

(21) Berdagué, P.; Courtieu, J.; Maitlis, P. M. *J. Chem. Soc., Chem. Commun.* **1994**, 1313.

(22) Collard, D. M.; Lillya, C. P. *J. Am. Chem. Soc.* **1989**, *111*, 1829.

(23) Cammidge, A. N.; Bushby, R. J. In *Handbook of Liquid Crystals*; Demus, D., Goodby, J. W., Gray, G. W., Spiess, H. W., Vill, V., Eds.; Wiley VCH: New York, 1998; Vol. 2B, pp 693-748.

Chapter 3: Metal-Containing [3+3] Schiff-Base Macrocycles

3.1 Background

Metal complexes can be used for numerous applications, including catalysts,[1] sensors,[2] and oxygen carriers.[3,4] Some metal complexes, such as metalloporphyrins and metallophthalocyanines, are being applied in biological studies. By making use of coordination chemistry, the metal complexes can be linked together by multidentate ligands, such as 4,4'-bipyridine, imidazole and pyrazine, which act bridging ligands. The bridging ligands connect the metal complexes into dimeric structures and one-dimensional metallopolymers, depending on the nature, geometry and length of the bridging ligands. The resulting linked metal complexes may have applications as nanowires and nonlinear optical (NLO) materials.

The Schiff-base compounds derived from substituted salicylaldehydes are very good ligands for the binding of metal ions because they have an N-O binding site that can chelate to the metal ions. If there is only one N-O binding site on the Schiff-base ligand (e.g., compound **42** in Fig. 3-1), a metal complex with one metal atom coordinated to two ligands (e.g., compound **45** in Fig. 3-2) will be obtained. Schiff-base compounds that have N_2O_2 pocket, such as salens and salphens (compounds **43** and **44**, respectively, in Fig. 3-2), are widely used as ligands. The resultant Schiff-base metal complexes (e.g., compound **46** in Fig. 3-2) have been used in catalytic,[5] polymeric,[6] and redox chemistry.[7,8]

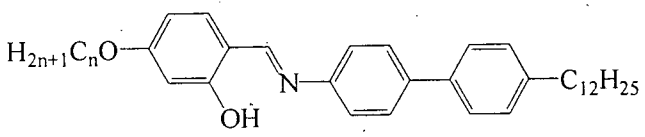

42

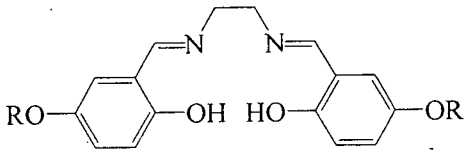

43

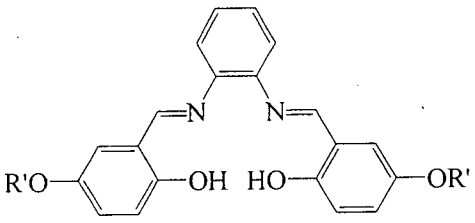

44

Figure 3-1: Examples of Schiff-base compounds with one N-O binding site (**42**) and N_2O_2 pocket (**43** and **44**)

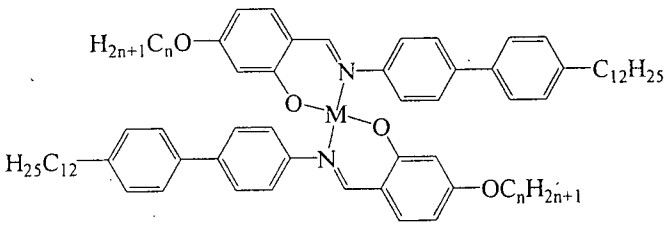

45

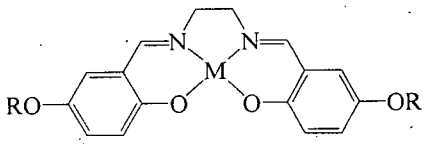

46

Figure 3-2: Examples of Schiff-base metal complexes

Metal complexes that form liquid crystals, metallomesogens, have received a lot of attention because their liquid crystalline properties and the shape of their organic counterparts can be changed by the addition of the metal atoms.[9,10] Metal-containing liquid crystalline complexes can also be obtained from non-mesogenic ligands. The incorporation of the metal atoms can induce mesomorphism in those non-liquid

crystalline organic ligands because the metal atoms are large and have easily polarizable electron density; the polarizability is a key factor in liquid crystallinity.[9,11] Another factor that determines whether a complex will form a liquid crystal is its axial ratio.[9,12] Therefore, the introduction of the metal atom should retain the axial ratio of the complex and thus the coordination geometry of the metal atom is best to be square planar.[12] The metal atoms commonly used to make metal-containing liquid crystals are Ni(II), Pt(II) and Pd(II), since they prefer square planar geometry. Incorporation of paramagnetic metal ions, such as Co(II) and Cu(II), can impart magnetic properties to the liquid crystals. The alignment of paramagnetic liquid crystals can be altered by an external magnetic field, enabling them to be used in display technology.[12,13]

The metal-containing [3+3] Schiff-base macrocycles highlighted in this chapter are synthesized by reacting the hexakisdecyloxy [3+3] Schiff-base macrocycle (**37**, see Chapter 2) with the first-row transition metals, excluding scandium, titanium and chromium (compounds **47-53**). The macrocycle is expected to coordinate at least three metal atoms since it has three N_2O_2 salphen-like pockets (Fig. 3-3). The introduction of the transition metal atoms to the macrocycle has two purposes. First, the metal-containing macrocycles have the potential to be stacked into nanotubes by intermolecular bridging ligands through coordination chemistry. The resulting nanotubes may also act as nanowires. Second, incorporation of metals may induce liquid crystallinity in the corresponding organic macrocycle. If the metal-containing macrocycles exhibit mesomorphism, the mesophase is likely to be nematic discotic or tubular.

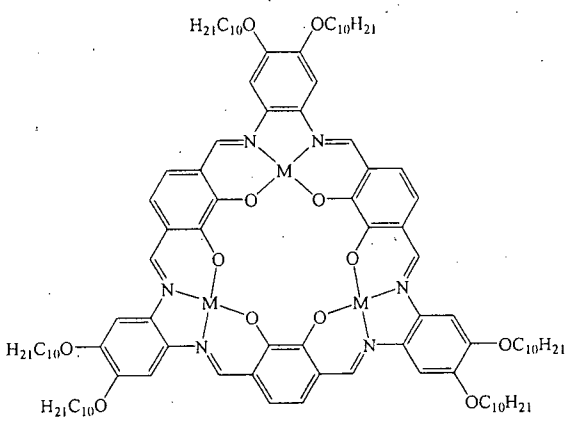

47 M = VO
48 M = Mn
49 M = Fe
50 M = Co
51 M = Ni
52 M = Cu
53 M = Zn

Figure 3-3: Target metal-containing [3+3] Schiff-base macrocycles

3.2 Experimental

Materials: Vanadyl acetylacetonate, manganese(II) acetylacetonate, iron(II) acetylacetonate, cobalt(II) acetylacetonate, nickel(II) acetylacetonate, copper(II) acetylacetonate, and zinc(II) acetylacetonate were obtained from Aldrich. Deuterated solvents were obtained from Cambridge Isotope Laboratories, Inc.. Tetrahydrofuran was dried and distilled from sodium/benzophenone under nitrogen. Hexakisdecyloxy and hexakisdodecyloxy [3+3] Schiff-base macrocycles (compounds **37** and **38**) were prepared by the procedure described in Chapter 2.

Equipment: All reactions were carried out under nitrogen unless otherwise stated. The 300MHz ^{1}H and 75.5 MHz ^{13}C NMR spectra were recorded on a Bruker AV-300

spectrometer. The IR spectra were obtained from dispersions in potassium bromide using a Bomens MB-series spectrometer. The ESR spectrum was obtained on a Bruker ECS-106 EPR spectrometer in a 20 μL quartz capillary. The UV-Vis spectra were obtained in dichloromethane on a Varian Cary 5000 UV-Vis/near-IR spectrometer using a 1 cm cuvette. Electrospray (ESI) mass spectra were obtained at the UBC Microanalytical Services Laboratory on a Micromass LCT time-of-flight (TOF) mass spectrometer equipped with an electrospray ion source. The sample was analyzed in methanol:chloroform at 1 μM. Matrix assisted laser desorption/ionization (MALDI) mass spectra were obtained at the UBC Microanalytical Services Laboratory on a Bruker Biflex IV time-of-flight (TOF) mass spectrometer equipped with a MALDI ion source The differential scanning calorimetry (DSC) thermograms were obtained on a Perkin Elmer Diamond DSC. An Olympus BX41 polarizing optical microscopy (POM) equipped with a heating stage was used to look for the liquid crystalline texture. The elemental analysis was performed on a Carlo Erba Elemental Analyzer EA 1108 at the UBC Microanalytical Services Laboratory and Canadian Microanalytical Service Ltd..

Synthesis of Compound 47. Compound **37** (0.050 g, 0.0303 mmol) and vanadyl acetylacetonate (0.025 g, 0.0938 mmol) were dissolved in tetrahydrofuran (20 mL) to give a dark red solution. The solution was heated to reflux at 90 °C for 24 h. After cooling to room temperature, the solvent was removed by rotary evaporation and a black solid was obtained. The black solid was then washed with hot methanol (200 mL) to remove any excess vanadyl acetylacetonate. Compound **47** was obtained as a black, shiny, thin film (0.053 g, 95%).

Data for Compound 47. ^{1}H NMR (300 MHz, chloroform-d_1) δ 1.30 (broad), 0.93 (broad) ppm; UV-Vis (dichloromethane): λ_{max} (ε) = 394 nm (5.78×10^4 $cm^{-1}M^{-1}$), 447 nm (7.76×10^4 $cm^{-1}M^{-1}$); ESI-MS: m/*z* = 1847.8 ($(M+H)^+$, 22%), 1869.8 ($(M+Na)^+$, 100%); IR (KBr): υ = 3440 (w), 2924 (vs), 2853 (s), 1601 (s), 1562 (w), 1556 (w), 1510 (m), 1451 (s), 1366 (m), 1336 (m), 1272 (s), 1216 (w), 1189 (m), 986 (m), 855 (w), 798 (w), 756 (w), 721 (w) cm^{-1}; Anal. Cal'd for $C_{102}H_{144}N_6O_{15}V_3$: 66.33% C, 7.86% H, 4.55% N, 8.27% V; Found: 64.95% C, 8.00% H, 4.46% N, 6.34% V.

Synthesis of Compound 48. Compound **37** (0.050 g, 0.0303 mmol) and manganese(II) acetylacetonate (0.024 g, 0.0938 mmol) were dissolved in tetrahydrofuran (40mL) to give a deep red solution. The solution was heated to reflux at 90 °C under nitrogen for 24 h. After cooling to room temperature, the solvent was removed by rotary evaporation and a black solid was obtained. The black solid was then washed with hot methanol (200 mL) to remove any excess manganese(II) acetylacetonate. Compound **48** was obtained as a deep red, shiny, thin film (0.049 g, 89%).

Data for Compound 48. ^{1}H NMR (300 MHz, chloroform-d_1) δ 1.29 (broad), 0.88 (broad) ppm; UV-Vis (dichloromethane): λ_{max} (ε) = 359 nm (5.07×10^4 $cm^{-1}M^{-1}$), 389 nm (5.14×10^4 $cm^{-1}M^{-1}$); MALDI-TOF-MS: m/*z* = 1834.1 ($(M+Na)^+$, 10%); IR (KBr): υ = 3453 (w), 2953 (sh), 2924 (vs), 2853 (vs), 1608 (s), 1507 (m), 1457 (m), 1389 (w), 1323 (w), 1268 (m), 1223 (w), 1177 (m), 1164 (m), 1108 (m), 1014 (m), 920 (w), 842 (w), 757 (w), 720 (m) cm^{-1}; Anal. Cal'd for $C_{102}H_{144}N_6O_{12}Mn_3$: 67.64% C, 8.01% H, 4.64% N, 9.10% Mn; Found: 64.36% C, 7.68% H, 4.65% N, 8.53% Mn.

Synthesis of Compound 49. Compound **37** (0.050 g, 0.0303 mmol) and iron(II) acetylacetonate (0.024 g, 0.0938 mmol) were dissolved in tetrahydrofuran (40 mL) to give a dark red solution. The solution was heated to reflux at 90 °C under nitrogen for 24 h. After cooling to room temperature, the solvent was removed by rotary evaporation and a black solid was obtained. The black solid was then washed with hot methanol (200 mL) to remove any excess iron(II) acetylacetonate. Compound **49** was obtained as a black, shiny, thin film (0.044 g, 80%).

Data for Compound 49. ^{1}H NMR (300 MHz, chloroform-d_1) δ 1.30 (broad) ppm; UV-Vis (dichloromethane): λ_{max} (ε) = 367 nm (2.25×10^4 $cm^{-1}M^{-1}$); MALDI-TOF-MS: m/z = 1813.8 ($(M+H)^+$, 100%), 1836.8 ($(M+Na)^+$, 95%); IR (KBr): υ = 3438 (m), 2952 (sh), 2924 (vs), 2853 (vs), 1604 (s), 1523 (m), 1509 (m), 1451 (m), 1377 (m), 1361 (m), 1332 (m), 1223 (w), 1169 (m), 1014 (m), 927 (w), 838 (m), 759 (w), 721 (w) cm^{-1}; Anal. Cal'd for $C_{102}H_{144}N_6O_{12}Fe_3$: 67.54% C, 8.00% H, 4.63% N, 9.24% Fe; Found: 65.11% C, 7.92% H, 4.55% N, 6.78% Fe.

Synthesis of Compound 50. Compound **37** (0.050 g, 0.0303 mmol) and cobalt(II) acetylacetonate (0.024 g, 0.0938 mmol) were dissolved in tetrahydrofuran (40 mL) to give a dark red solution. The solution was heated to reflux at 90 °C under nitrogen for 24 h. After cooling to room temperature, the solvent was removed by rotary evaporation and a black solid was obtained. The black solid was then washed with hot methanol (200 mL) to remove any excess cobalt(II) acetylacetonate. Compound **50** was obtained as a black, shiny, thin film (0.038 g, 69%).

Data for Compound 50. ^{1}H NMR (300 MHz, chloroform-d_1) δ 1.27 (broad), 0.85 (broad) ppm; UV-Vis (dichloromethane): λ_{max} (ε) = 259 nm (2.46×10^4 $cm^{-1}M^{-1}$), 375 nm (1.88×10^4 $cm^{-1}M^{-1}$); MALDI-TOF-MS: m/*z* = 1845.8 ($(M+Na)^+$, 100%); IR (KBr): υ = 3383 (w), 2953 (sh), 2923 (vs), 2853 (vs), 1600 (s), 1521 (s), 1457 (s), 1391 (m), 1344 (m), 1279 (s), 1221 (w), 1190 (m), 1106 (m), 1015 (m), 925 (w), 856 (w), 821 (w), 765 (w), 720 (m) cm^{-1}.

Synthesis of Compound 51. Compound **37** (0.050 g, 0.0303 mmol) and nickel(II) acetylacetonate (0.024 g, 0.0938 mmol) were dissolved in tetrahydrofuran (40 mL) to give a dark red solution. The solution was heated to reflux at 90 °C under nitrogen for 24 h. After cooling to room temperature, the solvent was removed by rotary evaporation and a black solid was obtained. The black solid was then washed with hot methanol (200 mL) to remove any excess nickel(II) acetylacetonate. Compound **51** was obtained as a black, shiny, thin film (0.038 g, 69%).

Data for Compound 51. ^{1}H NMR (300 MHz, chloroform-d_1) δ 1.23 (broad), 0.91 (broad) ppm; UV-Vis (dichloromethane): λ_{max} (ε) = 260 nm (4.68×10^4 $cm^{-1}M^{-1}$), 386 nm (2.46×10^4 $cm^{-1}M^{-1}$); MALDI-TOF-MS: m/*z* = 1821.9 ($(M+H)^+$, 77%), 1843.9 ($(M+Na)^+$, 75%); IR (KBr): υ = 3399 (w), 2924 (vs), 2853 (vs), 1604 (s), 1519 (m), 1506 (w), 1456 (s), 1395 (w), 1378 (w), 1360 (m), 1281 (s), 1247 (w), 1190 (m), 1111 (m), 1014 (m), 925 (w), 856 (w), 820 (w), 767 (w), 747 (w), 720 (m) cm^{-1}.

Synthesis of Compound 52. Compound **37** (0.050 g, 0.0303 mmol) and copper(II) acetylacetonate (0.025 g, 0.0938 mmol) were dissolved in tetrahydrofuran (40 mL) to give a deep red solution. The solution was heated to reflux at 90 °C under nitrogen for 24 h. After cooling to room temperature, the solvent was removed by rotary evaporation and a black solid was obtained. The black solid was then washed with hot methanol (200 mL) to remove any excess copper(II) acetylacetonate. Compound **52** was obtained as a black, shiny, thin film (0.039 g, 70%).

Data for Compound 52. ^{1}H NMR (300 MHz, chloroform-d_1) δ 3.87 (broad), 1.25 (broad), 0.87 (broad) ppm; UV-Vis (dichloromethane): λ_{max} (ε) = 260 nm (3.93×10^4 $cm^{-1}M^{-1}$), 368 nm (1.65×10^4 $cm^{-1}M^{-1}$); MADLI-TOF-MS: m/*z* = 1836.4 ($(M+H)^+$, 65%), 1858.4 ($(M+Na)^+$, 45%); IR (KBr): υ = 3424 (m), 2953 (sh), 2924 (vs), 2853 (vs), 1603 (s), 1559 (w), 1522 (m), 1507 (m), 1467 (s), 1452 (s), 1393 (w), 1366 (w), 1339 (w), 1272 (s), 1217 (w), 1185 (m), 1110 (m), 1014 (m), 937 (w), 859 (w), 826 (w), 746 (m), 721 (s) cm^{-1}; Anal. Cal'd for $C_{102}H_{144}N_6O_{12}Cu_3$: 66.69% C, 7.90% H, 4.58% N, 10.38% Cu; Found: 64.27% C, 7.83% H, 4.38% N, 8.35% Cu.

Synthesis of Compound 53. Compound **37** (0.050 g, 0.0303 mmol) and zinc(II) acetylacetonate (0.025 g, 0.0938 mmol) were dissolved in tetrahydrofuran (40 mL) to give a dark red solution. The solution was heated to reflux at 90 °C under nitrogen for 24 h. After cooling to room temperature, the solvent was removed by rotary evaporation and a black solid was obtained. The black solid was then washed with hot methanol (200

mL) to remove any excess zinc(II) acetylacetonate. Compound **53** was obtained as a deep red, shiny, thin film (0.046 g, 84%).

Data for Compound 53. ^{1}H NMR (300 MHz, chloroform-d_1) δ 8.30 (broad, 6H, C*H*=N), 6.63 (broad, 12H, aromatic C*H*), 4.03 (broad, 12H, OCH_2), 1.83 (broad, 12H, CH_2), 1.28 (broad, 86H, CH_2), 0.88 (broad, 18H, CH_3) ppm; UV-Vis (dichloromethane): λ_{max} (ε) = 261 nm (2.71×10^4 $cm^{-1}M^{-1}$), 362 nm (4.20×10^4 $cm^{-1}M^{-1}$), 409 nm (4.40×10^4 $cm^{-1}M^{-1}$); MALDI-TOF-MS: m/*z* = 1843.9 ($(M+H)^+$, 100%); IR (KBr): υ = 3444 (w), 2952 (sh), 2924 (vs), 2853 (s), 1610 (s), 1507 (m), 1462 (s), 1391 (w), 1324 (w), 1267 (m), 1221 (w), 1179 (w), 1112 (w), 1014 (w), 945 (w), 838 (w), 720 (s) cm^{-1}.

Synthesis of Compound 54. Compound **38** (0.050 g, 0.0303 mmol) and vanadyl acetylacetonate (0.025 g, 0.0938 mmol) were dissolved in tetrahydrofuran (20 mL) to give a dark red solution. The solution was heated to reflux at 90 °C under nitrogen for 24 h. After cooling to room temperature, the solvent was removed by rotary evaporation and a black solid was obtained. The black solid was then washed with hot methanol (200 mL) to remove any excess vanadyl acetylacetonate. Compound **54** was obtained as a black, shiny, thin film (0.048 g, 87%).

Data for Compound 54. ^{1}H NMR (300 MHz, chloroform-d_1) δ 3.97 (broad), 3.47 (broad), 1.29 (broad), 0.89 (broad) ppm; UV-Vis (dichloromethane): λ_{max} (ε) = 264 nm (7.42×10^4 $cm^{-1}M^{-1}$), 398 nm (6.34×10^4 $cm^{-1}M^{-1}$), 451 nm (1.01×10^5 $cm^{-1}M^{-1}$); ESI-MS: m/*z* = 2015.9 ($(M+H)^+$, 100%), 2037.9 ($(M+Na)^+$, 55 %); HR-ESI-MS $(M+H)^+$:

2016.0998 (calculated), 2016.0980 (found), $(M+Na)^+$: 2038.0818 (calculated), 2038.0883; IR (KBr): 3428 (w), 2923 (vs), 2853 (s), 1601 (s), 1555 (w), 1509 (m), 1450 (vs), 1364 (m), 1336 (m), 1270 (vs), 1216 (w), 1189 (m), 1108 (m), 982 (m), 852 (w), 760 (w), 722 (w) cm^{-1}.

3.3 Discussion

The reactions of the first-row transition metal starting materials with hexakisdecyloxy [3+3] Schiff-base macrocycle were performed under a nitrogen atmosphere using dry solvent (Scheme 3-1). An inert environment was used because water may cause the macrocycle to dissociate during the metallation, since the formation of the Schiff-base macrocycle is a reversible reaction (Scheme 2-1).

The metallations of the vanadyl(II)- and nickel(II)- [3+3] Schiff-base macrocycles were first performed with vanadyl(II) sulfate and nickel(II) acetate in ethanol (Scheme 3-2). The organic macrocycle was insoluble in ethanol and when the metal salts were added to the reaction flask, black solids formed. The black solids did not dissolve throughout the reaction period and were then filtered after the reaction completed. It was noticed that the resulting black solids were not soluble in any solvents. At first it was believed that the metal-containing macrocyclic molecules might have been stacked together if the nickel(II) complex was partially oxidized. A few drops of hydrazine were then added to the resulting metal complexes in dichloromethane. However, none of the

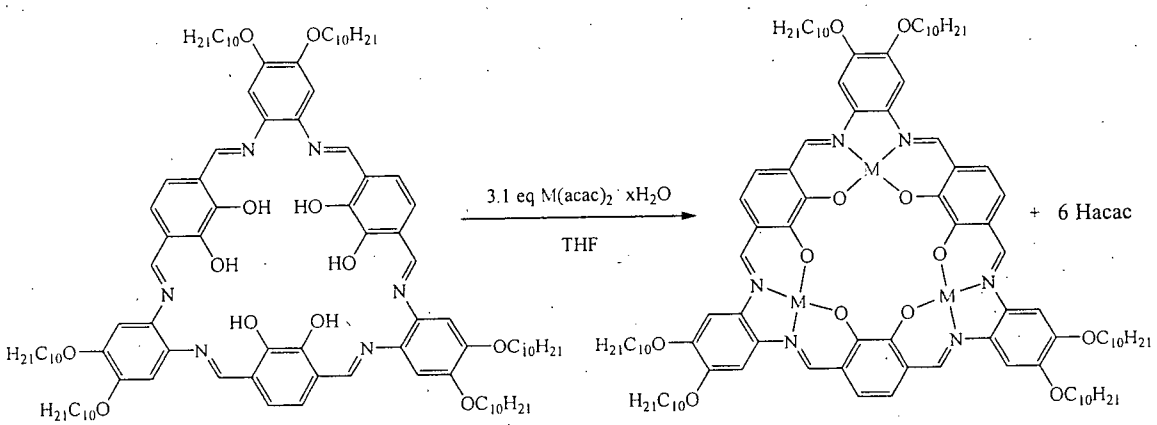

37

47 M = VO
48 M = Mn
49 M = Fe
50 M = Co
51 M = Ni
52 M = Cu
53 M = Zn

Scheme 3-1: Metallation of hexakisdecyloxy [3+3] Schiff-base macrocycle

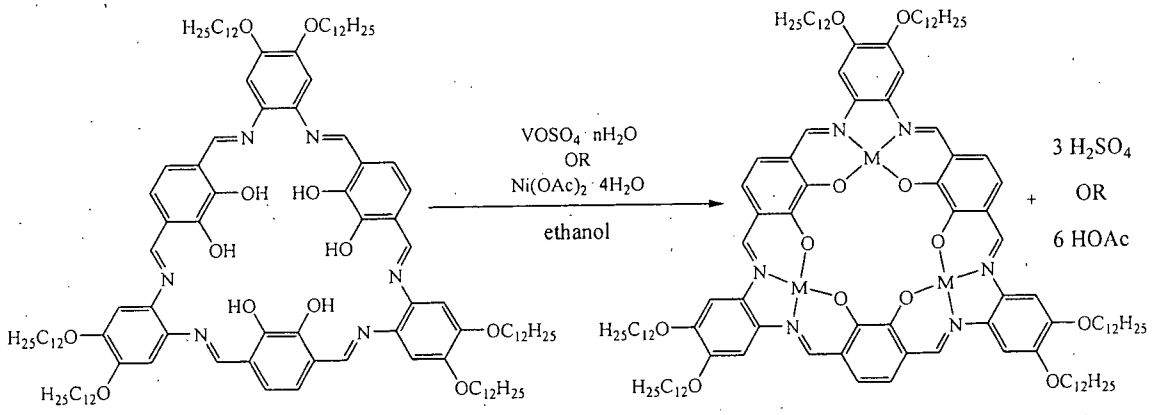

38

54 M = VO
55 M = Ni

Scheme 3-2: Metallation of VO(II) and Ni(II) ions to hexakisdodecyloxy [3+3] Schiff-base macrocycle (**38**) at a different approach

black solids dissolved. It was then thought that the acid generated during the metallation might oxidize the metal atoms, thus leading to the insoluble metal-containing macrocycles. Therefore, the reaction was performed under the same conditions as

previously mentioned in Scheme 3-2, but with the introduction of triethylamine to neutralize the acid generated during the reaction (Scheme 3-3). As a result, very dark red solids were obtained and they were soluble in solvents such as dichloromethane and tetrahydrofuran. The products were characterized by electrospray mass spectroscopy and the correct masses were observed.

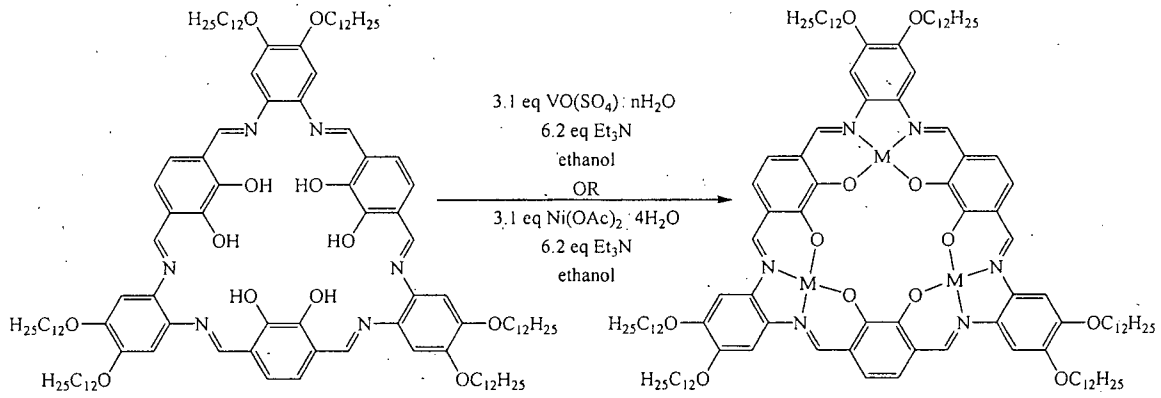

38

54 M = VO
55 M = Ni

Scheme 3-3: Metallation of VO(II) and Ni(II) ions to hexakisdodecyloxy [3+3] Schiff-base macrocycle (**38**) with the use of triethylamine

The final approach to the metallations was to prepare the metal-containing macrocycles by reacting the organic macrocyclic ligands with metal(II) chelates. There are two advantages of using metal(II) chelates as the sources of metal ions. First of all, no strong acid would be generated during the metallations. Second, the reaction could be performed in a solvent in which both the organic macrocycles and the metal(II) chelates are soluble. The metal chelates were chosen to be metal(II) acetylacetonates and the reactions were performed as shown in Scheme 3-1. Any excess metal(II) acetylacetonate left after the metallations could be washed off with hot methanol or acetonitrile. The

resultant metal-containing macrocycles are nearly black in color. They are soluble in chloroform, dichloromethane and tetrahydrofuran. The color of the metal complexes in solution is far more intense than that of the organic macrocycle at the same concentration. The metal-containing [3+3] Schiff-base macrocycles (**47-53**) were mainly characterized by ^{1}H NMR spectroscopy, mass spectrometry, UV-Vis spectroscopy and IR spectroscopy.

A sample of each transition metal complexes was prepared in chloroform-d_1, giving very dark red solutions. All of the peaks on all the ^{1}H NMR spectra were very broad. For the vanadyl-, manganese-, iron-, cobalt- and copper-containing macrocycles, this was expected since the metals are paramagnetic (Fig. 3-4). The spectra all showed very broad peaks between 0-3 ppm assigned to the alkoxy substituents. Although the ^{1}H NMR spectra of these paramagnetic metal complexes were not able to provide information about the structure of the resultant metal-containing macrocycles, they do indicate that no organic impurities (e.g., solvent, metal-free macrocycle or acetylacetone) are present in the product.

The nickel-containing Schiff-base macrocycle **51** was expected to give a ^{1}H NMR spectrum with sharp peaks because the geometry of the nickel metal centres were presumed to be square planar (d^8, S = 0). However, the ^{1}H NMR spectrum obtained for this metal complex showed only two broad peaks, similar to the spectrum of the paramagnetic metal complexes mentioned earlier. This suggests that the nickel atoms are not square planar. According to the PM3 calculation from Section 2.3, the organic

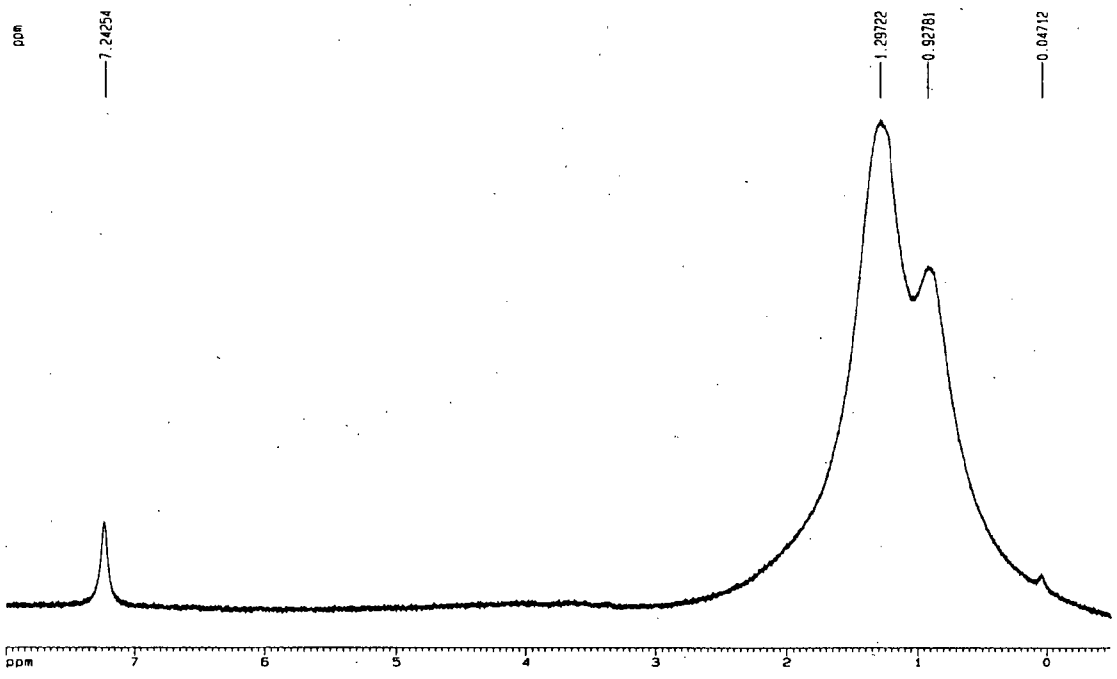

Figure 3-4: ^{1}H NMR spectrum of the vanadyl-containing macrocycle **47**

Schiff-base macrocyclic ligand is not planar and is twisted at the diformylcatechol moieties (Fig. 2-10). Therefore, in order for three nickel atoms to coordinate to the N_2O_2 salphen-like pockets of the macrocycle, they must arrange themselves in a geometry that would fit the shape of the pockets and thus the propensity of being square planar is lower. Accordingly, a possible geometry for the nickel centres would be tetrahedral, in which the electron configuration would have two unpaired electrons and thus the complex is paramagnetic. Another possible reason for obtaining a broad ^{1}H NMR spectrum of the nickel complex would be the oxidation state of the nickel atoms. It is possible that some of the nickel atoms were oxidized from a +2 oxidation state to +3 oxidation state, leading to paramagnetism.

The ^{1}H NMR spectrum of the zinc-containing Schiff-base macrocycle **53** is different than the spectra obtained for the other transition metal complexes. On this

spectrum, not only the peaks corresponding to the alkyl protons could be seen, but also the -OCH_2- protons, the aromatic protons and imine protons could also be observed. In addition, no hydroxyl protons were observed at 13-14 ppm (Fig. 3-5). The absence of the hydroxyl peak coincides with the coordination of the zinc atoms in the N_2O_2 salphen-like pockets of the macrocycle. It should be noted that the imine peak was shifted upfield by 0.2 ppm from that of macrocycle **37**. It was expected that the peaks on the ^1H NMR spectrum of the zinc-containing macrocycle would be sharp because the zinc(II) centres have a d^{10} electron configuration and thus the complex is diamagnetic. The geometry of the zinc centres would not affect the diamagnetism of this complex because all the d-orbitals are filled. However, the peaks in the ^1H NMR spectrum are broad. This may be due to the overall shape of the resulting zinc-containing macrocycle. As mentioned in Chapter 2, the PM3 calculated shape of the metal-free macrocycle was not planar. But since it was flexible enough to fluctuate in solution during the NMR time scale, the ^1H NMR spectrum exhibited an overall proton environment identical to the one that would be obtained for the completely flat macrocyclic ring. The incorporation of the zinc ions would increase the rigidity of the macrocycle and thus the fluctuation of the resulting macrocyclic metal complex in solution would be unlikely to occur on the NMR time scale. The protons on the macrocyclic ring would be locked in position and hence different environments would occur. The broad aromatic and imine peaks may be due to the overlapping of the aromatic and imine protons at different locations on the periphery.

The IR absorption spectra of the metal-containing [3+3] Schiff-base macrocycles were obtained (Fig. 3-6). The position of the IR bands is similar to those of the metal-

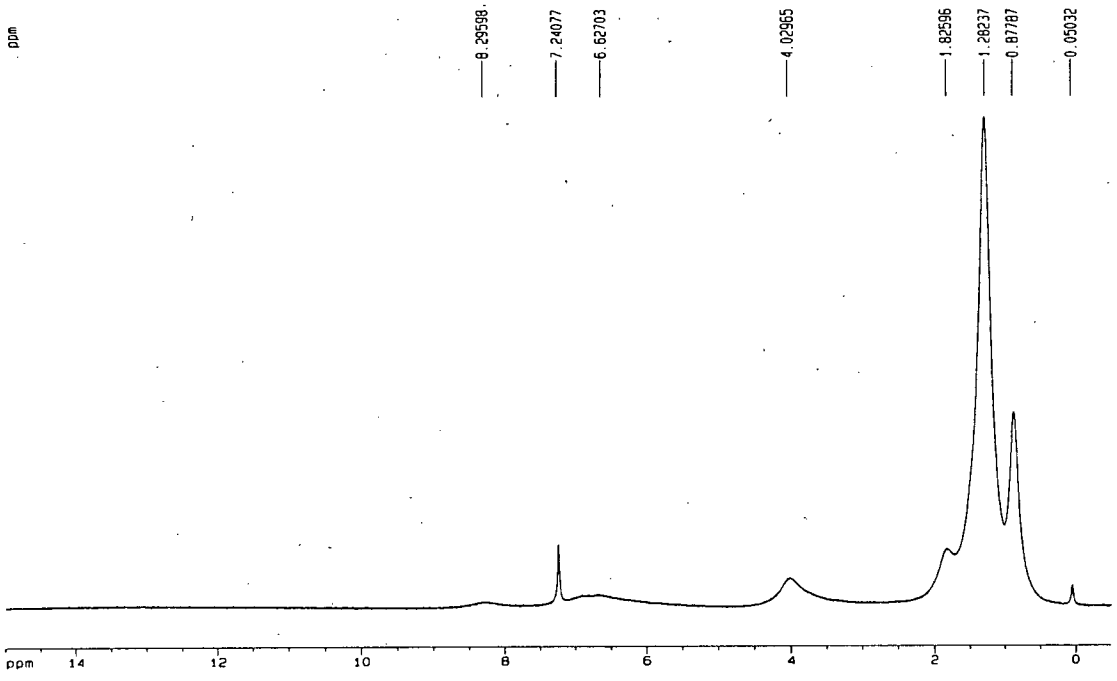

Figure 3-5: ^{1}H NMR spectrum of the zinc-containing macrocycle **53**

free macrocycles. The metal complexes have an absorption band of 1604 cm^{-1} on average that corresponds to the stretching frequency of the imine C=N bond, which is slightly lower than the imine C=N stretching frequency of the metal-free macrocycles. Two strong IR bands at around 2920 and 2850 cm^{-1} correspond to the C-H stretching frequencies of the alkoxy substituents on the periphery of the macrocyclic rings. Although the resultant metal-containing macrocycles do not contain any hydroxyl groups, the IR spectra display a broad OH absorption band at about 3400 cm^{-1}. This is likely due to the coordination of water molecules to the metal centres. In the IR spectrum of the vanadyl-containing macrocycle, there is another significant absorption band at 980 cm^{-1}. This absorption band corresponds to the stretching frequency of the V=O bond. It indicates the vanadyl centres did not form a ···V-O-V-O-V··· polymer with other V=O bonds from the neighbouring vanadyl-containing macrocycles during the metallation,

otherwise, a stretching frequency of 860 cm^{-1} would be observed. IR spectroscopy also confirmed the absence of metal-free macrocycle and C=O groups, which may form by hydrolysis of macrocycle **37**, in the products.

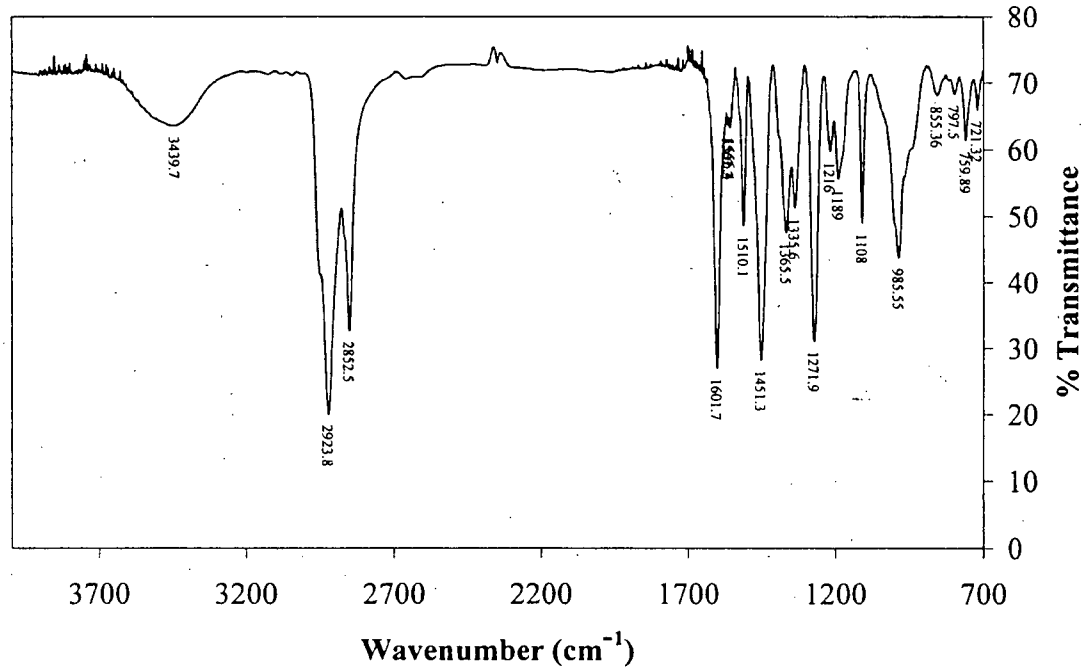

Figure 3-6: IR spectrum of the vanadyl-containing macrocycle **47**

The UV-Vis spectra of the metal-containing macrocycles showed bands between 250 and 410 nm. The peaks are listed in Table 3-1. The UV-Vis spectra of the vanadyl-, manganese- and zinc-containing macrocycles display two broad bands between 350 and 450 nm. These may be ligand-to-metal charge transfer (LMCT) or metal-to-ligand charge transfer (MLCT) bands. The intensities of those two bands in both the manganese- and zinc-containing macrocycles spectra are close to each other (Fig. 3-7). However, for the vanadyl-containing macrocycle, the band centred at 447 nm has an intensity that is 1.3 times stronger than the other one (Fig. 3-8). There may be an

overlapping LMCT band from O to V of the vanadyl centres in this region. For the iron-, cobalt-, nickel- and copper-containing macrocycles, their UV-Vis spectra show one broad

Table 3-1: The absorption bands of each metal-containing macrocycle

Metal	Wavelength (nm)	ε ($cm^{-1}M^{-1}$)	Wavelength (nm)	ε ($cm^{-1}M^{-1}$)	Wavelength (nm)	ε ($cm^{-1}M^{-1}$)
VO	395	$5.78x10^4$	447	$7.76x10^4$		
Mn	359	$5.07x10^4$	389	$5.14x10^4$		
Fe	367	$2.25x10^4$				
Co	259	$2.46x10^4$	375	$1.88x10^4$		
Ni	260	$4.68x10^4$	386	$2.46x10^4$		
Cu	260	$3.93x10^4$	369	$1.65x10^4$		
Zn	261	$2.71x10^4$	362	$4.20x10^4$	409	$4.40x10^4$

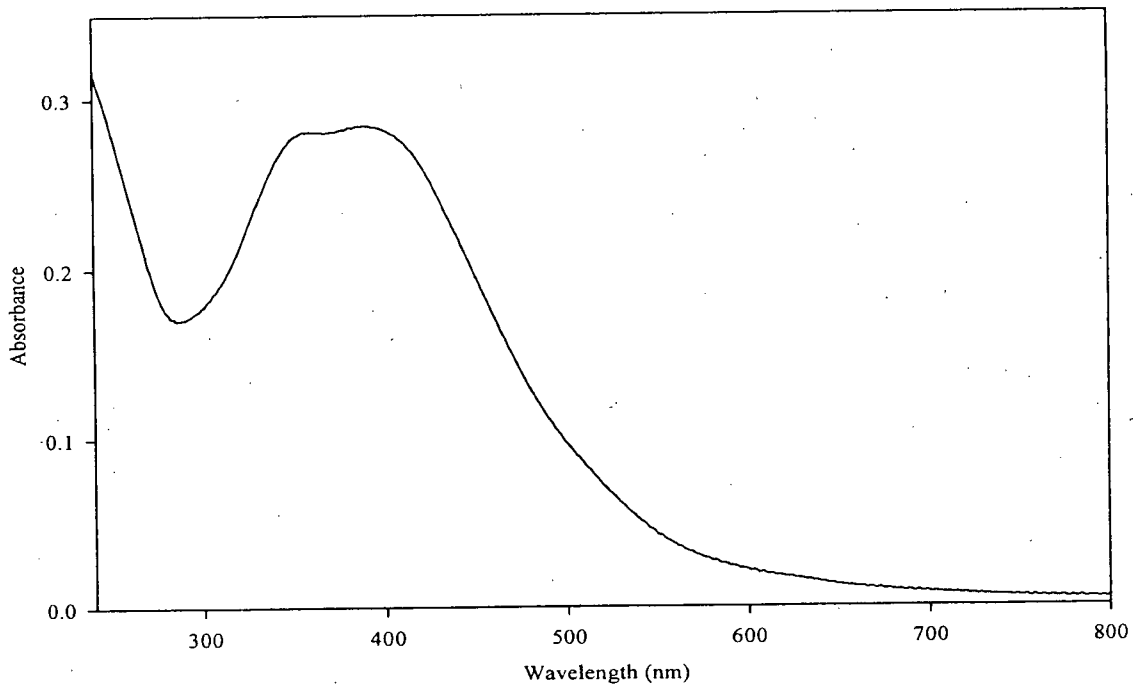

Figure 3-7: UV-Vis spectrum of the manganese-containing macrocycle **48**

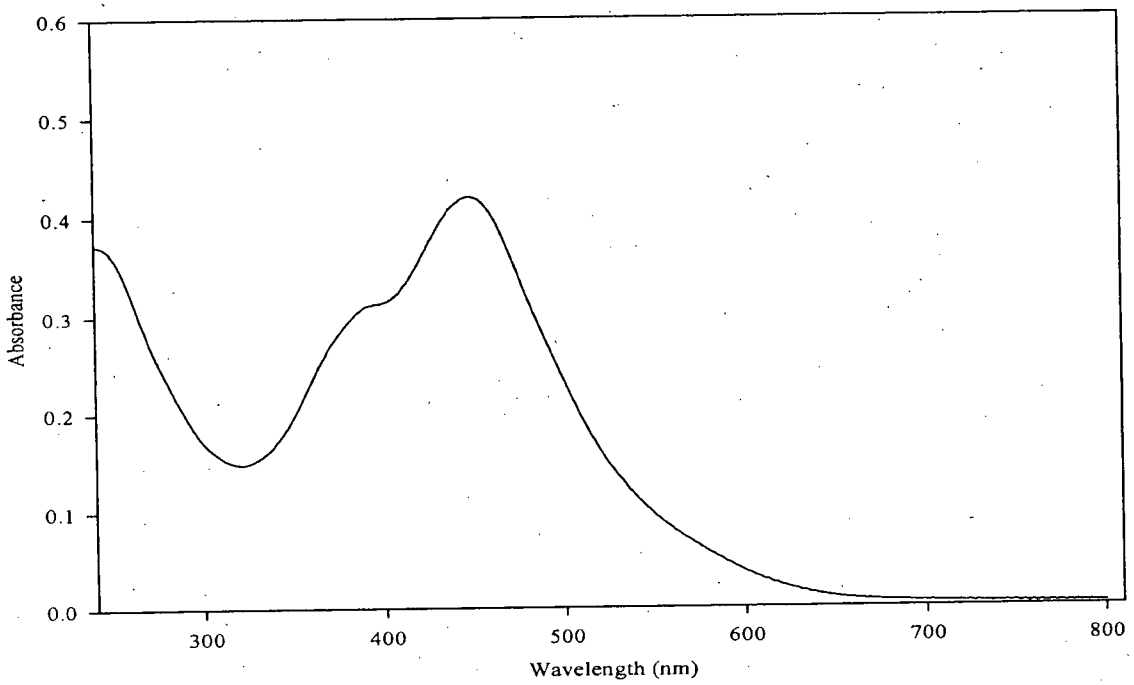

Figure 3-8: UV-Vis spectrum of the vanadyl-containing macrocycle **47**

band between 365-390 nm. This broad band is speculated to be an overlap of the two bands from the spectra of vanadyl-, manganese- and zinc-containing macrocycles.

ESR spectroscopy has been performed on the vanadyl-containing macrocycle **47** (Fig. 3-9). In the complex, the V(IV) ion has a single unpaired electron and a nuclear spin (I) of 7/2. According to the 2nI+1 equation for line splitting, an ESR spectrum with eight lines should be obtained. However, only one broad signal was observed on the spectrum. The ESR spectrum of related vanadyl salphen complex **56**[14] (Fig. 3-10) shows the expected octet pattern. The interval from one end of the octet to the other end is the same as the interval of the broad ESR signal of the vanadyl-containing macrocycle. There appears to be a significant interaction between the unpaired electrons of the vanadium atoms, leading to the single broad ESR signal. The interaction can be

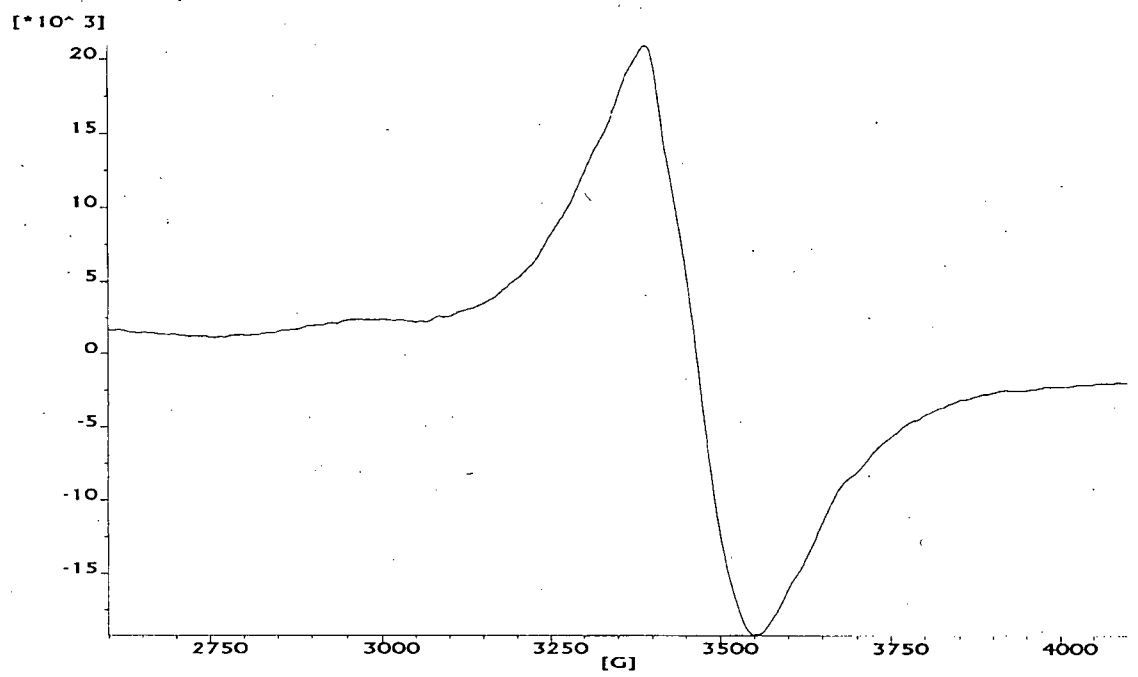

Figure 3-9: ESR spectrum of the vanadyl-containing macrocycle **47** (2.71×10^{-5} M in chloroform)

investigated by synthesizing two vanadyl-containing model complexes (compounds **57** and **58**). Compound **57** has only one vanadyl centre and the rest of the N_2O_2 salphen-like pockets each coordinate a zinc atom (Fig. 3-11a). Compound **58**, on the other hand, has two pockets binding vanadyl ions and the other pocket has a zinc ion (Fig. 3-11b). An ESR spectrum of compound **57** should show an octet pattern. As for compound **58**, a broad ESR signal, similar to the one obtained for the macrocycle with three vanadyl centres, may result from the interaction between the two unpaired electrons. The use of these model compounds should simplify the spectra and allow modeling of the electronic exchange in the macrocycles.

The metal-containing [3+3] Schiff-base macrocycles were also characterized by

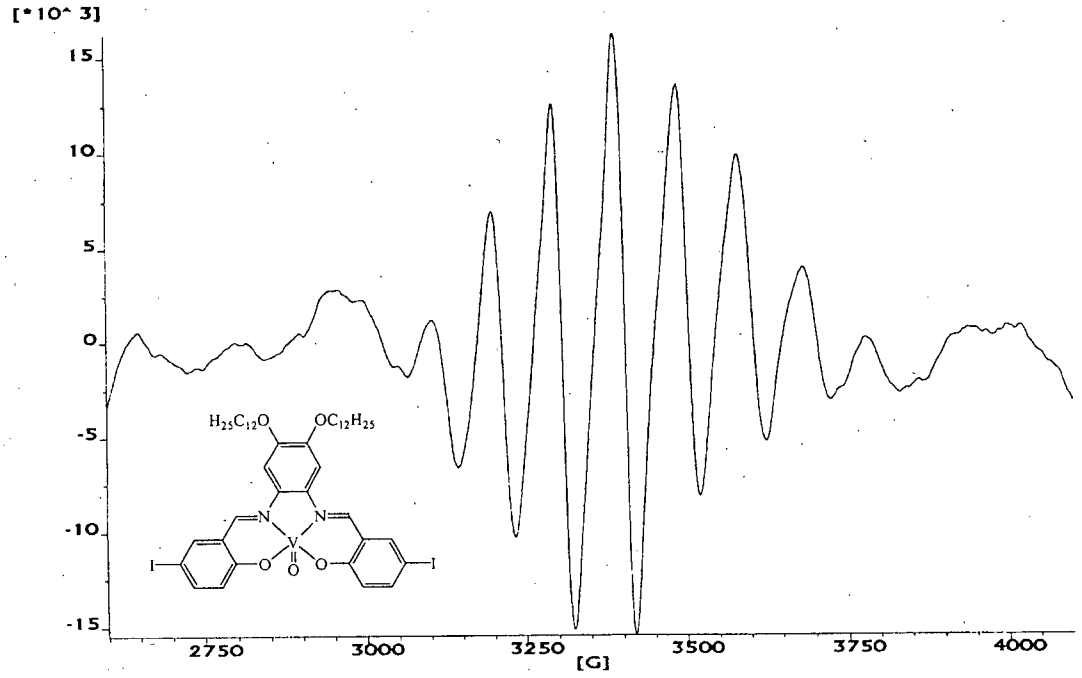

Figure 3-10: ESR spectrum of related vanadyl salphen complex **54**

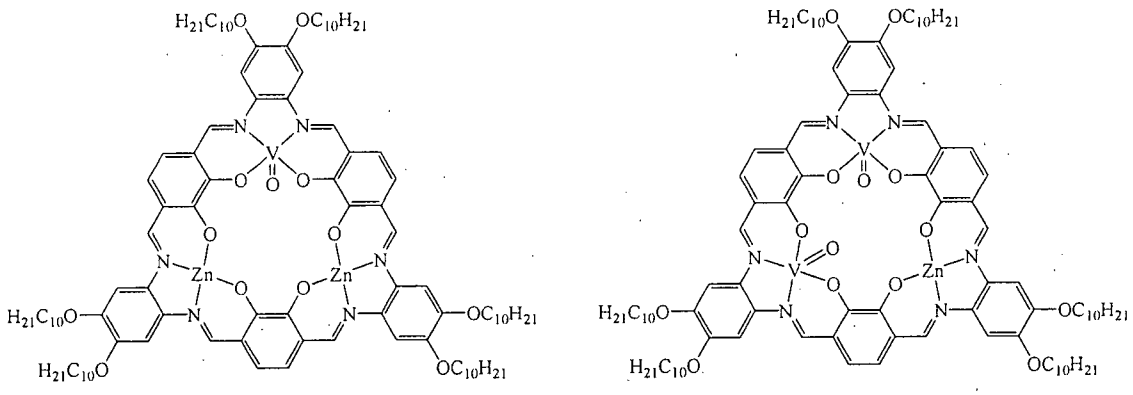

57 **58**

Figure 3-11: Chemical structures of compound **57** and compound **58**

either electrospray mass spectrometry (ESI-MS) or matrix assisted laser desorption ionization time-of-flight mass spectrometry (MALDI-TOF-MS). As the ^{1}H NMR spectra of the metal-containing macrocycles are broad and do not unambiguously confirm the

formation of the target complexes, both ESI-MS and MALDI-TOF-MS are very helpful techniques to identify the products. Both hexakisdecyloxy and hexakisdodecyloxy vanadyl-containing macrocycles (**47** and **54**) were characterized by ESI-MS. The ESI-MS of the vanadyl-containing macrocycle **54** shows the correct molecular weight of the target complex (Fig. 3-12). Moreover, a molecular weight corresponding to the target complex with the coordination of a sodium ion is observed. A strong affinity of sodium ions was also observed for the metal-free [3+3] Schiff-base macrocycle.[15] Furthermore, a molecular weight of a dimeric species of the target metal complex without any oxygen atoms is also observed at m/*z* = 2007. It is suspected that the dimerization occurred when the vanadyl-containing macrocycle was ionized when performing the ESI-MS. As for the hexakisdecyloxy vanadyl-containing macrocycle (**47**), the mass spectrum of the ESI-MS displays mainly the molecular weight of the target metallomacrocycle with the coordination of the sodium ion (Fig. 3-13). The sodium ion likely comes from the glassware used during the sample preparation.

The zinc-, cobalt-, nickel- and copper-containing macrocycle were characterized by MALDI-TOF-MS. For the zinc-containing macrocycle **53**, the correct molecular weight is observed at m/*z* = 1843.5 and there is only one major signal on the spectrum (Fig. 3-14). Therefore, a hexakisdecyloxy [3+3] Schiff-base macrocycle with three zinc centres was obtained. As for the cobalt-containing macrocycle **50**, the mass spectrum from MALDI-TOF-MS displays mainly the molecular weight of the target metallomacrocycle with the coordination of the sodium ion (Fig. 3-15). For the nickel-

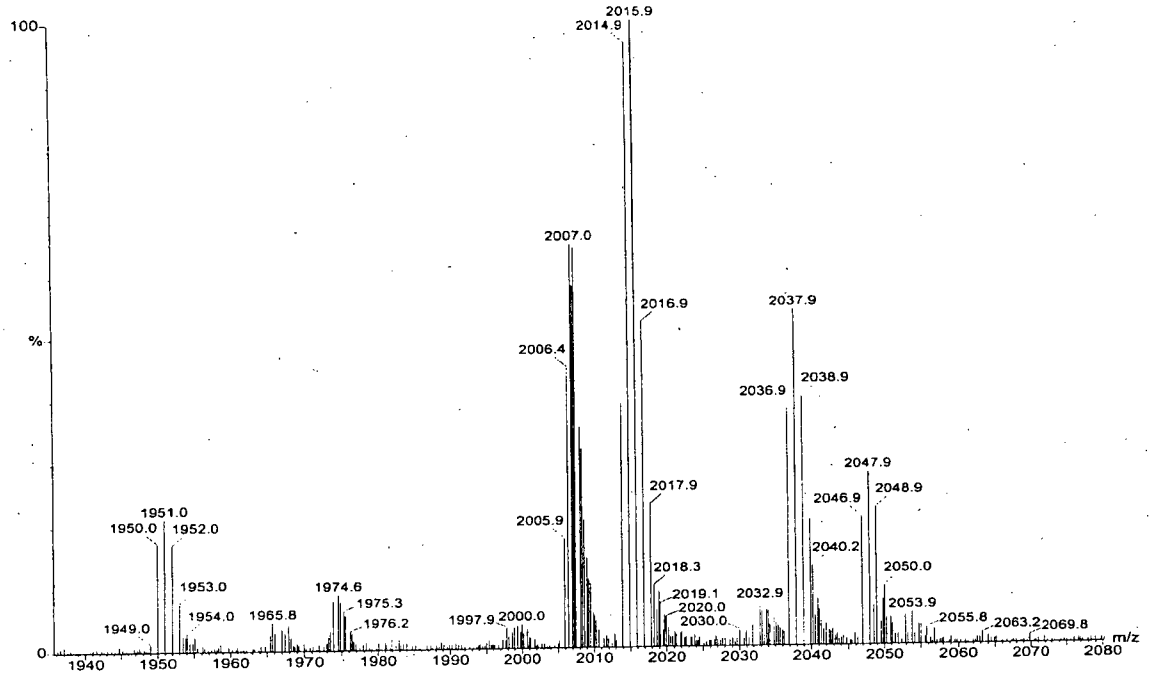

Figure 3-12: ESI mass spectrum of the vanadyl-containing macrocycle **54**

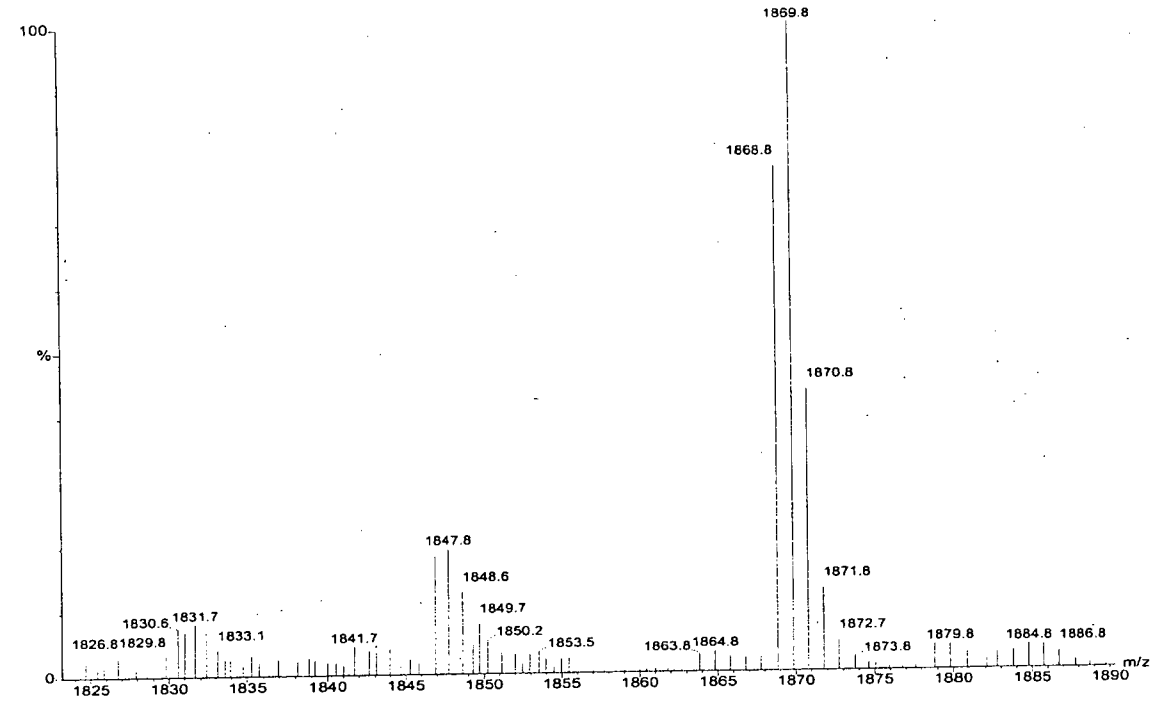

Figure 3-13: ESI mass spectrum of the vanadyl-containing macrocycle **47**

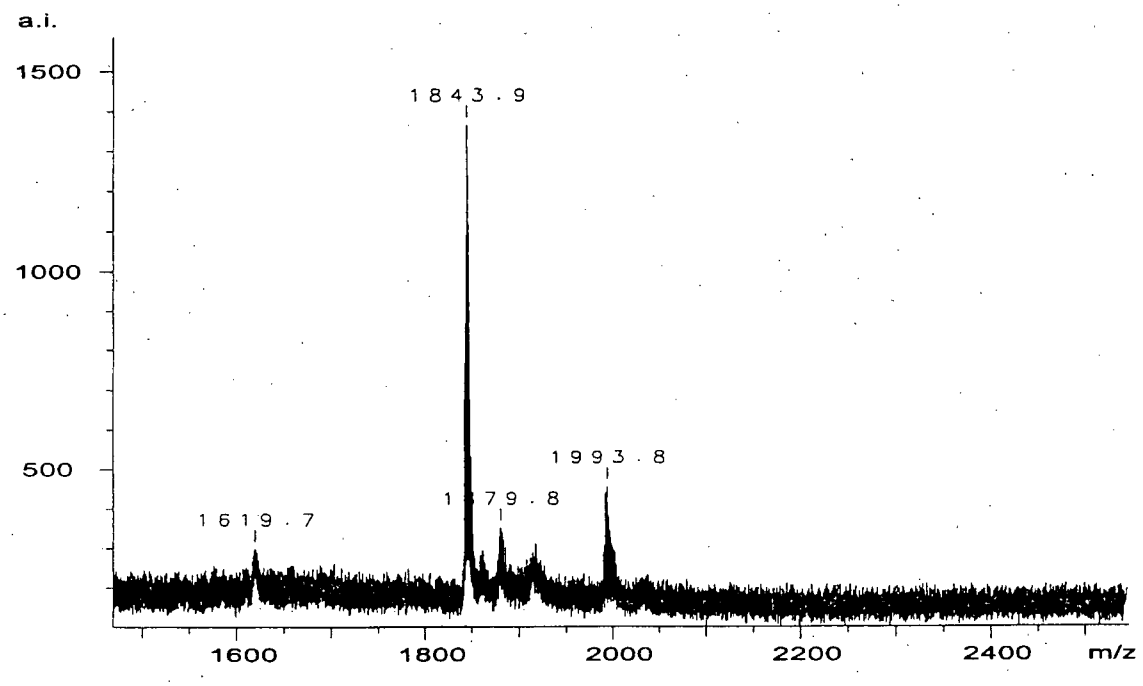

Figure 3-14: MALDI-TOF mass spectrum of the zinc-containing macrocycle **53**

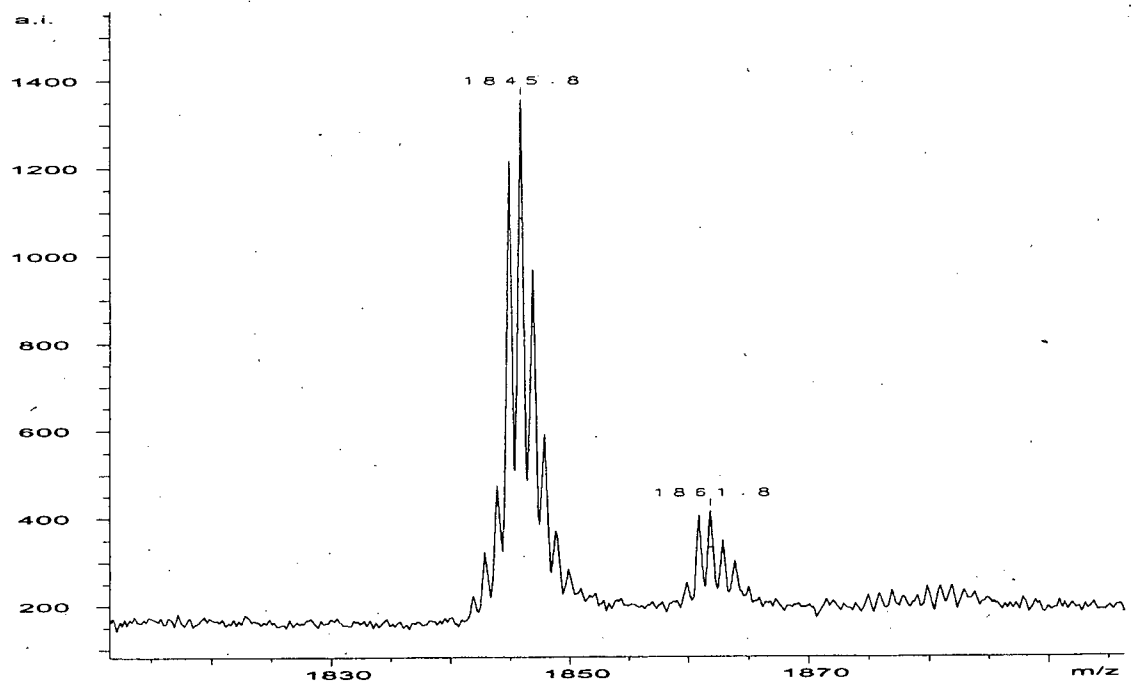

Figure 3-15: MALDI-TOF mass spectrum of the cobalt-containing macrocycle **50**

and copper-containing macrocycles (**51** and **52**), the signal of the target molecular weight is observed (Fig. 3-16 and 3-17). Other than $(M+H)^+$ and $(M+Na)^+$, a signal corresponding to the metallomacrocycle with four nickel atoms and four copper atoms, respectively, was present in the MALDI-TOF sample. These were not observed before in other metal-containing [3+3] Schiff-base macrocycles. When the metallated macrocycles were resynthesized with four equivalents of the corresponding metal chelates, the MALDI-TOF-MS spectra show no significant change in the ratio between the macrocycles with three metal atoms and four metal atoms. Therefore, the metallo-macrocycles with four metal atoms were probably formed during ionization. By using ESI-MS, a mass spectrum that shows only the metal-containing macrocycle with three metal atoms was obtained.

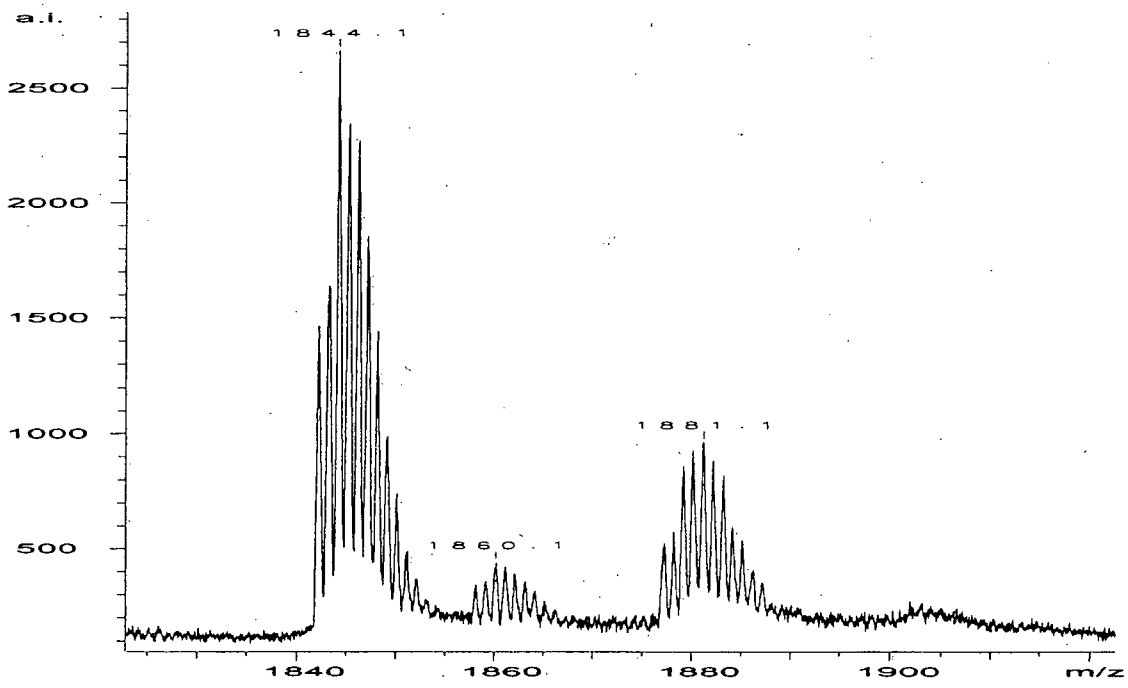

Figure 3-16: MALDI-TOF mass spectrum of the nickel-containing macrocycle **51**

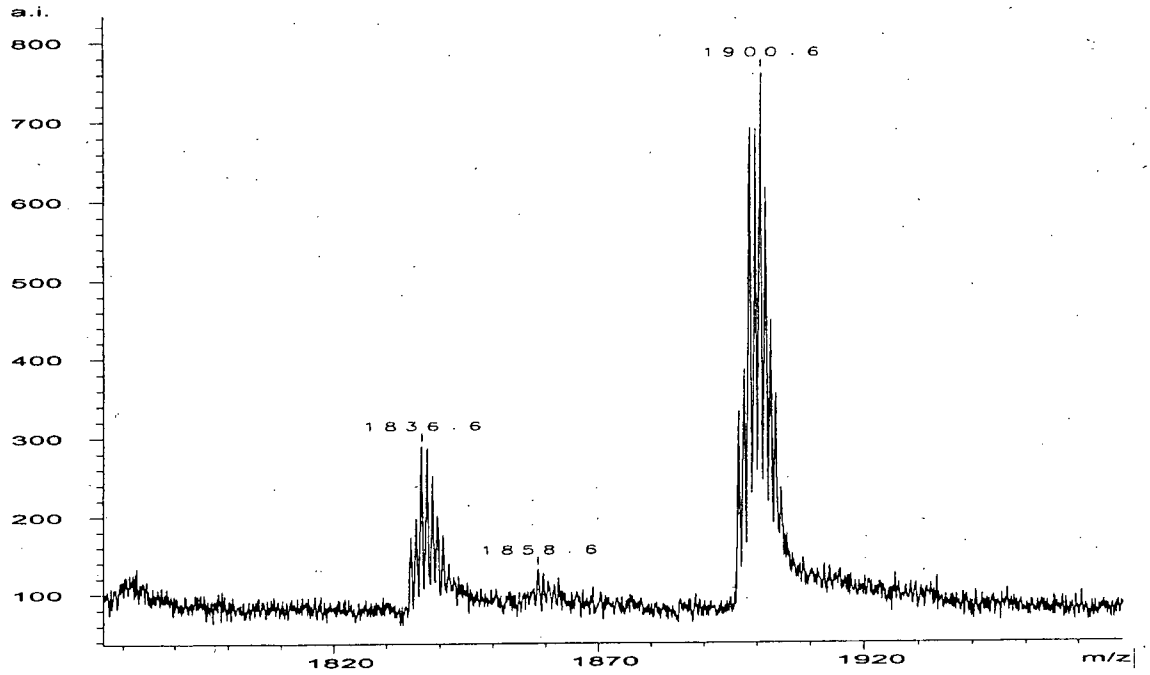

Figure 3-17: MALDI-TOF mass spectrum of the copper-containing macrocycle **52**

The vanadyl-, manganese-, iron- and copper-containing macrocycles were characterized by elemental analysis. The composition of each metal complex is listed in Table 3-2. It was noticed that the measured values for carbon are 1.5 to 3.5% lower than the calculated values. The lower values were due to the coordination of one or two water molecules to each metal centre. Table 3-3 shows the analyses with three and six water molecules. From the analyses, all the complexes have one water molecule coordinated to each metal, except for manganese which has two. The metal contents were also found to be lower than the expected values. Although the metal complexes were dried before the analysis, they might have physisorbed water that affected the analyses.

All of the metal-containing hexakisdecyloxy [3+3] Schiff-base macrocycles were tested with differential scanning calorimetry (DSC) and polarizing optical microscope

Table 3-2: The results of the elemental analysis of compounds **47**, **48**, **49** and **52**

	Compound **47** (% Cal'd / % Found)	Compound **48** (% Cal'd / % Found)	Compound **49** (% Cal'd / % Found)	Compound **52** (% Cal'd / % Found)
C	66.33 / 64.95	67.64 / 64.36	67.54 / 65.11	66.69 / 64.27
H	7.86 / 8.00	8.01 / 7.68	8.00 / 7.92	7.90 / 7.83
N	4.55 / 4.46	4.64 / 4.65	4.63 / 4.55	4.58 / 4.38

Table 3-3: The analyses of compounds **47**, **48**, **49** and **52** with three and six water molecules

	Compound **47**	Compound **48**	Compound **49**	Compound **52**
C (% Cal'd for no H_2O / 3 H_2O / 6 H_2O)	66.33 / 64.44 / 62.66	67.64 / 65.68 / 63.83	67.54 / 65.59 / 63.74	66.69 / 64.79 / 62.99
H (% Cal'd for no H_2O / 3 H_2O / 6 H_2O)	7.86 / 7.95 / 8.04	8.01 / 8.11 / 8.19	8.00 / 8.09 / 8.18	7.90 / 8.00 / 8.08
N (% Cal'd for no H_2O / 3 H_2O / 6 H_2O)	4.55 / 4.42 / 4.30	4.64 / 4.51 / 4.38	4.63 / 4.50 / 4.37	4.58 / 4.44 / 4.32

(POM) for liquid crystallinity. Although the organic counterpart did not exhibit mesomorphism, the incorporation of the metal atoms in the macrocycle might induce liquid crystallinity. However, no phase transition was observed on the DSC for any of the metal complexes even when the temperature was raised to 450 °C. Moreover, no sign of melting was observed on the POM as well. The melting point of the metal complexes may be lowered by increasing the length of the alkoxy side chains or by introducing chirality into the alkoxy substituents. In addition, the change in the side chain substituents can also assist the induction of liquid crystallinity.

The next step is to try stacking the transition metal-containing [3+3] Schiff-base macrocycles into nanotubes with different bridging ligands. The candidates that will be

used as the bridging ligands are 4,4'-bipyridine and pyrazine, as these two ligands can linearly bridge two metal atoms. Since each metallomacrocyclic molecule has three metal centres to which bridging ligands can coordinate, it creates a potential difficulty during the formation of the nanotubes. In order to synthesize the nanotubes with the use of bridging ligands, one metallomacrocycle has to stack perfectly onto another. However, it is possible that the reversibility of this coordination will facilitate the assembly process. As for the vanadyl-containing [3+3] Schiff-base macrocycle, it may form nanotubes without the use of bridging ligands because the V=O bonds can be polymerized into ···V-O-V-O-V··· chain with the neighboring molecules. However, the same problem as in the case of using bridging ligands to form the nanotubes may arise. Once these new nanotubes can be synthesized successfully, they will be characterized to determine their properties and potential applications.

In summary, the target metal-containing [3+3] Schiff-base macrocycles were obtained. They were characterized by ^{1}H NMR spectroscopy, IR spectroscopy, UV-Vis spectroscopy, and ESI and MADLI-TOF mass spectrometries. Future attempts to obtain the liquid crystalline metal-containing macrocycles will involve modifying the chain length and the functional group of the substituents. Moreover, attempts to obtain the target nanotubes will also be done.

3.4 References

(1) Crabtree, R. H. In *The Organometallic Chemistry of the Transition Metals*; Wiley-Interscience: Toronto, 2001, pp 222-258.

(2) Piotrowski, H.; Polborn, K.; Hilt, G.; Severin, K. *J. Am. Chem. Soc.* **2001**, *123*, 2699.

(3) Hoffman, B. M.; Weschler, C. J.; Basolo, F. *J. Am. Chem. Soc.* **1976**, *98*, 5473.

(4) Chen, D.; Martell, A. E. *Inorg. Chem.* **1987**, *26*, 1026.

(5) Patel, S. A.; Sinha, S.; Mishra, A. N.; Kamath, B. V.; Ram, R. N. *J. Mol. Catal. A: Chem.* **2003**, *192*, 53.

(6) Reddinger, J. L.; Reynolds, J. R. *Macromolecules* **1997**, *30*, 673.

(7) Kingsborough, R. P.; Swager, T. M. *Adv. Mater.* **1998**, *10*, 1100.

(8) Kingsborough, R. P.; Swager, T. M. *J. Am. Chem. Soc.* **1999**, *121*, 8825.

(9) Van Duen, R.; Binnemans, K. *Liq. Cryst.* **2001**, *28*, 621.

(10) Serrette, A.; Carroll, P. J.; Swager, T. M. *J. Am. Chem. Soc.* **1992**, *114*, 1887.

(11) Giroud-Godquin, A. M. In *Handbook of Liquid Crystals*; Demus, D., Goodby, J. W., Gray, G. W., Spiess, H. W., Vill, V., Eds.; Wiley VCH: New York, 1998; Vol. 2B, pp 901-932.

(12) Shaffer, T. D.; Sheth, K. A. *Mol. Cryst. Liq. Cryst.* **1989**, *172*, 27.

(13) Binnemans, K.; Lodewyckx, K.; Donnio, B.; Guillon, D. *Chem. Eur. J.* **2002**, *8*, 1101.

(14) Leung, A. C. W.; Chong, J. H.; Patrick, B. O.; MacLachlan, M. J. *Macromolecules* **2003**, *36*, 5051.

(15) Gallant, A. J.; MacLachlan, M. J. *Angew. Chem. Int. Ed.* **2003**, *42*, 5307.

Chapter 4: [6+6] Schiff-Base Macrocycles

4.1 Background

Macrocycles with rigid, non-collapsible, unsaturated hydrocarbon backbones have received a great deal of attention.[1] These substances can serve as shape-persistent cavities that have the capability to uptake molecules. The selectivity of the absorption of molecules within the cavities is subject to the size of and functionalities present on the macrocyclic ring. Unsaturation in the backbone will increase the π-stacking tendency between the neighbouring macrocyclic molecules; more extensive conjugation throughout the ring system will result in stronger π-stacking interactions. The π-π interaction of the macrocycles with their neighbouring macrocycles can lead to their aggregation to form nanotubes, which may have novel properties and potential applications.

Numerous types of conjugated macrocycles with different shapes have been designed and synthesized. For example, as described in Chapter 2, triangular [3+3] Schiff-base macrocycles have been investigated. This chapter describes my efforts to synthesize our next target Schiff-base macrocycle, which may be obtained by a [6+6] cyclocondensation of suitable dialdehyde and diamine building units (Fig. 4-1). The employment of Schiff-base chemistry provides a versatile and convenient approach towards the modular construction of macrocyclic structures. Both Moore[1-4] and Höger[5,6] have synthesized fully conjugated hexagonal macrocycles (Fig. 4-2a and b), which

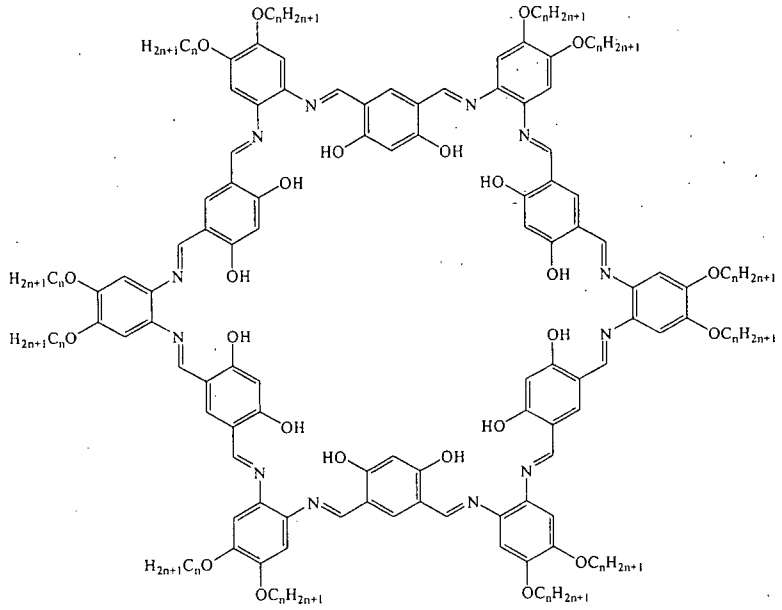

28

Figure 4-1: Chemical structure of the target [6+6] Schiff-base macrocycle

contain phenylene and ethynylene units. Our target hexagonal [6+6] Schiff-base macrocycles are also rigid and conjugated, and have twelve alkoxy substituents on the periphery in order to promote solubility. Unlike the phenyleneethynylene macrocycles, our target [6+6] macrocycle has six salphen sites that can coordinate metal atoms. The target macrocycle can be reacted with metal salts or metal chelates to form the metal complexes (Fig. 4-3), which could be potentially stacked into nanotubes with the use of bridging ligands. As the phenyleneethynylene macrocycles have been reported to exhibit mesophases,[3,6] the target [6+6] Schiff-base macrocycle has the potential to exhibit liquid crystallinity under certain conditions. In this chapter, my attempts to synthesize these macrocycles will be highlighted. Moreover, future work on this project will be discussed.

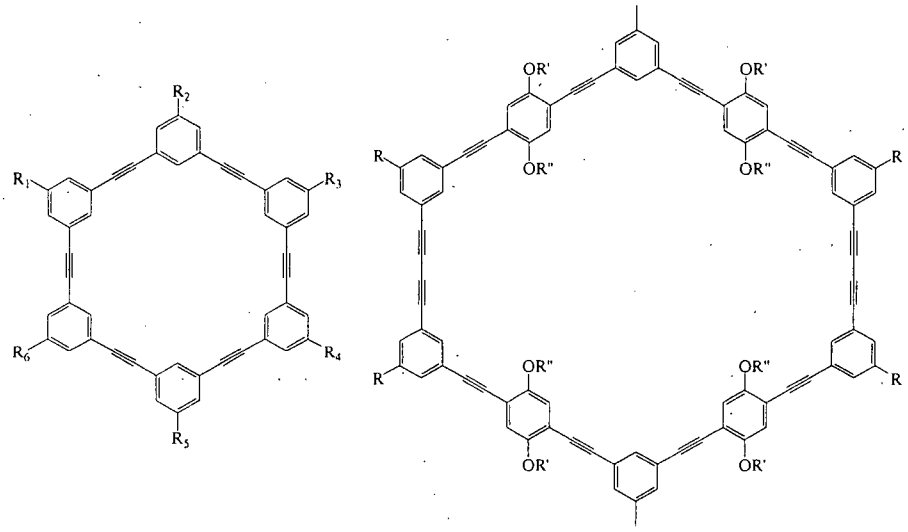

59 60

Figure 4-2: Chemical structure of Moore macrocycle (**59**) and Höger macrocycle (**60**)

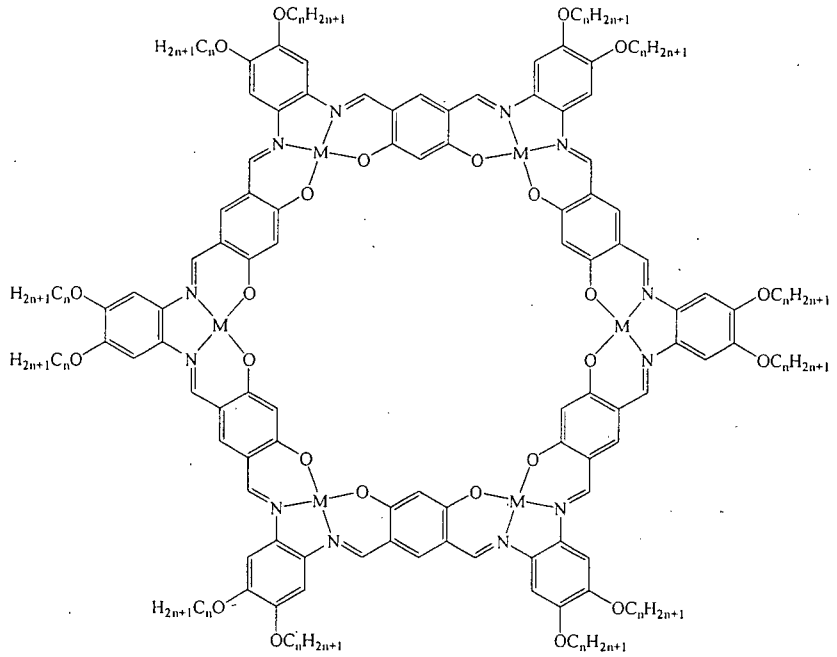

61

Figure 4-3: Chemical structure of the target metal-containing [6+6] Schiff-base macrocycle

4.2 Experimental

Materials: Deuterated solvents were obtained from Cambridge Isotope Laboratories, Inc.. Diethylether and dichloromethane were dried by passage over alumina columns. Dimethylformamide and ethanol were purged with nitrogen gas before use. 4,6-Diformyl-1,3-dihydroxybenzene (**62**) and 4,5-diamino-1,2-dialkoxybenzene (**63**) were prepared by literature methods.[7,8]

Equipment: All reactions were carried out under nitrogen unless otherwise noted. The 300MHz ^{1}H and 75.5 MHz ^{13}C NMR spectra were recorded on a Bruker AV-300 spectrometer. The IR spectra were obtained from dispersions in potassium bromide using a Bomens MB-series spectrometer. The UV-Vis spectra were performed in dichloromethane on a Varian Cary 5000 UV-Vis/near-IR spectrometer using a 1 cm cuvette. Electrospray (ESI) mass spectra were obtained at the UBC Microanalytical Services Laboratory on a Micromass LCT time-of-flight (TOF) mass spectrometer equipped with an electrospray ion source. The sample was analyzed in methanol:dichloromethane at 1 μM. The melting point was obtained on a Fisher-John's melting point apparatus and was corrected.

Synthesis of Compound 65. 4,6-Diformyl-1,3-dihydroxybenzene (**62**) (0.100 g, 0.602 mmol) and 4,5-diamino-1,2-dihexyloxybenzene (**64**) (0.371 g, 1.20 mmol) were added to a 100 mL Schlenk flask under nitrogen. Ethanol (40 mL) was added via syringe into the flask, giving an orange solution and orange-red solids. The mixture was stirred at

ambient temperature for 2 d. The red precipitate was isolated by filtration and compound **65** was obtained (0.425 g, 94%).

Data of Compound 65. ^{1}H NMR (300 MHz, chloroform-d_1) δ 14.01 (s, 2H, O*H*), 8.43 (s, 2H, C*H*=N), 7.36 (s, 1H, aromatic C*H*), 6.71 (s, 2H, aromatic C*H*), 6.51 (s, 1H, aromatic C*H*), 6.32 (s, 2H, aromatic C*H*), 3.944 (t, 8H, OCH_2), 3.86 (broad, 4H, NH_2), 1.76 (m, 8H, CH_2), 1.42 (m, 8H, CH_2), 1.33 (m, 16H, CH_2), 0.89 (t, 12H, CH_3) ppm; ^{13}C NMR (75.5 MHz, chloroform-d_1) δ 166.7 (*C*H=N), 158.9, 151.8, 143.7, 137.8, 137.4, 127.8, 115.0, 107.8, 105.5, 103.8 (aromatic *C*H), 72.6, 70.6 (O*C*H_2), 33.1, 33.0, 31.0, 30.6, 27.1, 24.0 (*C*H_2), 15.4 (*C*H_3) ppm; UV-Vis (dichloromethane): λ_{max} (ε) = 262 nm (2.91×10^4 $cm^{-1}M^{-1}$), 289 nm (3.20×10^4 $cm^{-1}M^{-1}$), 418 nm (3.48×10^4 $cm^{-1}M^{-1}$); ESI-MS: m/*z* = 747.6 ($(M+H)^+$, 10%), 769.6 ($(M+Na)^+$, 100 %); IR (KBr): υ = 3394 (m), 3292 (w), 3168 (m), 2955 (s), 2928 (s), 2856 (s), 1634 (vs), 1576 (s), 1522 (vs), 1466 (s), 1429 (s), 1388 (m), 1363 (s), 1332 (s), 1289 (vs), 1261 (s), 1241 (s), 1229 (w), 1207 (m), 1178 (vs), 1165 (m), 1137 (m), 1069 (w), 1045 (m), 1014 (w), 997 (m), 951 (m), 930 (w), 906 (w), 872 (w), 838 (s), 787 (w), 758 (w), 721 (w) cm^{-1}; Mp = 120-121 °C

Attempted synthesis of the [6+6] Schiff-base macrocycle. 4,6-Diformyl-1,3-dihydroxybenzene (**62**) (0.100 g, 0.602 mmol) and 4,5-diamino-1,2-dihexyloxybenzene (**64**) (0.253 g, 0.602 mmol) were added to a 100 mL Schlenk flask under nitrogen. Tetrahydrofuran (20 mL) and 2-methoxyethanol (20 mL) were sequentially added via syringe into the flask, giving a bright orange solution. The solution was stirred at 90 °C for two days, giving a red solution. After cooling the solution to room temperature, acetonitrile was added to the flask and a red precipitate was formed. The red solid was

isolated by filtration and was characterized by ^{1}H NMR spectroscopy and ESI mass spectrometry, which showed a mixture of species.

Attempted synthesis of the [6+6] Schiff-base macrocycle with template. 4,6-Diformyl-1,3-dihydroxybenzene (**62**) (0.100 g, 0.602 mmol), 4,5-diamino-1,2-didodecyloxybenzene (**34**) (0.287 g, 0.602 mmol) and hexahydroxytriphenylene (**67**) (0.033 g, 0.100 mmol) were added to a 100 mL Schlenk flask under nitrogen. Toluene (35 mL) and acetonitrile (15 mL) were sequentially added via syringe into the flask, giving an orange solution. The solution was stirred under reflux at 90 °C for 18 hours, and red precipitate was observed. After cooling the solution to room temperature, the red solid was isolated by filtration and was characterized by ^{1}H NMR spectroscopy and ESI mass spectrometry, which showed a mixture of species.

4.3 Discussion

In theory, the target dodecakisalkoxy [6+6] Schiff-base macrocycles can be synthesized by a one-pot synthesis through the condensation of 4,6-diformyl-1,3-dihydroxybenzene (**62**) and 4,5-diamino-1,2-dialkyloxybenzene (**63**) (Scheme 4-1). I have tried numerous approaches to synthesize the target [6+6] Schiff-base macrocycle in a one-pot synthesis. Reaction conditions, such as the use of solvents, the temperature of the reactions and the reaction time, were varied. The solvents that were used to perform

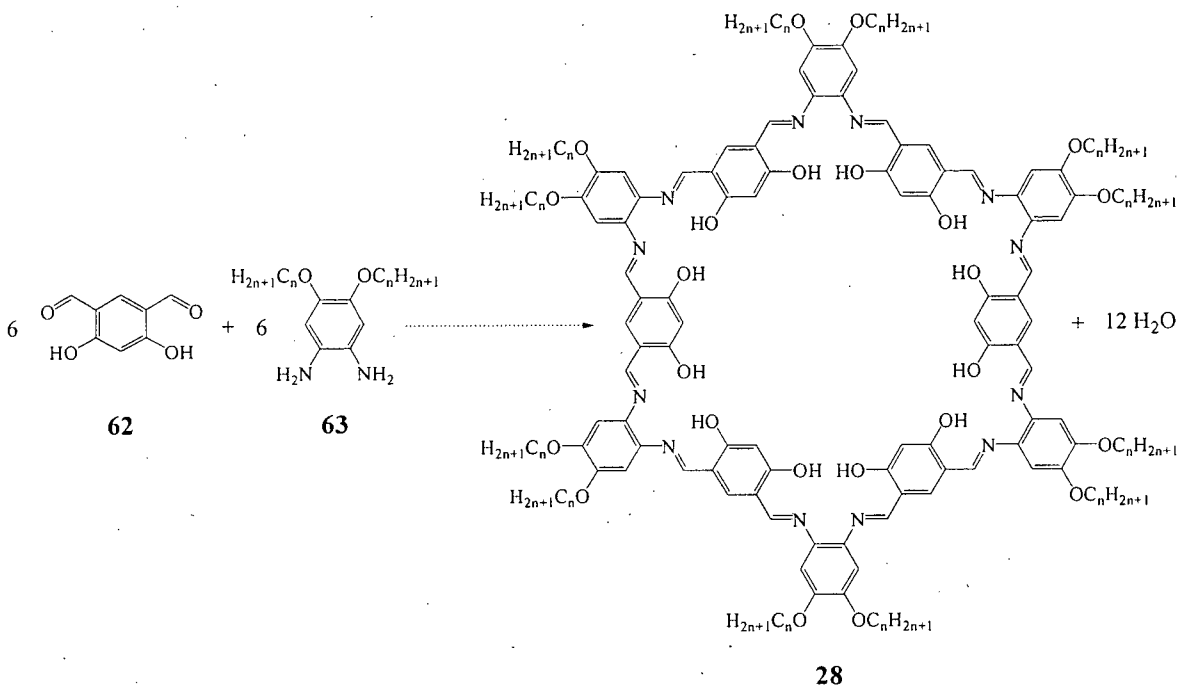

Scheme 4-1: Synthesis of the [6+6] Schiff-base macrocycles

the reactions were dichloromethane, acetonitrile, methanol, ethanol, tetrahydrofuran and 2-methoxyethanol. Moreover, solvent mixtures were used for some of the test reactions.

Compounds **62** and **63** (n = 6) were reacted in different solvents at different temperatures under a nitrogen atmosphere. The solvent or mixture of solvents were chosen to enhance the hydrogen bonding between the imine nitrogen and the hydroxyl group. It is believed that the hydrogen bond plays an important role in the formation of the Schiff-base macrocycles. Without hydrogen bonding, the imine C=N bond may form in a different direction (Fig. 4-4) and thus the Schiff-base macrocycle will not be obtained. The conditions and the results of the test reactions are listed in Table 4-1. All the resulting products were obtained as red solids and were characterized by ^{1}H NMR

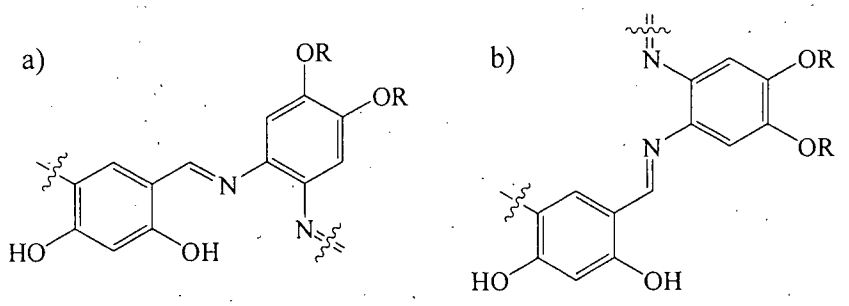

Figure 4-4: System a) with and b) without hydrogen bonding

Table 4-1: Test reactions of compound **62** with compound **64**

Trial	Diol:Diamine	Solvent(s)	Temp.	Reaction time	Product(s)
1	1:1	EtOH	ambient	overnight	mixture of species
2	1:1	CH_2Cl_2/MeCN	ambient	overnight	mixture of species
3	1:1	THF	ambient	3 d	compound **65**
4	1:1	THF	90 °C	2 d	compound **65**
5	1:1	MeOH	80 °C	2 d	compound **65**
6	1:1	2-methoxyethanol	90 °C	4 d	mixture of species
7	1:1	2-methoxyethanol/THF	90 °C	4 d	mixture of species

spectroscopy. The ^{1}H NMR spectra of the products obtained from the test reactions in ethanol and a dichloromethane/acetonitrile mixture showed that several species were present. Imine protons were observed in the spectra, which shows the starting materials underwent Schiff-base condensation. Accordingly, the target macrocycle may result if a longer reaction time and/or heat were applied to the system. For the test reactions that used tetrahydrofuran as the solvent, only compound **65** was obtained, despite varying the reaction time and temperature. Moreover, compound **65** was also obtained for the test reaction that used methanol as the solvent and that was heated under reflux for two days. The two starting materials, compounds **62** and **64**, were used in a 1:1 ratio in all the test

reactions. However, the major product, compound **65**, that is obtained in the third, fourth and fifth test reactions, was formed by a 1:2 ratio of compounds **62** and **64**. According to these results, compound **65** seems to be a very stable intermediate in the [6+6] Schiff-base condensation process. For the sixth and seventh trials of the test reaction, using 2-methoxyethanol and a mixture of 2-methoxyethanol and tetrahydrofuran as the solvents, respectively, the resulting products were characterized by both ^{1}H NMR spectroscopy and electrospray mass spectrometry. The ^{1}H NMR spectra show a very broad peak in both the aromatic and imine regions. This is suggestive of the target macrocycle because the [6+6] Schiff-base macrocycle might have slow dynamics and give a broad signal. However, the ESI-MS spectra show that the resultant products are mixtures of species that have molecular weights similar to larger fragments of the macrocycle (Fig. 4-5).

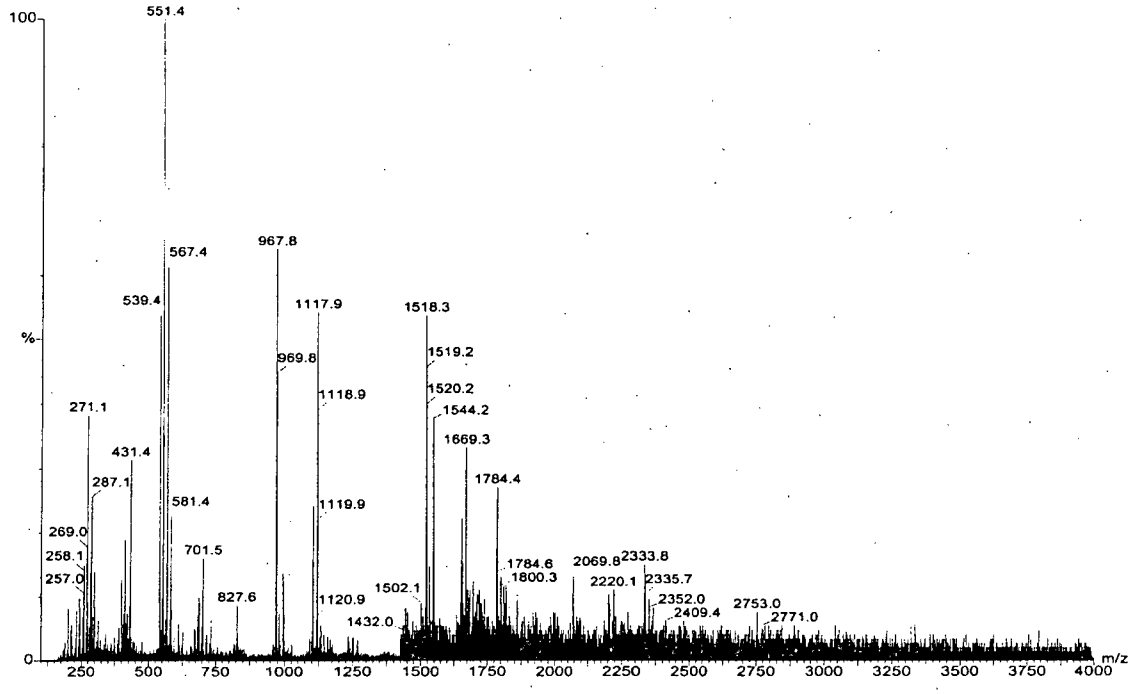

Figure 4-5: ESI mass spectrum of the product when 2-methoxyethanol was used as solvent

Therefore, 2-methoxyethanol might be a good solvent to be used in the future investigations of this reaction. The sixth and seventh test reactions were reattempted with 4,5-diamino-1,2-didecyloxybenzene (compound **33**) instead of 4,5-diamino-1,2-dihexyloxybenzene (compound **64**), but the same results were obtained. The reaction was also performed in the presence of molecular sieves in order to remove water generated during the reaction. However, the product was still a mixture of species.

Synthesis of the target macrocycle was also attempted using a templating method. The choice of the template and the conditions of the test reactions are listed in Table 4-2. The template may help to bring the starting materials together and hold them in the correct position for the reaction to take place.[9]

Table 4-2: Test reactions of the [6+6] Schiff-base cyclocondensation using a templating method

Trial	Template	Diol:Diamine:Template	Solvent(s)	Temp.	Reaction Time	Product(s)
8	zinc acetate dihydrate	1:1:1	MeOH	80 °C	overnight	mixture of species
9	hexahydroxy-triphenylene	6:6:1	toluene/MeCN	90 °C	18 h	mixture of species
10	hexahydroxy-triphenylene	6:6:1	toluene/MeCN	90 °C	3 d	mixture of species
11	hexahydroxy-triphenylene	6:6:1	$CHCl_3$/MeCN	90 °C	3 d	mixture of species

Zinc(II) acetate dihydrate was used as the template as it was expected to form the zinc-containing [6+6] Schiff-base macrocycle (Scheme 4-2). Compounds **62**, **64** and zinc acetate dihydrate were combined in methanol and heated to reflux overnight. The zinc

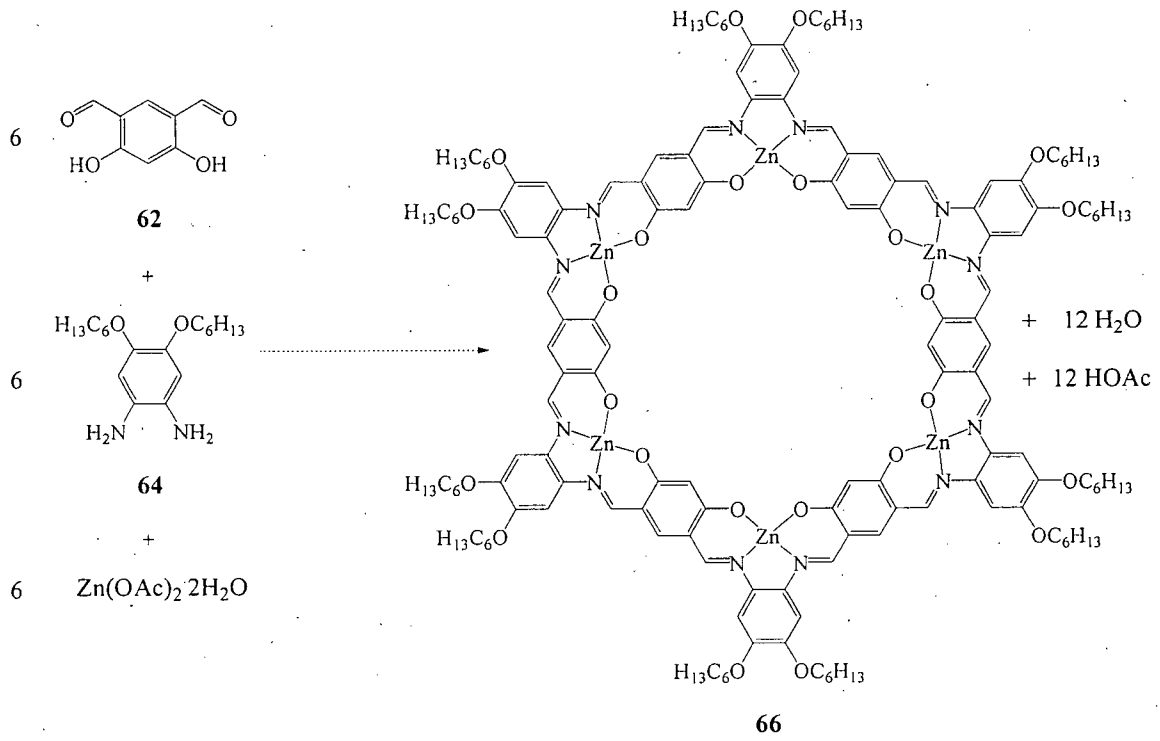

Scheme 4-2: Synthesis of [6+6] Schiff-base macrocycle with zinc template

ions should have coordinated to the salphen pockets during the reaction. If that was the case, the resulting zinc-containing salphen moieties could lead to the formation of the target macrocycle. The peaks on the ^{1}H NMR spectrum of the product are broad, which was expected, since the zinc-containing [3+3] Schiff-base macrocycle also had broad peaks. However, according to the ESI-MS, the product was a mixture of species. This metal templating reaction can be retried with different solvents or mixture of solvents, and with metal chelates in future studies.

We also tried templating with a molecule that should fit in the cavity of the macrocycle. Hexahydroxytriphenylene (**67**) was chosen as the template because it can hydrogen bond to the starting materials and help to stabilize the product. 4,6-Diformyl-1,3-dihydroxybenzene (**62**) and 4,5-diamino-1,2-didodecyloxybenzene (**34**) were reacted

in the presence of hexahydroxytriphenylene (**67**) in different mixtures of solvents and heated to reflux for different periods of time (Scheme 4-3 and Table 4-2). Red solids were obtained as the products of these reactions, and were analyzed by ^{1}H NMR spectroscopy. It was found that the product of the ninth test reaction was a mixture of species. For the tenth and eleventh test reactions, the products were mainly compounds similar to compound **65**.

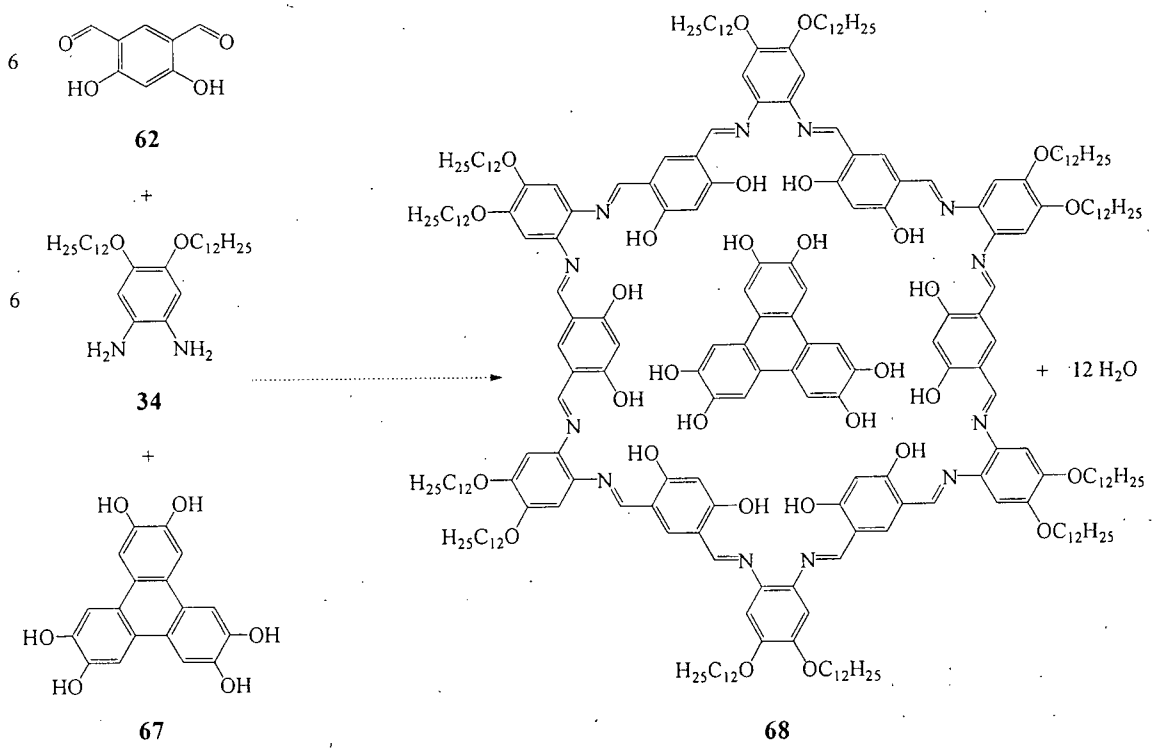

Scheme 4-3: Proposed synthesis of [6+6] Schiff-base macrocycle using hexahydroxytriphenylene as template

Compound **65** was prepared according to the procedure listed in the experimental section of this chapter and was characterized by ^{1}H and ^{13}C NMR spectroscopy, IR spectroscopy, UV-Vis spectroscopy and electrospray mass spectrometry. The peaks of the ^{1}H and ^{13}C NMR spectra of compound **65** correspond to the correct number of proton

and carbon environments (Fig. 4-6 and Fig. 4-7). In the IR spectrum of compound **65** (Fig. 4-8), three bands at 2955, 2928, and 2856 cm^{-1} are the C-H stretching frequencies of the alkoxy substituents on the periphery of phenyl ring. The absorption band at 3394 cm^{-1} corresponds to the stretching frequency of the N-H bond. There is a very strong absorption band at 1633 cm^{-1}, which is the imine C=N stretching frequency. The UV-Vis spectrum of compound **65** shows three peaks centred at 262, 289, and 418 nm (Fig. 4-9). The band centred at 418 nm likely corresponds to the π to π^* transition of the π-electron of the conjugation from one end to the other end of the compound. The ESI-MS spectrum (Fig. 4-10) displays mainly the molecular weight of compound **65** with the coordination of the sodium ion. The sodium ion likely comes from the glassware used during the sample preparation.

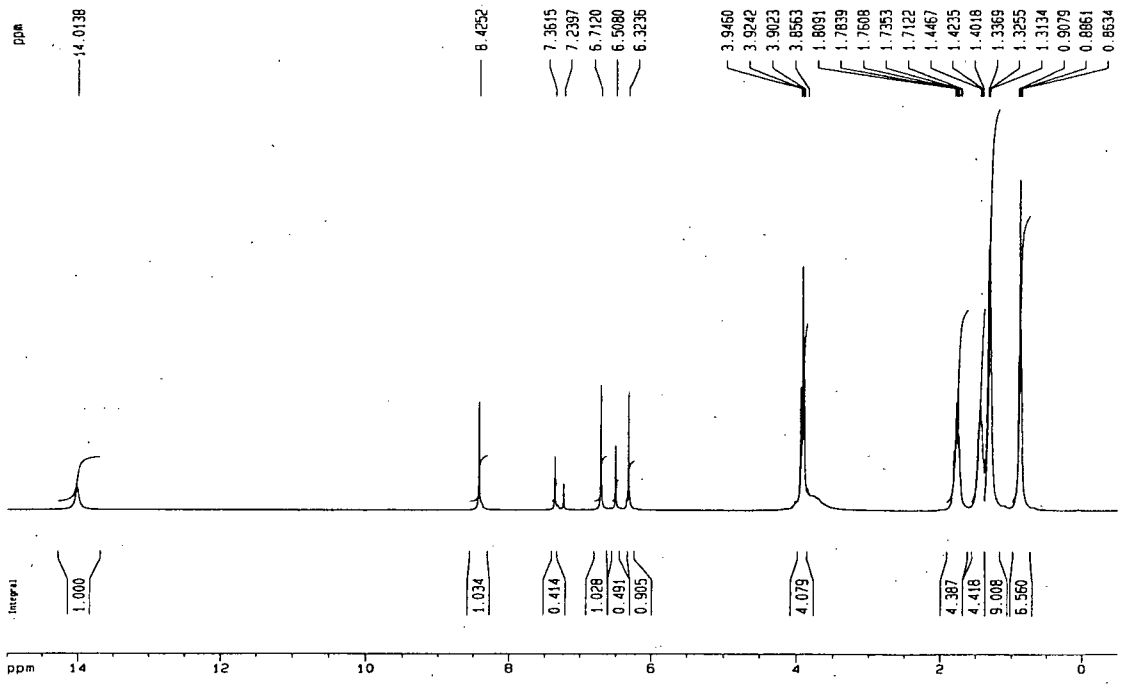

Figure 4-6: ^1H NMR spectrum of compound **65**

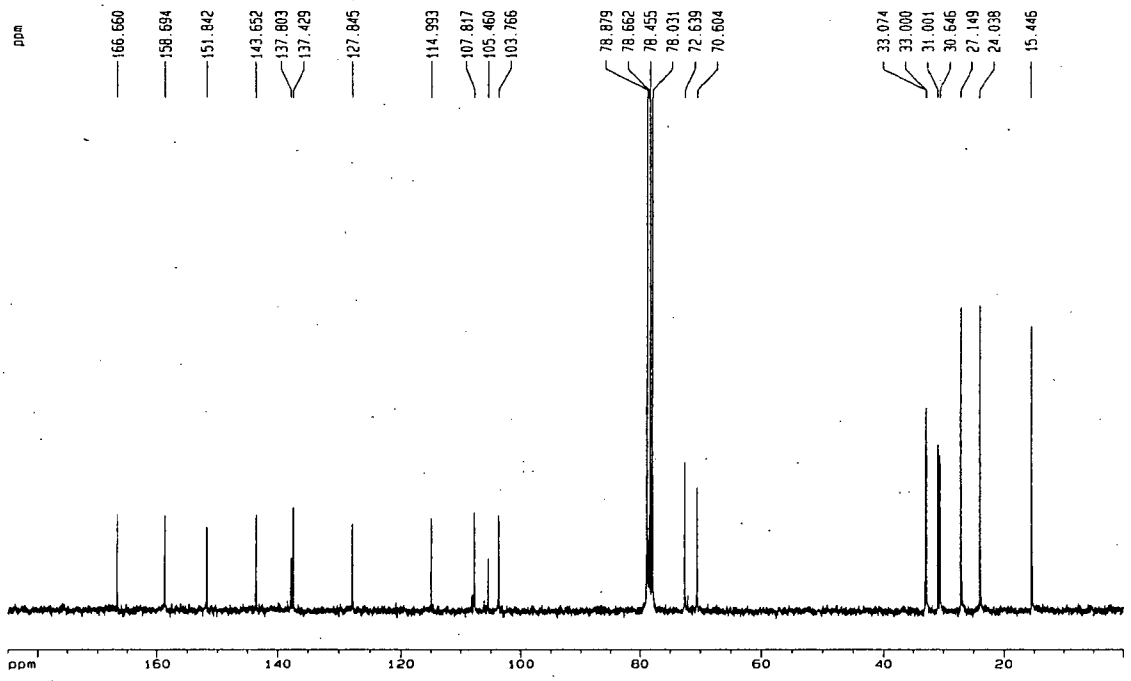

Figure 4-7: ^{13}C NMR spectrum of compound **65**

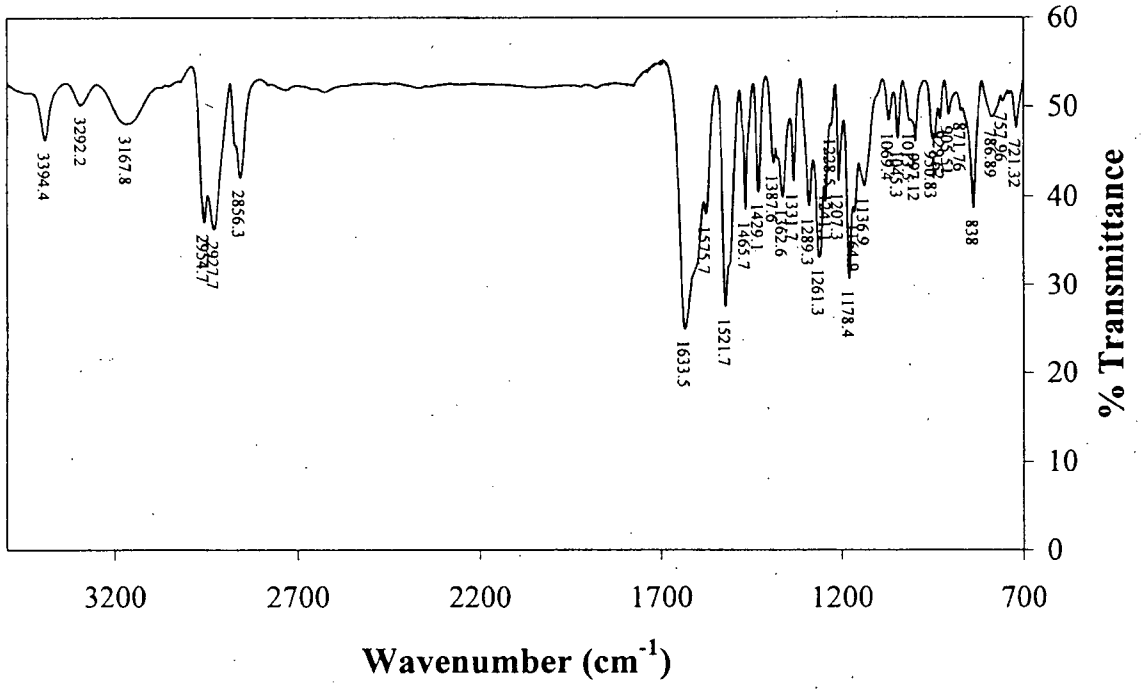

Figure 4-8: IR spectrum of compound **65**

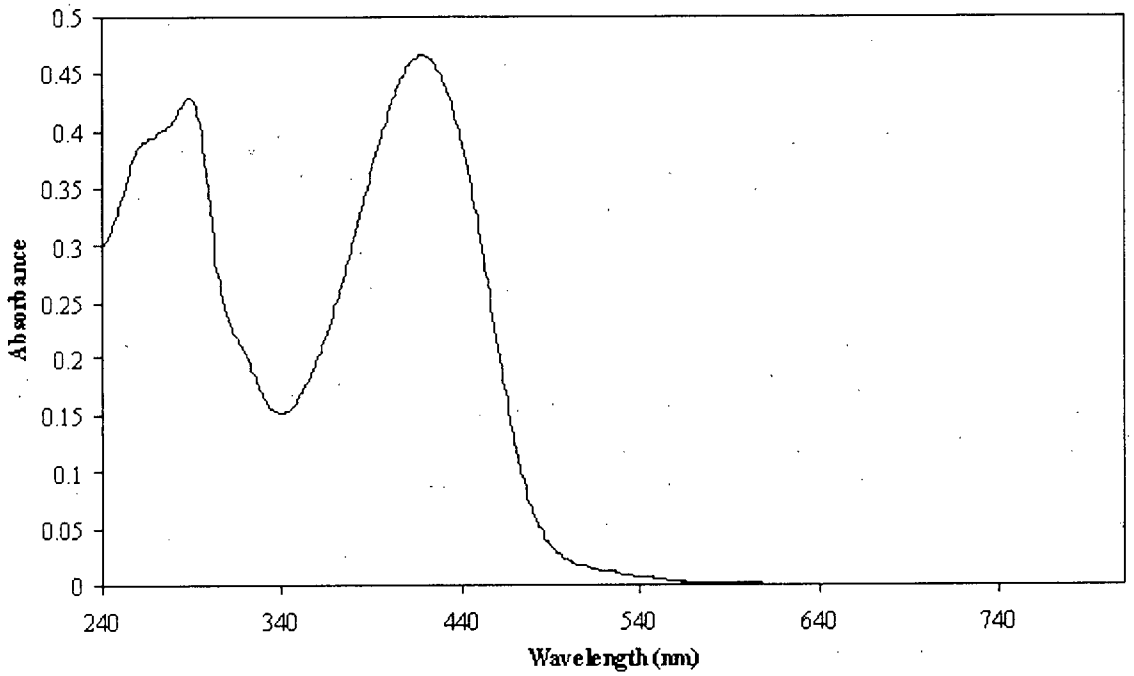

Figure 4-9: UV-Vis spectrum of compound **65**

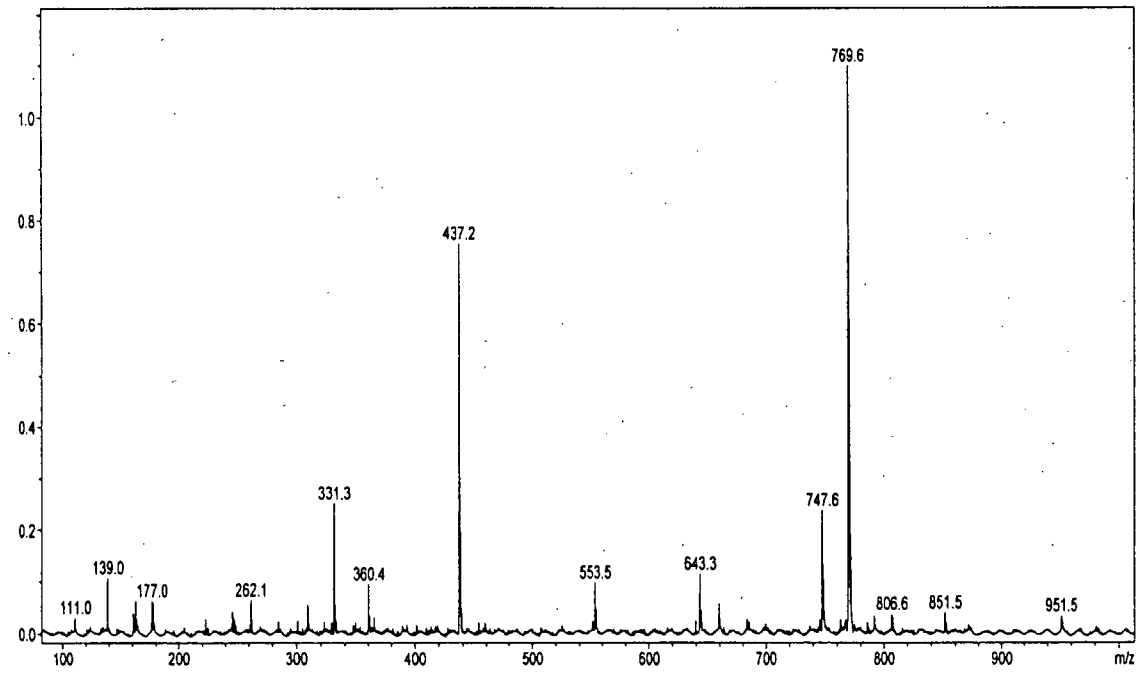

Figure 4-10: ESI mass spectrum of compound **65**

Compound **65** was synthesized to help understand more of the chemistry of needed to form the target [6+6] Schiff-base macrocycle. Compound **65** has been used as a starting material and reacted with 4,6-diformyl-1,3-dihydroxybenzene (compound **62**), but the product obtained was a mixture of species. Capping compound **65** with derivatives of salicylaldehyde was attempted in different solvents at different temperatures (Scheme 4-4 and Table 4-3). The products from each reaction were analyzed by ^{1}H NMR spectroscopy and were all found to be mixtures of species. For the test reactions that were performed in the presence of molecular sieves and zinc acetate dihydrate, the target product was not obtained. The best cases among the test reactions were the first and second trials. According to the ^{1}H NMR spectra of those two trials, the products seemed to be a mixture of the target di-capped compound (**71**), the mono-capped compound (**73**) and/or the dihexyloxy salphen (**74**) (Fig. 4-11). The lack of completion of the reaction and the formation of the salphen might be due to water in

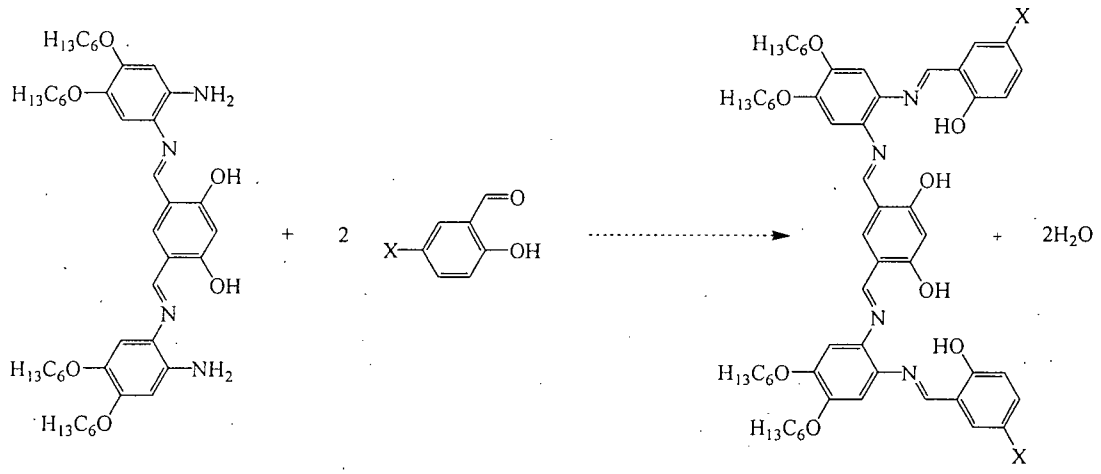

65 **69** X = H, **70** X = I → **71** X = H, **72** X = I + $2H_2O$

Scheme 4-4: Capping compound **65** with derivatives of salicylaldehyde

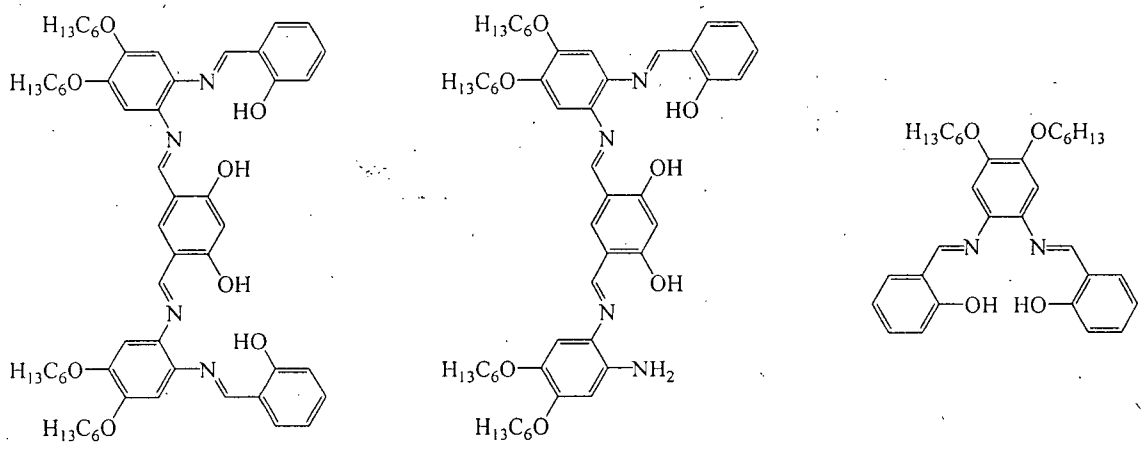

Figure 4-11: Chemical structures of compounds **71**, **73** and **74**

solution, since the formation of compound **71** is reversible in the presence of water. The capping reaction will be reattempted under a nitrogen atmosphere in order to obtain the di-capped compound.

In summary, the target [6+6] Schiff-base macrocycle was not obtained. However, a smaller fragment of the target macrocycle, compound **65**, was observed in many trials of the condensation. Compound **65** was synthesized and capping with salicylaldehyde to form compound **71** was attempted, but, unfortunately, the desired product could not be obtained. In the future, more test reactions will be done on compound **65** in order to obtain compound **71**. Future attempts to synthesize the target macrocycle will involve using a step-wise approach, using a Dean-Stark apparatus and modifying the conditions of the one-pot synthesis. Once the [6+6] Schiff-base macrocycle is obtained, metallation with different transition metals will follow.

Table 4-3: Test reactions of the capped compound **65** under different conditions

Trial	Cap	Solvent(s)	Air/N_2	Temp	Reaction Time	Extra	Product(s)
1	salicylaldehyde	CH_2Cl_2	air	ambient	overnight		mixture of species
2	salicylaldehyde	THF	air	ambient	overnight		mixture of species
3	salicylaldehyde	CH_2Cl_2	air	50 °C	4 d	molecular sieves	mixture of species
4	salicylaldehyde	THF/EtOH	air	ambient	5 h		mixture of species
5	salicylaldehyde	THF/EtOH	air	ambient	overnight		mixture of species
6	salicylaldehyde	THF/EtOH	air	ambient	2 d	molecular sieves	mixture of species
7	salicylaldehyde	THF/EtOH	air	ambient	2 d	2 eq. $Zn(OAc)_2 2H_2O$	mixture of species
8	salicylaldehyde	THF	N_2	90 °C	2 d		mixture of species
9	salicylaldehyde	1,2-dichloro-benzene	air	180 °C	4 h		mixture of species
10	salicylaldehyde	1,2-dichloro-benzene	air	180 °C	overnight		mixture of species
11	salicylaldehyde	1,2-dichloro-benzene	air	180 °C	overnight	2 eq. $Zn(OAc)_2 2H_2O$	mixture of species
12	5-iodo-salicylaldehyde	EtOH	air	90 °C	overnight		mixture of species
13	5-iodo-salicylaldehyde	CH_2Cl_2	air	50 °C	overnight		mixture of species
14	5-iodo-salicylaldehyde	THF	air	90 °C	2 d		mixture of species

4.4 References

(1) Zhao, D.; Moore, J. S. *J. Chem. Soc., Chem. Commun.* **2003**, 807.

(2) Zhang, J.; Moore, J. S. *J. Am. Chem. Soc.* **1992**, *114*, 9701.

(3) Zhang, J.; Moore, J. S. *J. Am. Chem. Soc.* **1994**, *116*, 2655.

(4) Zhang, J.; Moore, J. S. *Angew. Chem. Int. Ed.* **1992**, *31*, 922.

(5) Höger, S.; Meckenstock, A-D.; Müller, S. *Chem. Eur. J.* **1998**, *4*, 2423.

(6) Höger, S.; Enkelmann, V.; Bonrad, K.; Tschierske, C. *Angew. Chem. Int. Ed.* **2000**, *39*, 2267.

(7) Worden, L. R.; Kaufman, K. D.; Smith, P. J.; Widiger, G. N. *J. Chem. Soc., Chem. Commun.* **1970**, 227.

(8) Yilmaz, I.; Bekâroğlu, Ö. *J. Chem. Res* **1998**, (*S*) 374; (*M*) 1585.

(9) Cox, B. G.; Schneider, H. In *Coordination and Transport Properties of Macrocyclic Compounds in Solution*; Elsevier: New York, 1992; pp 335-400.